European Polymer Journal 117 (2019) 304–336

Contents lists available at ScienceDirect

European Polymer Journal

journal homepage: www.elsevier.com/locate/europolj

Advancements in nanofibers for wound dressing: A review

Rushikesh S. Ambekar, Balasubramanian Kandasubramanian*

Rapid Prototype & Electrospinning Lab, Department of Metallurgical and Materials Engineering, DIAT (DU), Ministry of Defence, Girinagar, Pune 411025, India

ARTICLE INFO

Keywords:
Wound healing
Wound dressing
Electrospinning
Biodegradable polymers
Antibiotic drugs

ABSTRACT

Chronic wound healing is an intricate time-consuming process (healing time ~12 weeks), susceptible to external biological attack such as bacteria (e.g. *E. coli, B. subtilis, S. aureus* etc.) promoting wound infection and exhibit a negative effect on the immune system, therefore, it is a necessity to form a controlled environment for wound healing with the help of suitable barrier. Over the past few decades, various topical formulations of wound barriers like films, hydrogels, emulsions and nano/micro-fibers have been explored. The drug-embedded fibers are the potential candidate for wound healing as a barrier owing to the large specific surface area (for surface functionalization), enormous porosity ~60–90% (for oxy-permeability), reticulated nano-porosity (for inhibition of the microorganism) and advanced electrospinning methodology which facilitates sustained drug release. Wound bed exhibits 37 °C temperature and 7.4 pH (typically for blood) condition which triggers the drug release and nano/micro-fiber degradation simultaneously. Drug-embedded nano/micro-fiber consists of a matrix with excellent biocompatibility, appreciable biodegradation rate (e.g. Chitin nanofiber-20% degradation in 15 days) and a drug with a superior antibiotic, antimicrobial property, besides certain drug (e.g. Captopril) also promote vasodilation which increases in-vascular permeability leading to rapid movement of leukocytes into the affected tissue, thereby reducing the healing time. In this review article, we discuss the consolidated recent advanced works on wound healing and wound dressing which implies the significance of wound dressing. In addition, the recent advancements in nano/micro-fiber fabrication methodology for drug release mechanism, and benefits of the fiber-based wound dressings compared to conventional wound dressings have been extensively discussed.

1. Introduction

Humans recognized the importance of wound healing from the ancient period, however, the wide research was conducted in the period of world war I, in which the use of metallic projectiles and shrapnels caused injuries, which gave rise to new types of wounds. Simultaneously, contaminated battlefields were also susceptible to wound infection, and immediately after world war II, the demand for surgical dressings also increased due to improved and dangerous projectiles and ammunitions [1].

The wound is a discontinuity in the tissue occurring due to an exogenous laceration on the skin causing trauma. An acute wound is the faster healing wound, whereas, the chronic wound is the time-consuming wound, thus it is under high risk of bacterial attack [2]. Wound healing is naturally more complicated than just four stages of Hemostasis, Inflammation, Proliferation and Remodeling, besides phagocytosis, chemotaxis process and some of the mediators are also required to trigger and terminate the wound healing stages on an appropriate occasion of healing [3].

Wound healing has been of considerable significance since few millenniums. In 1550 BCE, an ancient Egyptian document, Ebers Papyrus, mentioned the mixture containing grease (for barrier), honey (for antibacterial) and lint (for absorbent) for wound treatment [4]. Later, in 600 BCE, the Indian physician Sushruta mentioned wound healing [5,6] where he encouraged the use of Mustard seeds, Neem leaves, Cow's ghee and Salt. Later, scientists unveiled that mustard seeds have antibacterial and antifungal property, leaves of Neem have a good anti-fungal property and the mixture of cow's ghee with salt allows the gas permeation for improved wound healing [7]. Soon after, in 460–380 BCE, the Greek physician, Hippocrates, practiced the treatment of chronic wound with honey, wine and milk as honey (complex sugars) exhibits strong resistance towards gram-positive bacteria, whilst wine has good resistance to the growth of gram-negative bacteria and milk products, encompassing cytokines, acts as a buffer to control the pH of wound bed [8]. In 25 BCE-50 CE, the Roman encyclopaedist Cornelius Celsus published De Medicina book where he mentioned Scalpels, Curved forceps and surgical hook for wound closure treatment [9]. In 1865, Dr. Joseph Lister reported the importance of sterilized surgical gauze with carbolic acid for wound dressing. In 1846–1890, the Russian military surgeon Carl Reyher mentioned debridement

* Corresponding author.
E-mail address: meetkbs@gmail.com (B. Kandasubramanian).

https://doi.org/10.1016/j.eurpolymj.2019.05.020
Received 8 March 2019; Received in revised form 23 April 2019; Accepted 11 May 2019
Available online 13 May 2019
0014-3057/

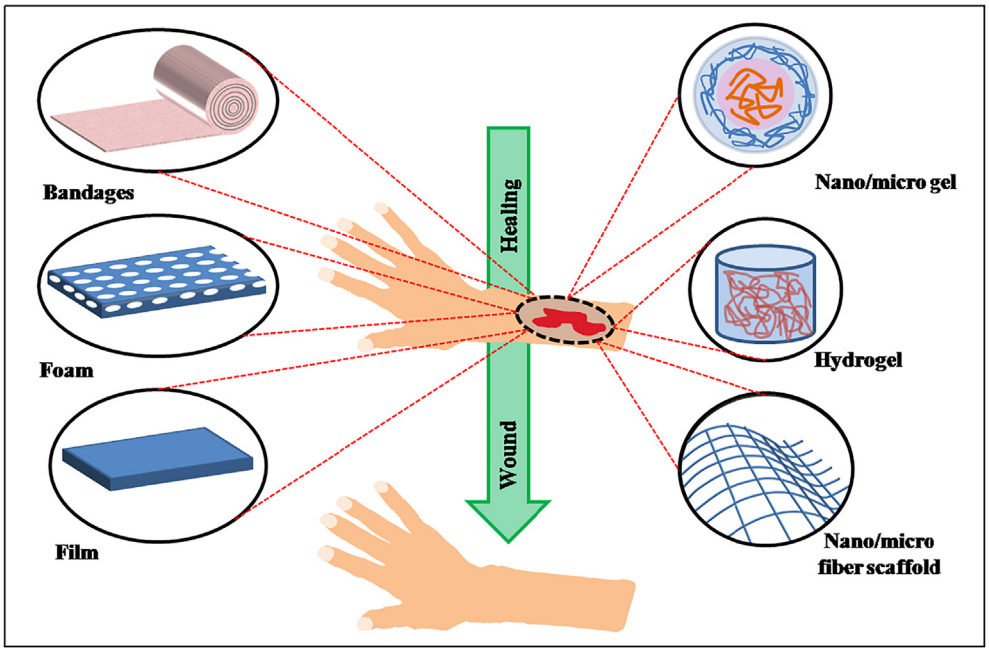

Fig. 1. Classification of wound dressing.

which is nothing but cleansing of wound from foreign body [1]. In 1955, Professors Lim and Wichterle synthesized first time poly-2-hydroxyethyl methacrylate based hydrogel for biomedical application [10]. In 1962, Winter's experimental data confirmed that moist wound heals faster than dry wound [11].

From 1980 onwards, topological formulations such as Membranes/sponges [12–18], Hydrogels [19–25], films [26–29], nanogel/microgel [30–32], Scaffolds/bandages [21,33–36] and nano/micro-fibers [37,38] have been investigated as shown in Fig. 1. Out of them, nano/micro-fibers provide the desired properties for wound dressing such as exudate's absorption, oxygen permeability, high surface area and antibacterial property, which is largely attributed to the evolution of nanotechnology [39–41].

The nanotechnology is the fastest emerging miniaturized technology having characteristics properties such as high specific surface area, surface chemistry (composition) [42], surface thermodynamics (wettability and free energy) [43–45] and surface physics (topography and roughness) [46], thus making it most favourable for biomedical applications such as drug delivery [47,48], bone tissue engineering [49–52], tissue engineering [53–55], skin tissue engineering [56–59], bio-adhesive [60], anti-bacterial [61] and anti-microbial application [62]. Recently, drug-loaded nanofiber scaffolds have enticed the attention of researchers in the field of skin tissue engineering due to its characteristics such as tailor-ability, drug release efficiency and biocompatibility that enhances the repairment of damaged tissue [63]. Various nanofiber fabrication methodologies such as Melt blowing, Rotary jet spinning, Hand spinning, Pressurized Gyration [64–67] and Electrospinning [39] have been developed for manufacturing drug-loaded nanofiber scaffold. The comparison of advantages and limitations of nanofiber fabrication methods are depicted in Table 1.

Drug released from the polymeric matrix scaffold is categorized into two types: burst release and sustained release. The burst release is the rapid release of drug, mainly due to the large surface area of nanofiber whereas later is release of constant drug concentration for a specific time, to avoid any side effect caused by drug overdose [68]. The burst release of drug depends on instrument geometry, surface characteristics of scaffold, dispersibility of drug in matrix, pore size, pore density, etc. [69]. The concentration of drug in the body should lie in therapeutic window, thus drug concentration depends on the drug release rate of the scaffold and therefore, scaffold should be designed in such a way that drug concentration should not cross the maximum safe concentration limit. To rectify this, the advanced electrospinning techniques act as a potential candidate owing to its sustained drug release due to coaxial and tri-axial configuration, better oxygen permeability, tunable fiber diameter and large specific surface area [70].

Electrospinning methodology facilitates the use of wide range of materials such as poly (L-lactic acid) (PLLA) [75], poly(ε-caprolactone) (PCL) [76,77], poly(ethylene glycol) (PEG) [78], poly lactic glycolic acid (PLGA) [79], chitosan [80,81], chitin [82], cellulose [83–86], poly (vinyl alcohol) (PVA) [87] wherein, these materials serve as a drug carrier owing to their excellent biocompatibility and biodegradability. Drugs such as captopril (to promote vasodilation) [88], tetracycline hydrochloride (for anti-biotic) [89], curcumin (for anti-infective, anti-oxidant, anti-inflammatory activity and anti-microbial) [90,91], titanium dioxide [92], activated carbon nanoparticles [93] etc. are being incorporated into the fibrous matrix for enhancing wound healing process [94].

The current review paper consolidates the advanced research works on wound healing and wound dressing using nanofibers and their respective drug delivery mechanisms, which are not available in solitary literature. In the present review, we have discussed the comprehensive wound healing process and the therapeutic approach for reducing the healing time by utilizing nanofibers scaffold such as uni-axial, coaxial, tri-axial and smart nanofibers scaffold. Simultaneously, the advanced micro/-nano fiber electrospinning techniques, as well as mathematical models for drug release and their respective mechanisms have also been extensively discussed. In addition, we have discussed the advantages of nanofiber-based wound dressing over the conventional wound dressing. Finally, we conclude the review by comparing commercial products and their feasibility for fiber-based dressing over the conventional dressing.

2. Fundamental aspects

For understanding the depth and severity of the wound, it is important to understand the structure of the skin since it is more complex than just three layers, i.e., epidermis, dermis and hypodermis. Wound such as superficial wound [95], deep dermal wound [35] and full thickness wound [96] have different depth of damage upto epidermis, dermis and hypodermis layer respectively, in the skin and accordingly, healing time increases as the depth of damage is more. Thus, in the

Table 1
Nano/micro-fiber fabrication methodology.

Method	Advantages	Disadvantages	Control fiber diameter	Ref. no.
Melt blowing	High productivity, Long and continuous fibers, free from solvent recovery issues	Thermal degradation of polymers, polymer limitations	Yes	[71]
Rotary jet spinning	Eco-friendly, Free from very high voltage	Requirement of high temperatures	No	[71]
Hand spinning	Highly concentrated and well-aligned nanofillers, independent on electric properties of polymer and solvent, high-quality nanofibers with higher efficiency	Low throughput	No	[72]
Pressurized Gyration	High productivity, Homogeneous fibers, better control on final product morphology, electric field is not required	Sometimes heating to very high temperature is necessary	Yes	[67,73]
Electrospinning	High surface to volume ratio, Continuous nonwoven long fibers, high aspect ratio, cost-effective, core and sheath fiber composite, possibility of developing random and orientedfibers	Jet instability, no control over three-dimensional pore diameter, too many variables to control	Yes	[74]

following section, we have discussed the anatomy of skin and wound.

2.1. Anatomy of skin

The skin is the largest organ of the human body which comprises three layers: epidermis, dermis and hypodermis as depicted in Fig. 2. The epidermis is further divided into 5 sub-layers, i.e. stratum corneum, stratum lucidum, stratum granlosum, stratum spinosum and stratum germinativum. The epidermis is made up of keratinocytes, melanocytes, langerhans and merkel cells that help to maintain the body temperature [97]. The dermis can be further divided into two types based on the distance from the epidermis called papillary region and reticular region. The dermis contains the hair follicles, sweat glands, sebaceous glands, apocrine glands, lymphatic and blood vessels. It consists of connective tissue and also provides the cushioning effect to the body from external stress and strain [98,99]. The hypodermis is not a segment of skin but a subcutaneous tissue which lies below the dermis that consists of fibroblast, macrophages and adipocytes cells. It assists in coupling of dermis with bone and muscles. The bacterial count varies with different regions of the skin i.e., on the upper layer of skin, bacteria such as Staphylococci species [100–102] are commonly found which are not harmful at lower bacterial count, however gram-negative bacteria are harmful and causes wound infection in case of ruptured skin [103,104].

2.2. Wound

The wound can be elucidated as an interruption of normal anatomic structure and function which can occur due to thermal, physical, mechanical and electrical damage to the skin. The external damage results in superficial wound on above sub-dermis or it might be deep-lying wound which can damage dermis, epidermis and hypodermis and sometimes sweat glands, hair follicles and blood vessels [105–107].

2.3. Classification of wound

The wound is classified according to various factors as shown in Fig. 3.

The wound is classified according to healing time, acute wound is the one that heals without external support and in minimum time [108–110], whereas the chronic wound is the delayed acute wound which takes longer time to heal due to diabetic ulcer. Acute wound is healed through orderly manner but chronic wound does not follow the order of the wound healing stages [111–113].

Further, the wound is classified according to depth of wound, superficial wound which involve only epidermal layer of skin undergoes scar-less healing within 10 days [95,114]. The deep dermal wound also known as partial thickness wound, heals within 10–21 days via scar formation and re-epithelialization [35,115]. Full-thickness wound happens due to damage of dermis as well as hypodermis and requires more healing time (> 21 days) [96,116].

The wound is also categorized on the basis of complexity of wound, simple wound deals with the skin tissue or dermal layer [117], complex wound deals with significant tissue loss [118,119] and complicated wound deals with an infected complex wound or infected complex wound with diseases like haematoma, ischaemia etc. [120,121].

Further, the wound is categorized according to cause of wound, traumatic is the cause of wound when the patient employs the deep anxiety, it can be experienced when civilian and military surgeons suggest for saline treatment of wound to disinfect from bacteria [122], Iatrogenic is a wound infection caused due to medical examination or surgery [123,124] and burn is caused due to thermal shock on the skin and the portion of burnt wound is susceptible to bacterial attack owing to the damage of macrophages and neutrophils [125–130].

Based on contamination or postoperative infection, they are also classified as clean wound (Class I) which is infection-free, however bacteria which are already present on skin contaminate the wound.

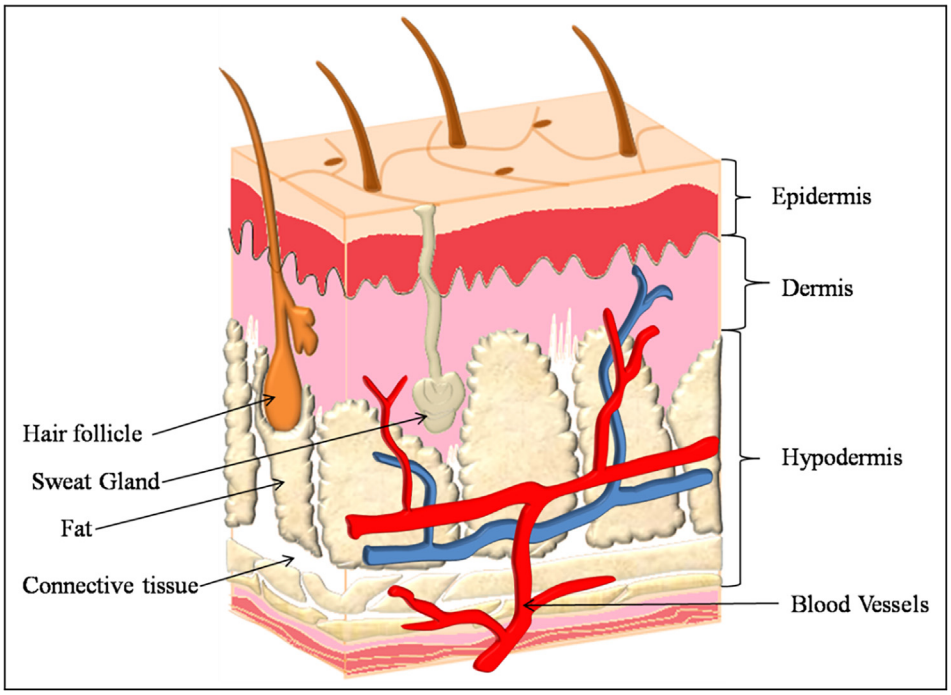

Fig. 2. Structure of human skin.

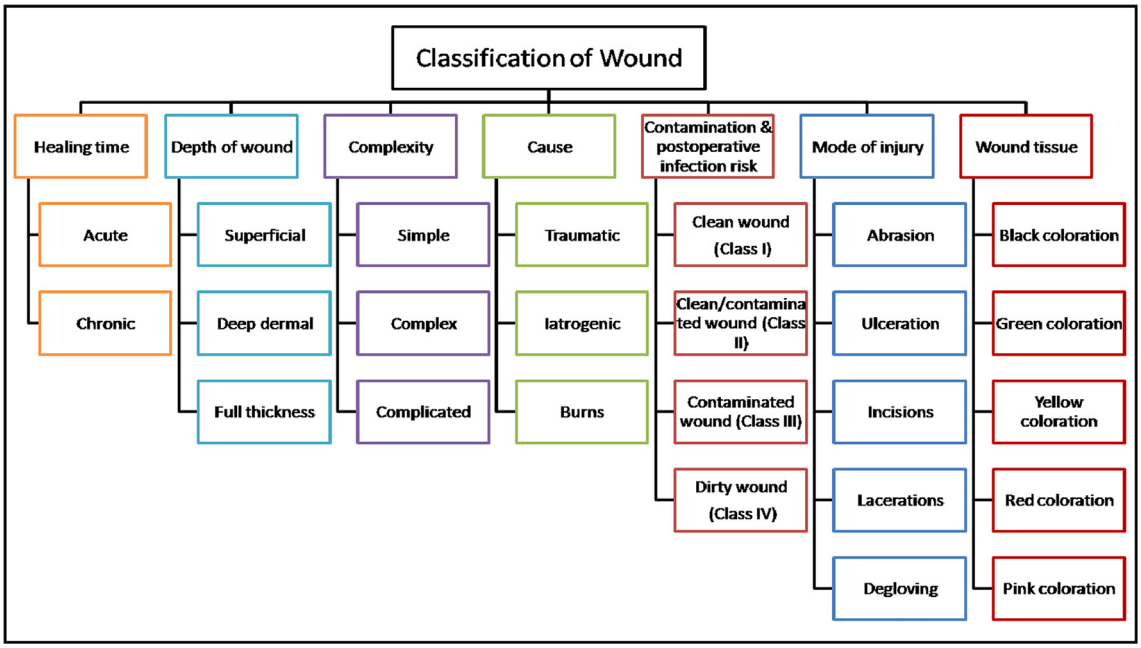

Fig. 3. Classification of wound.

Clean/contaminated wound (Class II) includes wound on alimentary and respiratory system without loss of tissue fluid, and contaminated wound (Class III) includes non-purulent inflammation whereas dirty wound (class IV) includes purulent inflammation [130–132].

The wound can be classified according to mode of injury, abrasion wound healing includes the subcutaneous layer such as epidermis and blood oozing shows that abrasion has reached that extent [133–136]. Ulceration wound healing includes the wound which takes more than 6 month for healing due to different types of ulcers such as Pressure ulcers, venous leg ulcers, diabetic neuropathic foot ulcers etc. [137,138], Incision is wound that occurs due to surgical cut inside the skin with sharp object but this type undergoes faster wound closure ideally within 6 h [139–143]. Laceration is wound arising due to contact of skin with blunt object or sometimes due to heavy swimming because the wound is infected by Aeromonas hydrophila bacteria, which is most commonly found in fresh water [144–147]. Degloving is occurs due to skin sheared away from underlying fascia, in this case the wound healing is challenging because of edema and bleeding of underlying tissue [148,149].

The wound can be classified according to colour of the harmful and contaminated tissue, this contains necrotic tissue, infected tissue, sloughy tissue, granulating tissue and epithelial tissue exhibits black, green, yellow, red and pink coloration respectively [2,150,151].

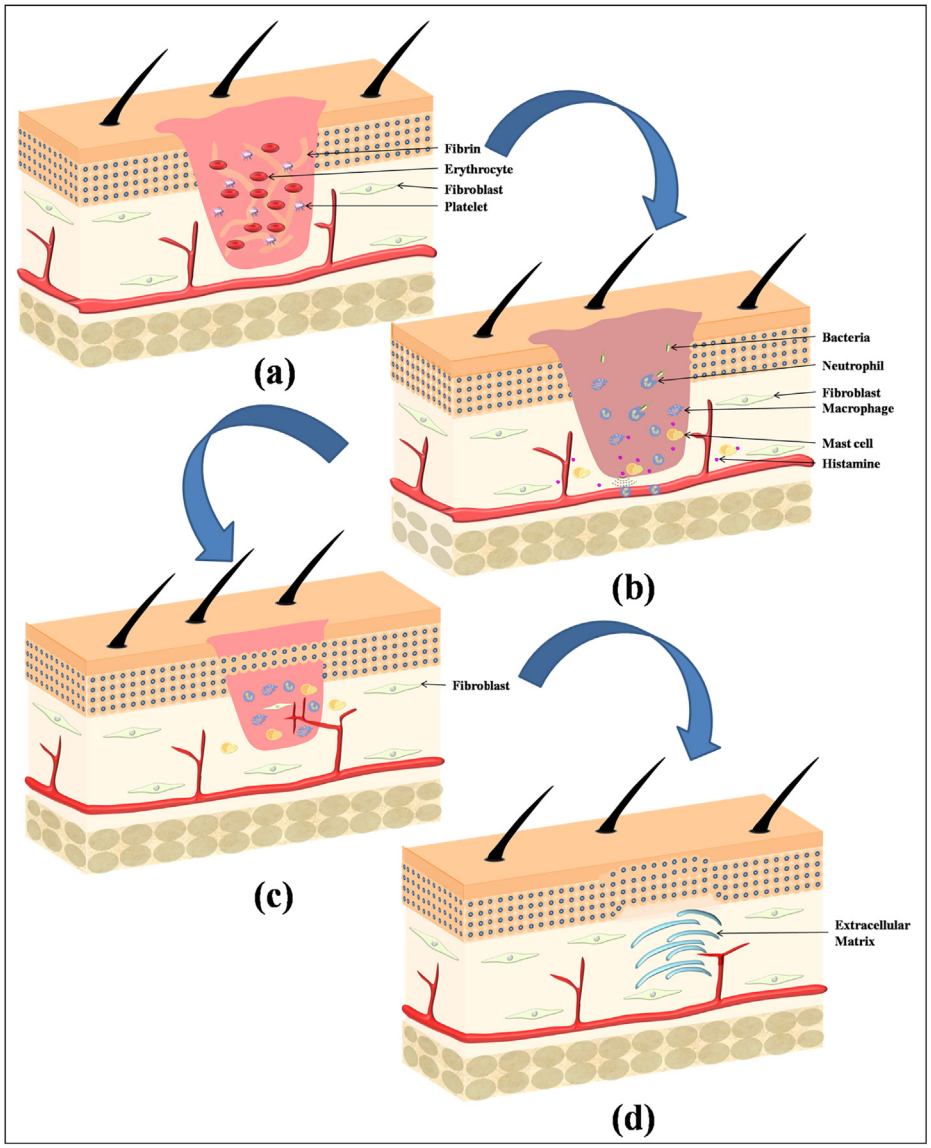

Fig. 4. Wound healing stages (a) Hemostasis stage (b) Inflammation stage (c) Proliferation stage (d) Remodeling stage.

3. Wound healing stages

There are four wound healing stages hemostasis, inflammation, proliferation and remodelling as illustrated in Fig. 4.

3.1. Hemostasis stage

Hemostasis is an instantaneous response towards injury to stop the blood loss and it also allows to execute the functions of other organs without interrupting in spite of injury via configuration of momentary scaffold plug (as illustrated in Fig. 4(a)). The pernicious effect causes micro vascular lesion, vasoconstriction occurs due to neuronal reflex mechanism which is beneficial for preventing blood loss from arteriole. The first response to skin injury (Extrinsic structure) occurs by accumulation of thrombocyte and inflammatory cells binding with the structural protein such as collagen (Intrinsic structure) in the extracellular matrix [152]. The thrombocyte is able to secrete the number of protein such as thrombospondin, von Willebrand factor (vWF), sphingosine-1-phosphate, and fibronectin to enhance invigoration of thrombocytes and growth factors such as insulin growth factor (IGF), platelet-derived growth factor (PDGF), interleukin 1 (IL-1), transforming growth factors (TGF-α, TGF-β) to assist in the post-hemostasis stages of the wound healing. The release of clotting factors stimulates the fibrin matrix deposition to insure the stability of momentary scaffold plug [153].

The momentary scaffold plug has developed the environment suitable for posting of fibroblasts, leukocytes, keratinocytes and endothelial cells in further stages and act as a bank of growth factor. Thrombocyte influences the migration of leukocytes from blood vessels to towards injury via releasing chemical signals. Zhang et al. investigated the drug release study of captopril-loaded poly(lactic-*co*-glycolic acid) (PLGA) biodegradable nanofibers, in which captopril drug is well known to promote vasodilation [88].

3.2. Inflammation stage

Inflammation assists in attraction of leukocyte to the injury via activating various mediators and chemotactic factors in 24–48 h of post-injury, 3 days required to complete the Inflammation phase. The characteristics sign of the inflammation can be observed because the mast cells release the fragments filled with enzymes such as histamine which is also act as a mediator and this mediator also has special importance because it dilates the blood vessels. The vasodilatation allows the efficient migration of neutrophils towards wound injury site (as

illustrated in Fig. 4(b)). The swelling of the wound causes due to accumulation of the body fluid is another sign of inflammation. The prime task of the neutrophils is to eliminate the foreign body, pathogens, dead cells and damaged matrix component via phagocytosis process [153] and it also acts as a chemical pairing with other cells in the phase, further the cleansing start by releasing proteinases and antimicrobial substances [154]. The thrombocyte releases the chemical signals which are responsible for attraction of neutrophils to approach the wound site and adhere to the endothelial cells further induct the neutrophils via cell adhesion molecule for binding with endothelial cell. After 48 h of injury cytokines, growth factors, and chemokines migration stimulate monocytes and lymphocytes and distinguish into macrophages that phagocytes survived pathogens, necrotic tissues and debris, this event starts the granulation tissue formation. Macrophages and neutrophils have similar task but macrophage is able to serve better than neutrophils for proteolytic degradation. In inflammation phase macrophages (like TNF-α, tumor necrosis factor-α, TGF-β, PDGF) and cytokines (like IL-6, IL-1) produces growth factor which helps later in post-inflammation stage for proliferation of fibroblast and endothelial cells. At last the macrophages phagocytes the neutrophils and the depletion of inflammatory cells shows initiation of proliferation stage [153]. Merrell et al. found that curcumin loaded PCL nanofiber has potential application in wound dressing as curcumin has a strong anti-oxidant, anti-infective and anti-inflammatory properties [155].

3.3. Proliferation stage

The proliferation phase assist to convert the momentary scaffold plug to permanent tissue plug via sub-stages such as angiogenesis, granulation tissue formation, Re-epithelialization and wound contraction (as illustrated in Fig. 4(c)). The inflammatory cells releases the TGF-β and PDGF which attracts the fibroblasts, the proliferation stage started with migration of fibroblast and myofibroblasts. After 7 days, accumulation of massive extracellular matrix further support migration of the cells. Collagens are the essential structural protein for all the wound healing stages but it plays dominant job especially in proliferation and remodelling stages [156]. The restoration of new arteriole on wound site by endothelial cells is called Angiogenesis [157]. The angiogenesis begins with binding of endothelial cells of existing vessels and growth factors with the help of their receptors. The proliferation of endothelial cells only possible, when the basal lamina dissolved by the proteolytic enzymes of activated endothelial cells, this process is known as sprouting and these recently built sprouts form interconnected channels. Smooth muscle cells and pericytes assist in stabilization of vessels walls and once the blood flow starts the angiogenesis get completed [158].

The angiogenesis is important for the formation of granulation tissue owing to the recently formed arteriole supplies the nutrients and oxygen to the wound site, granulation tissue formation permits the re-epithelialization to begin. Inflammatory cytokines stimulate the re-epithelialization process as fibroblast produces the growth factors such as hepatocyte growth factor, keratinocyte growth factor and epidermal growth factor which attracts the keratinocytes to migrate towards the wound site and proliferate on the wound by forming the cover over the wound bed [159]. The combination of fibroblast and smooth muscle cell called myofibroblasts which has ability to close the wound by pulling the wound edge, this wound closing process is called wound contraction [160]. Xie et al., fabricated the growth factors (vascular endothelial growth factor) incorporated chitosan nanofibers to enhance the wound healing process as vascular endothelial growth factor is a key mediator for the angiogenesis and granulation tissue formation [161].

3.4. Remodelling stage

The remodelling is a final stage of wound healing (as illustrated in Fig. 4(d)) that starts from 2-week post-injury and can be last over 1 year. All the processes initiated in the inflammation and proliferation stages are going to terminate in the remodelling stage [162]. The sweat glands and hair follicles does not have capability to heal after serious wound damage [163]. Macrophages, endothelial cells and myofibroblasts exit the wound site or remaining undergoes apoptosis. The metabolic activity of wound healing is decline as the small arteriole aggregates into larger blood vessels. The ECM also acquire change such as reticular collagen (type III) produced in proliferation stage is replaced by fibrillar collagen (type I), the reorientation of replaced collagen is stimulated by the lysyl enzyme and matrix metalloproteinases which are secreted via the fibroblasts to increase the tensile strength of the newly formed tissue although tensile strength is not more than 80% of the unwounded tissue. Finally, the wound is repaired via apoptosis and migration of the cells from wound site and extracellular matrix degradation by matrix metalloproteinases [164,165]. The scar formation on the epidermis results owing to deficiency in anchoring of subcutaneous tissue called rete pegs and are liable for tight connection between epidermis and dermis [163]. The scar formation can be avoided by keeping the proper balance between synthesis and degradation.

3.5. Critical factors influence on wound healing

The various factors affect prolonged wound healing in aged patient was correlated with delayed leukocyte migration into the wound site and decrease in phagocytic capacity of macrophage [166–168]. Studies have revealed that stress causes considerable delay in wound healing owing to stress regulate the glucocorticoids and decreases the growth factors level of macrophages and cytokines such as TNF-α, IL-6 respectively, and stress also reduced the chemoattractants of IL-1α and IL-8 which are essential for inflammatory phase [169–172]. Obese patient experiences the highest chances of surgical wound infection, as well as the friction between skin, causes the ulceration. The primary caloric storage depends on adipose tissue, as adipose tissue secretes the adipokines which are affecting on the inflammatory response of the body [173–176]. The tobacco smoke content thousands of substances out of them nicotine, hydrogen cyanide and carbon monoxide are main interest regarding wound healing effect [177–180], nicotine causes vasocontraction leads to tissue blood flow reduction, hydrogen cyanide decreases the oxygen consumption of the tissue and carbon monoxide originate tissue hypoxia [181].

3.6. Significance of wound dressing

The wound dressing plays a vital role in wound healing process owing to wound dressing protects the wound from further exogenous microorganisms and pain. The wound dressing should be carefully chosen in such way that to avoid secondary trauma and damage when wound dressing changes is required [182]. The wound dressing is also used to absorb the exudates in case of burn and chronic wound as well as wound bed environment is also important, studies shows that the moist wound heals more efficiently than dry wound [183,184]. The wound dressing should be oxygen breathable as oxygen is needed for every wound healing stages. Currently, a large number of wound dressings are available but out of them the selecting the appropriate dressing is essential to promote the proliferation of fibroblast and allows re-epithelialisation [184]. The important function of dressing is to stop the bleeding in case of full-thickness wound and provide structural support to skin in case of wound cause by degloving.

3.7. Classification of wound dressing

The wound dressings are classified into 4 types: Passive dressing, Interactive dressing, advanced dressing and smart dressing on the basis of the affinity of dressing towards the wound (as shown in Fig. 5).

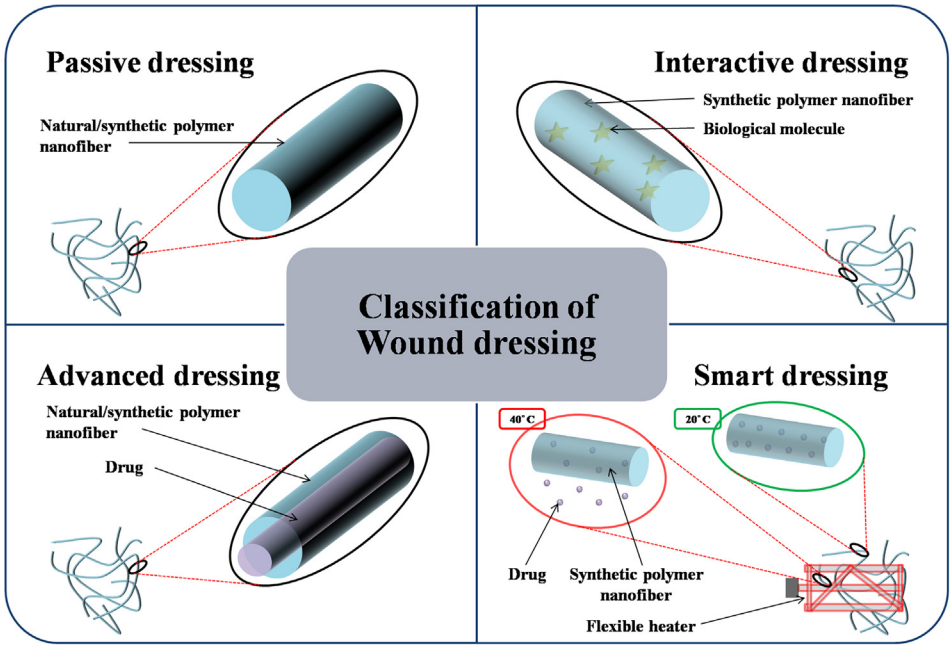

Fig. 5. Classification of fiber based wound dressing.

3.7.1. Passive dressing

The network of fiber establishes an environment which is suitable for wound healing by providing oxy-permeability due to their porous structure are called passive dressing. The passive dressing can be fabricated using natural as well as synthetic polymers and are most popular for the wounds which require suitable environment and protection from mechanical damage. Uppal et al. electrospun the hyaluronic acid to study the effect of electrospinning parameters such as applied voltage, spin length and flow rate on diameter of hyaluronic acid and also found that the air permeability of hyaluronic acid was greater than gauze with Vaseline [185].

3.7.2. Interactive dressing

The dressings which provide not only suitable environment but also assist in control of bacterial growth are called interactive dressing. Interactive dressing is the combination of non-biological polymer (synthetic polymer) and biological molecule owing to ease of processing, anti-bacterial property and wound site affinity respectively. The possibility of immunogenic reactions and impurities restricts the scope of the dressing. Liu et al. investigated the polylactide-polyglycolide (PLGA)/collagen nanofiber having 250 nm diameter and found that the PLGA/collagen nanofibers have an excellent affinity towards human fibroblast which is beneficial for accelerating wound healing in initial stage [79].

3.7.3. Advanced dressing

Drug-loaded nanofiber is part of advance interactive dressing which is capable of treating bacterial infection. There are three types of nanofibers in which drug can be incorporated: Drug-loaded uni-axial electrospun nanofibers, Drug-loaded biaxial electrospun nanofibers, Drug-loaded tri-axial electrospun nanofibers. In recent years, Drug loaded nanofibers were most commonly fabricated by the coaxial electrospinning technique consists of core/shell structure. Core contains drug whereas shell contains polymer matrix (as illustrated in Fig. 6). The dug release profile of core/shell nanofibers depends on shell thickness, wettability of polymer and drug, linear or crosslinked matrix, biodegradability, porosity etc. He et al. fabricated PLLA/tetracycline hydrochloride (TCH) nanofiber via coaxial electrospinning, in which PLLA (shell) act as a drug release carrier and tetracycline hydrochloride (core) act as antibiotic drug and found sustain drug release till 30 days [89]. Soltanova et al. investigated coaxial nanofiber consisting of hydrophilic drug ampicillin as a core and PCL as a sheath. They compared the blend nanofibers with coaxial nanofiber and found that blend nanofiber has 85% drug release in 4 h whereas coaxial nanofiber has 7% drug release in 4 h, thus the drug release profile of coaxial nanofibers were adjacent to zero-order kinetics [76].

3.7.4. Smart dressing

This dressing has the capability to perform multiple functions and also has ability to treat with real-time monitoring with the help of sensors incorporated in the smart dressing. These sensors were helpful to indicate the wound healing status. Schueren et al. PCL/chitosan nanofiber functionalized with Nitrazine yellow has potential application in wound healing [186]. Tamayol et al. developed the thermo-responsive nanofiber mesh to perform on-demand drug delivery and the drug was stimulated by biodegradable metallic heaters stacked on the nanofibers mesh [187].

4. Electrospinning

In the recent years, nanofibers have been extensively explored in the biomedical applications such as tissue engineering, drug delivery and wound dressing owing to its high aspect ratio, huge surface area, tailorability and persistent diameter [188]. Nanofibers are most widely fabricated via electrospinning due to its simplicity, reproducibility and cost-efficacious [189–191]. A high electric field was applied to the polymeric solution and collector plate, in which polymer solution itself act as an electrode having positive charge and on the other hand metallic collector has negative charge, this huge potential difference between electrode exerts electrostatic forces results in the nano/micro fiber formation [74,192–195]. The electrospinning technique contains three basic parts: high voltage source (to charge the electrodes), syringe with metallic needle (to convey the polymer solution), metallic collector or counter electrode (to deposit spun nanofiber) (as depicted in Fig. 7(a)) [192,196,197]. The properties of the final electrospun fibers relies on Solution properties such as viscoelasticity, surface tension, conductivity, dielectric characteristics and solvent volatility, Processing variables such as applied voltage (kV), needle tip to collector distance (cm), flow rate (μL/min), Environmental variables such as room temperature (°C) and humidity (%) [198–200]. The nanofiber deposited on

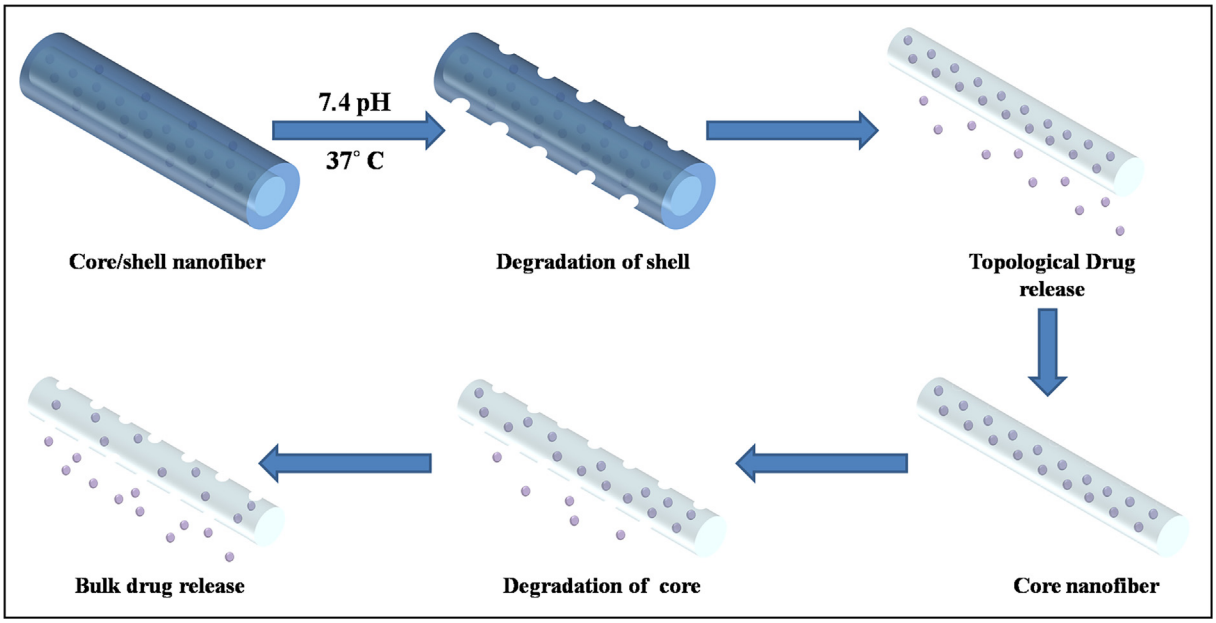

Fig. 6. Advanced dressing drug delivery.

metallic collector via evaporating the solvent mimic the ECM in the context of size and geometry [193,201]. The detailed parameters for electrospinning for different biopolymers are shown in Table 2.

Electrospinning has the capability to produce a broad diameter range of fibers from micrometers (10–100 μm) to sub-micrometer or nanometers (10–100 nm) [206–208]. Chew et al. and Wang et al. reported the effect of aligned electrospun scaffolds facilitate the guidance to cultured cells, resulting in elongation and orientation of cells along the major axis of the nanofibers [209–211], even though the dedicated fillers/drug can be damage in case of uniaxial electrospinning. Thus further uni-axial electrospinning was modified to coaxial electrospinning which is also called core-sheath electrospinning technique (as shown in Fig. 7(b)). The charge mainly contains the sheath polymer solution and thus cone shape of the sheath at the tip of the needle causes the core layer to deform, thus this was a popular technique owing to sheath layer maintaining the structural integrity of the core drug/fillers [212]. This technique was also utilized to fabricate hollow nanofibers via two ways: (1) Spinning the sheath polymer solution in the absence of core solution and (2) Selecting the core polymer solution in such way that post-spun core can be dissolved in solvent and sheath layer should be insoluble in that solvent that results in hollow fiber formation [213–216]. Srivastava et al. fabricated the heavy mineral oil/PVP + TiO_2 core/shell nanofibers having 100 nm average diameter and then heavy mineral oil was removed by dissolving in octane [217]. Core/shell nanofibers cannot provide sustain drug delivery as they have only one breathable barrier layer of the polymer matrix therefore multi-barrier layer nanofiber was preferred for sustain and prolong drug delivery.

Tri-axial electrospinning technique has capacity to produce multi-layer fibers, thus it has provision to add outer solution, middle solution and inner solution (as illustrated in Fig. 7(c)). The sustain, as well as dual drug delivery, can be possible in tri-axial electrospun fibers and it also facilitates the multiple properties in a single fiber [218] but Khalf et al. observed that selection of solvent for sheath layers was critical [219] and production rate of tri-axial electrospinning technique was also limited.

Constrains of production rate was successfully rectified in the modified electrospinning techniques. The production rate of the electrospinning was enhanced with the multi-needle and needleless electrospinning techniques. Needleless electrospinning is also called tip-less electrospinning (as depicted in Fig. 7(d)), Wu et al. acknowledged this technique, as PEO nanofibers were obtained with higher yield 260 times that of single jet electrospinning technique via circular cylindrical electrode [220].

5. Classification of nanofiber-based wound dressing

The nanofibers are classified on the basis of cladding such as uni-axial, coaxial and tri-axial nanofibers (as shown in Fig. 8). Uni-axial nanofibers were fabricated via facile electrospinning technique due to their easy geometry owing to their less processing parameters to control than other modified electrospinning. These fibers were further divided into 5 types: (1) Polymer nanofibers consisting of pristine natural or synthetic polymer, (2) Polymer blend nanofibers consisting of mixture of more than one polymers, (3) Biological molecule embedded polymer nanofibers such as growth factor, cells were embedded in polymer matrix, (4) Drug embedded polymer nanofiber consist of drug in a polymer matrix such as Chitosan, PVA, PCL, PLA and others, and (5) hybrid nanofiber consisting of more than one drug or combination of drug and biological molecule embedded nanofibers.

5.1. Uni-axial nanofibers

5.1.1. Polymer nanofibers

Polymer nanofibers fabricated via facile electrospinning technique, mainly biopolymers, has ease of processing, excellent biocompatibility and non-toxicity, also few polymers such as cellulose acetate possess the anti-bacterial property without addition of anti-bacterial agents. Yoshioka et al. reported bombyx mori silk nanofibers have diameter ranging from 180 to 260 nm and found that methanol treatment increases the mechanical properties compared to pristine nanofiber like yield strength from 33.6 to 96.1 MPa, Young's modulus from 1.4 to 3.2 GPa but the fracture strength decrease from 8.7% to 3.7% [221]. Uppal et al. studied the effect of electrospinning parameters on the diameter of Hyaluronic Acid nanofibers and found that the lower flow rate (0.1 mL/h) and spin length (2.5 cm) assisted for achieve the fine nanofiber (58 nm), they also observe that air permeability of hyaluronic acid (1642.5 $m^3/h/m^2$) was more compare to gauze with Vaseline (334.7 $m^3/h/m^2$) owing to presence of oxygen that speed up the wound healing process [185]. Kim et al. successfully mimicked the human skin pattern with the help of conductive mold to attain the better wound healing environment and the 14 days in-vitro test confirm that the

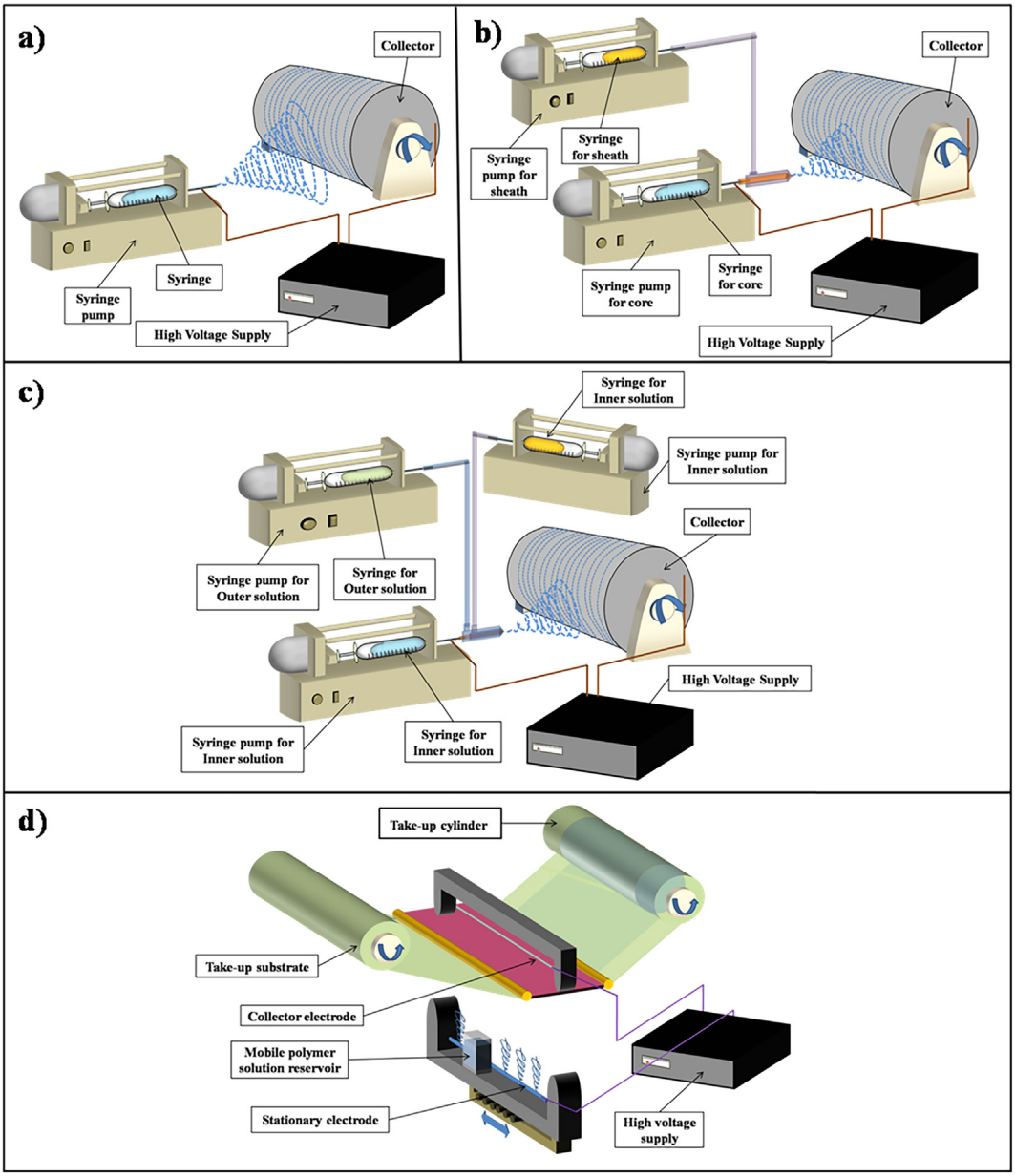

Fig. 7. Electrospinning methodologies (a) Uni-axial electrospinning technique. (b) Coaxial electrospinning technique. (c) Tri-axial electrospinning technique. (d) Needleless Electrospinning.

Table 2
Parameters of Electrospinning of different biopolymers.

Polymer	Solvent	Voltage	Flow rate	Tip collector distance	Fiber diameter	Ref
PCL	Chloroform	21 kV	0.1 mL/h	6 cm	250–3000 nm	[202]
Chitosan	Acetic acid	40 kV	20 μL/min	–	130 nm	[203]
PVA	Deionized water	22 kV	1 mL/h	10 cm	240 nm	[204]
PLLA	Dichloromethane:Acetone (2:1)	15 kV	0.8 mL/h	15 cm	1153 ± 112 nm	[88]
Cellulose Acetate	Acetone	25 kV	3 mL/h	10 cm	1000 nm	[205]

prepared nanofibers mat seeded cells successfully proliferate for 7 days and also heals the wound with a little scar formation [202]. Augustine et al. fabricated poly(ϵ-caprolactone) scaffold to study wound healing and the mechanism of cell proliferation via electrospinning technique. Tensile test shows that 15 wt% PCL (3.84 ± 0.25 MPa) has higher modulus than 5 wt% PCL (2.46 ± 0.26 MPa). Wettability study shows that PCL has 122 ± 5° whereas, 30 days immersed membrane in simulated body fluid has 72 ± 5° water contact angle. PCL showed excellent cell attachment, migration and proliferation of fibroblast cells which aided in guiding cell in the center of wound that results in faster wound healing [222]. Ishii et al. studied the effectiveness of stereocomplexed PLA nanofiber (complex of poly(L-lactide) and poly(D-lactide)) over the poly(L-lactide) (PLLA) and found that post in-vivo, number average molecular weight (M_n) of stereocomplexed PLA was almost same but the PLLA shows decrease in M_n from 3.8×10^5 to 1.8×10^5, the swelling of stereocomplexed PLA was also lower than

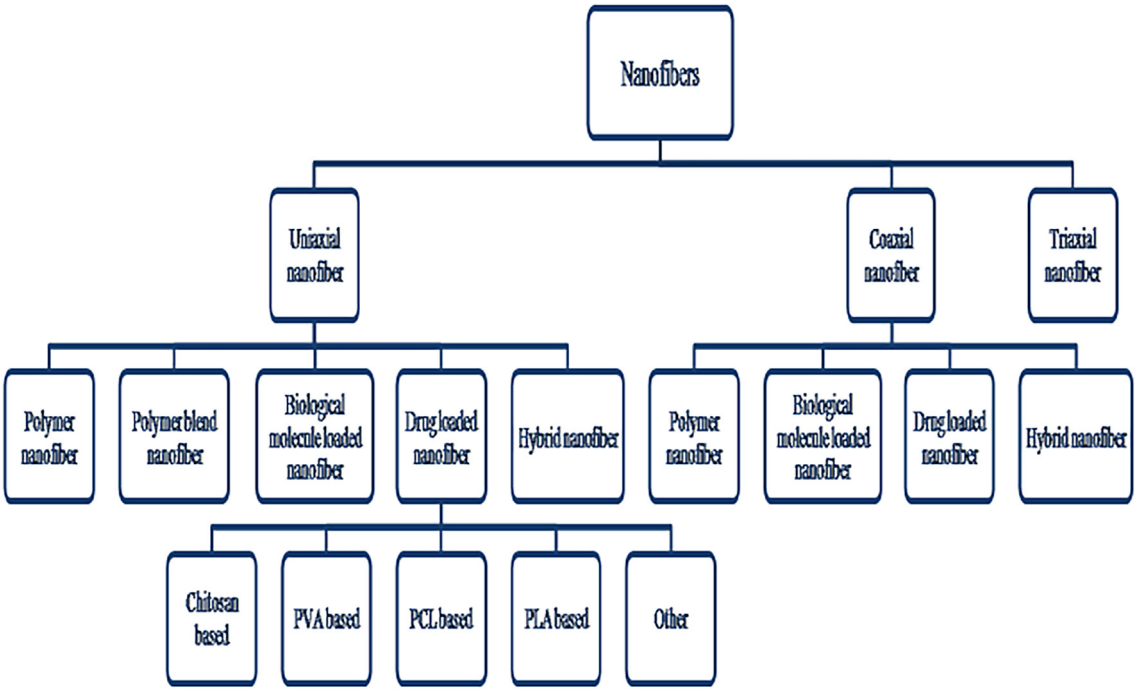

Fig. 8. Classification of nanofibers based wound dressing.

Table 3
Uni-axial polymer nanofibers.

Polymer	Fiber Diameter	Application	Condition	Properties/Results	Ref. no.
Bombyx mori silk fibroin	180–260 nm	Wound healing	–	Yield strength-96.1 MPa Young's modulus-3.2 Gpa	[221]
Hyaluronic acid (HA)	58 nm	Wound dressing	*In vivo*	Air permeability HA Nanofibers-1817 $m^3/h/m^2$ Gauze with Vaseline-322 $m^3/h/m^2$	[185]
PCL	250–3000 nm	Wound healing	*In vitro*	In vitro cell culture Proliferation duration-7 days	[202]
PCL	–	Wound healing	*In vitro*	Modulus 5% PCL membrane-2.46 ± 0.26 MPa 15% PCL membrane-3.84 ± 0.25 MPa	[222]
Poly(L-lactide) + Poly(D-lactide)	300 nm	Wound healing	*In vitro*	Crystallinity Before implantation – 61% 4 week after implantation – 49%	[223]
Cellulose acetate (CA)	1.0 μm	Wound dressing	–	Adsorption coefficient CA nanofibers – 420 against *E. coli*	[205]

PLLA, all this summarizes the swelling of stereocomplexed PLA while in-vitro lethargic degradation than PLLA nanofibers [223]. Since many years cellulose acetate is utilized for filtration, but for transportation of microorganism was first time attempted by Rieger et al., they spun the cellulose acetate nanofiber and compared the performance with commercial product such as Fisherbrand fabric and Sartorius membrane and also calculated the adsorption coefficient (K_{eq}) of microorganism (*E. coli* K12) wherein nanofiber mat (420) had very high values compared to Fisherbrand fabric (9.24) and Sartorius membrane (0.67) [205]. Polymer nanofibers can be useful for lower bacterial resistance to resist higher bacterial count, bacterial resistance capability of polymers enhanced by blending with high bacterial resistance polymers. Characteristics of uni-axial polymer nanofibers are consolidated in Table 3.

5.1.2. Nanofibers of polymer blends

Polymer blend nanofibers allows to design formulation according to need of application by tuning the polymer content as well as selecting the specific polymer to target unique property, thus polymer blend has tailored property; Yeo et al. fabricated the collagen and silk fibroin blend nanofiber, in which crosslinking stabilizes the collagen component by glutaraldehyde vapor whereas the crystallization to the β-sheet structure stabilizes the silk fibroin by water vapor and found that they successfully seeded the fibroblasts and normal human epidermal keratinocytes exerts excellent cellular behaviour and cytocompatibility in case of hybrid nanofibers compared to blend nanofiber [224]. Datta et al. reported that gelatin and oleoyl chitosan (grafted chitosan backbone with C_{18} oleoyl chain) nanofibers mat has superb in vitro cytocompatibility along with human amniotic membrane-derived stem cells in context of improved proliferation and adhesion. The wettability study demonstrated that concentration of oleoyl chitosan increases the contact angle (36–80°) and decreases the swelling of the nanofibers mat compared to gelatin nanofiber (420–380%) [225]. Dongargaonkar et al. also reported the blend nanofiber of gelatin and gelatin-dendrimer conjugates (highly branched polyamidoamine), further the silver acetate was added in the blend and treated with photoreactive PEG diacrylate to form a semi-interpenetrating networks. Constructed nanofibers degrade completely within 24 h, but only 8–13% silver released in 48 h shows resistance against *S. aureus* and *P. aeruginosa* owing to electrostatic interaction of silver with dendrimers conjugates slower the silver release [226]. Anjum et al. investigated the Poly (ε-caprolactone)/gelatin blend nanofibers for enhanced wound healing, In vivo analysis revealed that fabricated scaffold shows improved collagen deposition, axonal density and dermal as well as epidermal thickness. They observed that the poly (ε-caprolactone) coated gelatin (38%) has higher wound closure rate than poly (ε-caprolactone) blended gelatin (30%) [227]. Aydogdu et al. fabricated bacterial cellulose/poly-caprolactone blend nanofibrous scaffolds for wound dressing application via portable electrohydrodynamic gun. The SEM study shows that 384.24–953.13 nm diameter of as-prepared nanofibers as well as proliferation of human Saos-2 cells on as-spun nanofibers scaffold after 72 h confirm the biocompatibility of scaffold [228]. Levengood et al. studied the chitosan/poly(caprolactone) blend nanofibers for skin repair as the chitosan impart intrinsic biocompatibility whereas the poly

(caprolactone) impart the processing stability and mechanical strength. The wound recovery rate of spun nanofibrous mat were compared with commercially available air breathable and water tight wound dressing such as Tegaderm and found that on day 6 the nanofibers mat recovered 45% and tegaderm 5.9% whereas on day 14 both the dressing recovered 99% [229]. Tchemtchoua et al. compared the performance of the chitosan/PEG blend nanofibers with films and freeze-dried sponges for proliferation of fibroblasts, keratinocytes and endothelial cells. According to experimental data, they concluded that the chitosan/PEG blend nanofibers were a potential candidate for wound dressing due to accelerated re-epithelialization, boost in vascularization and productive remodelling of granulation tissue [230]. Pakravan et al. studied the chitosan/polyethylene oxide blend nanofiber in which chain stiffness of chitosan affects the processability and to rectify this, polyethylene oxide (10 wt%) was blended with chitosan where the strong Hydrogen bonding facilitates the facile electrospinning. Higher content of chitosan promotes ultra thin nanofibers spinning (123–63 nm) [231]. Zhang et al. fabricated electrospun chitosan/PVA nanofibers for improved wound healing. The cell adhesion and proliferation confirms the biocompatibility of nanofiber scaffold. The accelerated wound healing was observed due to the higher blood absorption capacity of as-prepared nanofibers which accelerate the homeostasis and tissue regeneration [232]. Zhou et al. investigated chitosan/PVA nanofibers, which was cross-linked with the help of aqueous glutaraldehyde solution and this crosslinked nanofibers were nontoxic to L929 cells as well as exert good in vitro biocompatibility. The equal content of chitosan and PVA are suitable for L929 cells are adhered well on accordingly 48 h of cell culture [233]. Quaternized chitosan was water soluble in all pH scale where the chitosan was only soluble below 6.5 pH, Ignatova et al. reported the blend of poly [(L-lactide)-*co*-(D, L-lactide)] (PLA)/chitosan (Ch) and PLA/Quaternized chitosan (QCh) nanofibers and also verified the antibacterial activity of QCh/PLA mat and QCh/PLA film against the *S. aureus* and *E. coli* cells. The equilibrium swelling degree in water of QCh/PLA and Ch/PLA was 160% and 170% respectively [234]. Ashraf et al. prepared the PVA and polyhydroxybutyrate (PHB) blend (50:50) nanofibers as well as the sole polymer nanofibers, as these miscible polymers exhibit good compatibility. Specific cell proliferation can be promoted via tuning the PVA concentration in the blend e.g. PVA/PHB (50:50) that promotes the human keratinocyte cell line and inhibit the dermal fibroblast cells, whereas PVA/PHB (5:95) promotes fibroblast cell growth and inhibit the human keratinocyte cell line [235]. Aytimur et al. fabricated PVA/PEG and PVA/PPG blend were the novel matrix for wound dressing, According to SEM micrograph PVA/PPG (75:25) and PVA/PEG (75:25) had higher colonization compared to PVA/PPG (50:50) and PVA/PEG (50:50) against *E. coli* cell culture medium. It was also observed that PVA/PPG (50:50) was bead-free and has uniform diameter (1.082 μm) that was suitable for wound dressing application [78]. Park et al. developed the biomimetic poly(glycolic acid) (PGA)/Chitin blend nanofiber scaffold but the difference in the solubility parameter of PGA (34.0 $J^{1/2}/cm^{3/2}$) and Chitin (17.8 $J^{1/2}/cm^{3/2}$) brings the immiscibility and degradation study indicates that entire PGA content was degraded within 45 days, the decline in chitin content (25–75%) causes the depletion of degradation value (30–13 days) whereas bovine serum albumin coated PGA/Chitin (25:75) was a satisfying candidate for cell attachment and proliferation of normal human fibroblast [236]. The blend nanofibers have higher bacterial resistance than pristine nanofibers but an affinity for improved cell adhesion and proliferation was not fulfilling to the required extent. Characteristics of uni-axial polymer blend nanofibers are consolidated in Table 4.

5.1.3. Biological molecule loaded nanofibers

Biological molecule embedded nanofibers exert excellent affinity towards the human body for cell adhesion and proliferation. The processing constrains of biological molecule was rectified by blending with synthetic polymers. Fan et al. prepared novel L-ascorbic acid 2-

Table 4
Uni-axial polymer blend nanofibers.

Materials		Fiber Diameter	Application	Condition	Properties/Results	Ref. no.
Polymer A	Polymer B					
Collagen (COL)	Silk fibroin (SF)	320–360 nm	Wound dressing	*In vitro*	Cell attachment 300 cells/0.53 mm^2	[224]
Gelatin	Oleoyl Chitosan (OC)	150–400 nm	Full-Thickness Excisional Wound Healing	*In vitro*	Water contact angle – 80° Swelling – 380%	[225]
Gelatin	Gelatin-dendrimer Conjugates	3.20 μm	Wound dressing	*In vitro*	Bacterial density Cell culture ~1×10^8 cfu/ml in 4 h	[226]
PCL	Gelatin (GE)	666 ± 164 nm	Wound healing	*In vitro*	Wound closure rate 38% in 21 days	[227]
PCL	Bacterial cellulose (BC)	384.24 nm	Wound dressing	-	Cell viability Control- 100% in 72 h 20%PCL/5%BC nanofibers- 100% in 72 h	[228]
Chitosan	PCL	177.640.5 nm	Acute and chronic wound healing	*In vitro*	Wound recovery 45% in 6 days	[229]
Chitosan	PEG	50–200 nm	Wound healing	*In vivo*	Cells spreading time- 3 days	[230]
Chitosan	Poly(ethylene oxide) (PEO)	60–120 nm	Wound dressing	-	Electric conductivity-3 mS/cm Viscoity-2.25 Pa.s	[231]
Chitosan	PVA	-	Wound healing	*In vitro*	Blood absorption Control- 1500% 2D nanofibers- 2500% 3D nanofibers- 4200%	[232]
Carboxyethyl chitosan (CECS)	PVA	131–456 nm	Wound dressing	*In vitro*	Adhesion study- L929 cells after 48 h	[233]
Poly[(L-lactide)-*co*-(D,L-lactide)] (PLA)	Chitosan (Ch) Quaternized Chitosan (QCh)	840 nm	Wound Dressing	-	Equilibrium swelling degree Ch/PLA nanofibers-170% QCh/PLA nanofibers-160%	[234]
Poly[(L-lactide)-*co*-(D,L-lactide)] (PLA)	Polyhydroxy Butyrate	~615 nm	Wound healing	*In vitro*	Cell culture PVA/PHB (50:50) nanofiber- promote the human keratinocyte cell line PVA/PHB (5:95) nanofiber- promote only fibroblast cell growth	[235]
PVA PVA	PEG PPG	1.082 μm	Wound dressing	-	Bacterial colonization PVA/50% PPG & PVA/50% PEG < PVA/25% PEG and PVA/25% PPG	[78]
Poly(glycolic acid) (PGA)	Chitin	140 nm	Wound dressing	*In vitro*	Degradation rate PGA degrade in 13 days	[236]

phosphate (VC-2-p)-loaded silk fibroin (SF) nanofibers mat, thus ethanol vapor post-treatment nanofibers mat stabilizes the unstable silk I to stable silk II. VC-2-p loaded SF imparts adhesion and proliferation of L929 cells and also observed the burst release of the VC-2-p from VC-2-p-loaded SF nanofibers mat (60–70% in 20 min) was also observed [237]. Selvaraj et al. investigated accelerated wound healing via Fenugreek loaded Silk Fibroin nanofibers as the fenugreek are well known for their anti-oxidant property, therefore, antioxidant activity of the nanofibers studied with 1,1-diphenyl-2-picrylhydrazyl (DPPH), revealed drastic increases in the antioxidant property from pristine silk fibers (5.6%) to Fenugreek loaded Silk Fibroin nanofibers (49.3%) and biocompatibility was also confirmed with the proliferation of fibroblast cell in 72 h of incubation time. silk fibroin–fenugreek (1:1) releases 73 ± 0.9% in 24 h whereas the silk fibroin–fenugreek (1:0.1) release 21.5 ± 0.9% in 24 h. This behaviour of burst release was due to trapped fenugreek in the surface pores and in second case the slow release was due to the lesser concentration of fenugreek as well as the hydrophobic nature of the silk fibroin [238]. Xi et al. reported electrospun poly-caprolactone and poly(citrate)-ε-poly-lysine (PCE) hybrid nanofibers for Multidrug resistance bacteria and to accelerate wound healing. SEM study shows that Fiber diameter of pure PCL nanofibers (212 ± 40 nm) was less compared to 50% PCE/PCL nanofibers (450 ± 100 nm). Wettability study shows that PCL has 130 ± 3° water contact angle which is hydrophobic in nature but the addition of 50% PCE in PCL affect significantly on the wettability and shows hydrophilic nature of hybrid nanofibers [239]. Satish et al., focused on the fabrication of Triiodothyronine loaded PCL for healing of chronic wound as the Triiodothyronine was a hormone acknowledged for tissue repair inspite of the initial burst release of around 70 ng the remaining was the sustained release from day 1 to day 4 (40–50 ng/day). Fluorescence image of FITC confirmed the uniform distribution of the Triiodothyronine hormone [240]. Xie et al. studied the effect of aligned poly(ε-caprolactone) nanofibers on wound closure with the help of peripheral ring electrode and central point electrode. In case of fibronectin-coated radially aligned nanofiber, at the first place the fibronectin was found only at the edges but 4 day post-incubation time they migrate towards the center, it results that fibronectin coated radially aligned nanofibers were a potential candidate for wound closure [241]. Most of the research was conducted on the randomly oriented Nanofibrous scaffold but Sun et al. attempted to mimick the basket-weave pattern of collagen to produce microenvironment with the assistance of PCL/Type I collagen (Col I) nanofibers specifically focused for chronic wound healing, wound closure study shows that crossed, aligned and random Nanofibrous scaffold recover wound 70%, 62% and 56% respectively. Interestingly, crossed Nanofibrous scaffold provides greater cells response of fibroblast in wound healing compared to random or aligned Nanofibrous scaffold [242]. Kang et al. investigated the nucleic acid-stimulated inflammatory response to prevent the exogenous microorganism. The PCL-poly(ethylenimine) (PEI) copolymer and pristine PCL were electrospun and further, to enhance the scavenging ability of nanofibers, they were treated with methanol to achieve highly cationic topology of the nanofibers. Methanol treated nanofibers shows declined wettability compared to non-methanol treated nanofibers [243]. Gao et al. bio mimicked the Extracellular Matrix with bioactive glass nanoparticles incorporated collagen/PCL nanofibrous scaffold. The wound closure study shows that bioactive glass nanoparticles incorporated collagen/PCL accelerated recovery 60% on day 7 and 90% on day 14 compared to collagen/PCL scaffold 50% on day 7 and 80% on day 14. The cell proliferation study also shows that on day 3 endothelial cells proliferation higher number in bioactive glass nanoparticles incorporated collagen/PCL compared to collagen/PCL [244]. Lee et al. investigated the development of growth factor-loaded PLGA–collagen scaffold which facilitates the sustained release of recombinant human platelet-derived growth factor (rhPDGF) for treatment of chronic wound healing. The wettability study illustrates that water contact angle of growth factor incorporated PLGA–collagen scaffold (97.2 ± 0.7°) lesser than PLGA–collagen scaffold (107.6 ± 1.0°) and pristine PLGA scaffold (113 ± 3.3°). The growth factor incorporated (PLGA)–collagen scaffold burst release (102 ± 3 ng ml^{-1} on day 1) the growth factor initially and then sustained release (5 ng ml^{-1}) for 21 days [245]. Liu et al. reported electrospun polylactide-polyglycolide (PLGA)/collagen nanofibers to biomimic the extracellular membranes for wound dressing application. The fiber diameter of PLGA/collagen nanofibers reduced with increment in collagen content and decline in wound area of as-spun nanofiber (5% in 21 days) was lower than commercial dressing (15% in 21 days) and gauze (20% in 21 days) [79]. Cai et al. prepared Chitosan/Silk Fibroin Nanofibers as the chitosan impart biodegradability, biocompatibility as well as antibacterial property. SEM micrograph confirms that an increase in chitosan content reduce the fiber diameter and incorporation of silk fibroin augments the mechanical properties (1.3–10.3 MPa). Cell attachment and proliferation of murine fibroblast on Chitosan/Silk Fibroin Nanofibers were verified via MTT assay in vitro and antibacterial effect of Chitosan/Silk Fibroin Nanofibers enhanced with increase in chitosan content against gram positive (*S. aureus*) and gram negative (*E. coli*) bacteria [80]. Charernsriwilaiwat et al. attempted the electrospinning of lysozyme loaded chitosan (2 wt %)–ethylenediaminetetraacetic acid (CS-EDTA)/PVA (30:70) nanofibers for wound healing. In vitro release study reveals burst release of 80% lysozyme within 30 min. and cumulative 90% drug in 4 h. The as-spun Nanofibrous mat shows higher healing effect than gauze in first 1–5 days and also shows equivalent healing rate to that of commercially available dressing [246]. Ma et al. studied bioactive glass (BG)-introduced multifunctional gelatin/chitosan (G/C) for healing of chronic wound. In wettability study, the water contact angle of BG-loaded G/C was increased due to higher bioactive glass content whereas the water intake capacity was reduced and higher bioactive glass content also enhances the mechanical properties. Bioactive glass (BG) possesses the higher resistance against A. viscosus and *E. coli* compared to commercially available 45S5 Bioglass® mainly due to presence of ZnO and CuO [247]. Dai et al. investigated curcumin incorporated gelatin nanofibers, as curcumin is well known for its anti-microbial activity since the ancient period in Asian countries but it also has limitations such as poor absorption, hydrophobicity and instability. To overcome this, gelatin was blended with curcumin to improve the hydrophobicity for wound healing. They found that the crosslinked curcumin loaded gelatin release the curcumin in sustain manner than without crosslinked blend and the wound closure recovery study shows that decreased wound area of curcumin/gelatin (2%) was lower than pristine gelatin (10%) [248]. Li et al. reported vitamin E TPGS and Vitamin A palmitate stable form of vitamin E and vitamin A respectively successfully incorporated into the gelatin nanofibers, thus nanofibers diameter are reduced as the increment in vitamin content. Release study of vitamin A shows initial burst release (20% in 8 h) and then sustain release (64% in 60 h) whereas the vitamin E shows initial burst release (30% in 10 h) and then sustain release (72% in 60 h). Vitamin E loaded fibers efficiently resist the growth of *S. aureus* and *E. coli* and vitamin loaded gelatin nanofiber facilitates the greater wound healing capacity compared to commercially available disinfectant gauze and cast film [249]. Chhabra et al. attempted doping of zinc oxide in Gelatin/poly-methyl vinyl ether-alt-maleic anhydride (PMVE/MA) matrix to fabricate electrospun nanofiber and stability of these nanofiber scaffolds was ensure via glutaraldehyde vapors crosslinking. The antibacterial study shows that higher *E. coli* bacteria adhere to pristine PMVE/MA Nanofibrous mat compared to nZnO-PMVE/MA Nanofibrous mat, nano zinc oxide inhibits the *E. coli* bacteria from adhering to the scaffold surface [250]. Samadian et al. studied the efficiency of cellulose acetate/gelatin/nanohydroxyapatite (CA/Gel/nHA) composite Nanofibrous scaffold for wound dressing. The higher nanohydroxyapatite content decreases the ultimate tensile strength of the scaffold as well as water vapor transmission rate of CA/Gel scaffold was also decreased with increase in nanohydroxyapatite content. The highest wound closure achieved was

66.26 ± 1.91% in 7 days and 93.56 ± 1.6% in 14 days for Ca/Gel + 25 mg nHA and this composition also promotes collagen production, neovascularization and re-epithelialization [251]. Unnithan et al. prepared polyurethane (PU)/CA-Zein blend electrospun nanofiber as polyurethane promotes cell attachment and proliferation, hydrophilicity and blood thickening ability. The SEM images revealed the cell attachment to pristine PU/CA/Zein and drug-loaded PU/CA/Zein nanofibers scaffold, as well as pristine PU and PU/CA/Zein, have not responded to the bacteria but drug loaded PU/CA/Zein promotes the antibacterial activity [252]. Kandhasamy et al. studied the effect of collagen (COL) coated Ostholamide (OSA) in Polyhydroxybutyrate (PHB)/Gelatin (GEL) matrix on the wound healing. In vitro degradation study reveal that PHB-GEL-COL nanofibers degrade 89.8% in 12 h and PHB-GEL-OSA-COL Nanofibers degrade 71.8% in 12 h, this reduction in degradation confirms that ostholamide has affinity to collagen, therefore, it resists the degradation of PHB-GEL-OSA-COL Nanofibers and existence of ostholamide contribute in antimicrobial activity, Antimicrobial study shows that zone of inhibition of PHB-GEL-OSA-COL Nanofibers against S. aureus and *P. aeruginosa* are 10 ± 2 mm and 14 ± 22 mm respectively [253]. Xi et al. investigated the effect of direction-dependent property of nanomaterial and cytophilic on the wound healing and cell adhesion and found that the polyurethane nanofiber was a potential candidate for cell tuning and guiding towards the nanofiber direction, alignment of nanofiber was also an important characteristic, as the anisotropic random nanofibers (5236 ± 2313) mat has highest capacity for cell proliferation than random nanofibers mat (2252 ± 683) and planar random nanofibers mat (1143 ± 521) [254]. The possibility of immunogenic reaction, as well as the impurities present in the raw material, limits the biological molecule loaded nanofibers from becoming a commercial product. Characteristics of Biological molecule loaded uni-axial polymer nanofibers are consolidated in Table 5.

5.1.4. Drug loaded nanofibers

The therapeutic approach wound healing was a traditional way of healing the wound but nowadays this drugs are blended with polymers (typical polymer structure depicted in Fig. 9) and spun into nanofibers and can have effective drug release than traditional therapy. Although these drugs were used due to their properties like anti-biotic, anti-bacterial, anti-inflammatory and some drug stimulates the healing events such as vasodilation, thus nanofibers possess extreme resistance against bacteria.

5.1.4.1. Drug-loaded chitosan-based nanofibers. Charernsriwilaiwat et al. studied the effect of Garcinia mangostana (GM) extracts with α-mangostin loaded chitosan-ethylenediaminetetraacetic acid/polyvinyl alcohol (CS-EDTA/PVA) electrospun nanofibers on wound healing. Swelling of nanofibers decreases (111.96–96.67%) while increasing α-mangostin content (1–3 wt%) and these swelling characteristic of nanofibers results in the burst release of α-mangostin (80% in 60 min). The α-mangostin GM extract loaded CS-EDTA/PVA nanofiber exhibit bacterial inhibition against *E. coli* and S. aureus [255]. Naseri et al. investigated the chitin nanocrystals (ChNC) reinforced chitosan/PEO nanofibers for wound dressing application. Water vapor transmission study shows that addition of chitin nanocrystal decrease the water vapor transmission rate of ChNC loaded chitosan/PEO (1290 $g\,m^{-2}\,day^{-1}$) compared to pristine chitosan/PEO (1353 $g\,m^{-2}\,day^{-1}$), but this problem can be overcome via crosslinking the nanofibers with genipin solution although crosslinking decline the surface area (59–35 $m^2\,g^{-1}$) [82]. Zupancic et al. reported novel metronidazole loaded chitosan/PEO nanofibers for treatment of local wound infection. Drug release study of 15% metronidazole loaded chitosan/PEO nanofiber shows burst release 60% in 10 min followed by 95% in next 2 h, this may be due to very high swelling of chitosan/PEO nanofibers (1000% in 1 h) [256]. Sadri et al. also electrospun the CS/PEO nanofibers with cefazolin drug to study its microbial property and found that 1% cefazolin loaded CS/PEO exert the anti-microbial activity against the *S. aureus* (ZOI-12 mm) and *E. coli* (ZOI-10 mm) bacteria. Drug release study of 1% cefazolin loaded CS/PEO (90:10) nanofiber indicates that initial burst release and then sustain release of cefazolin drug, this may be due to lower concentration and hydrogen bond exert affinity between chitosan and drug. The swelling study reveals that 1% cefazolin loaded CS/PEO (65% in 24 h) swells higher than pristine CS/PEO (58% in 24 h) [257]. Abdelgawad et al. introduced the environment-friendly rout to wound dressing of Silver nanoparticles embedded Chitosan/polyvinyl alcohol (PVOH) nanofibers were crosslinked by glutaraldhyde. The drug release study of 7 days immersion test shows that the augmented crosslinking time results in decline the Ag^+ ion release. Antibacterial test reveals that PVA/CS/AgNPs fiber exerts sufficient resistance against *E. coli* and also found that number of bacteria colonies reduced by increasing chitosan content (above 20%) in the system [258]. Charernsriwilaiwat et al. prepared the Chitosan (CS)/PVA nanofibers scaffold in which chitosan was loaded with ethylenediaminetetraacetic acid (EDTA), thiamine pyrophosphate (TPP) and hydroxybenzotriazole (HOBt). The cytotoxicity study confirms that as-prepared nanofiber was non-toxic towards normal human fibroblast cells and CS-EDTE/PVA and CS-HOBt/PVA has successfully restrict the gram-positive and gram-negative bacteria. They conclude that out of three formulations, CS-EDTE/PVA was a perfect choice of dressing as it results in excellent biocompatibility and antimicrobial resistance [259]. Mei et al. studied the effect of curcumin incorporated polypropylene carbonate (PPC)/grafted chitosan (g-CS) electrospun nanofibers on the wound healing improvement. In vivo study observed the 98.7 ± 10.3% wound closure ratio in case of 10% curcumin incorporated PPC/g-CS nanofibers scaffold on day 21 of post-injury. Drug release study validates initially on day 1 burst release and later 36.41% curcumin release was observed within 12 days [260]. Sadri et al. investigated the environment-friendly green tea extract added Chitosan/PEO nanofibers mat as a wound dressing. As-prepared nanofiber mat was treated with glutaraldehyde vapour to improve its hydrophilic property. GT added chitosan/PEO nanofiber exhibits antibacterial activity against gram-positive and gram-negative bacteria having inhibition zone 6 mm and 4 mm respectively [261]. Annur et al. reported silver nanoparticles incorporated Chitosan/PEO nanofibers scaffold, as silver nanoparticle was well known for its antibacterial property. SEM images of 1 wt% $AgNO_3$ incorporated chitosan/PEO nanofiber shows that 30% reduction in fiber diameter in 1.5 min of post-plasma treatment. The antibacterial study shows that 2 wt% $AgNO_3$ incorporated chitosan/PEO nanofiber (0.38 mm) exhibit higher zone of inhibition than pristine chitosan/PEO nanofiber (0.01 mm) [262]. Ali et al. introduced the Phenytoin (Ph) loaded chitosan (CS)/PEO nanofibers for accelerated wound healing events. The entrapment efficiency of phenytoin above 94% was observed and drug release study shows that initial burst release of Ph-loaded pluronic nanomicelles (20% in 2 h) whereas sustain release of Ph-loaded lecithin-coated PLGA NPs (33% in 48 h) [263]. Chitosan-based nanofibers have very high swelling rate, therefore, it shows faster drug release rate but grafting and blending can be utilized to tune the drug release rate. Characteristics of Drug-loaded chitosan-based uni-axial nanofibers are consolidated in Table 6.

5.1.4.2. Drug-loaded PVA based nanofibers. Kenawy et al. studied the Ketoprofen embedded PVA microfibers mat for wound dressing application, as Ketoprofen is well known for its anti-inflammatory property. The drug release study shows that burst release was observed in untreated hydrolyzed PVA fibers (85.24% in 2 h) compared to 1 h methanol treated (26.49% in 2 h) or 24 h methanol treated (10.42% in 2 h) fibers and also observed that 1 h methanol treated (33.28% in 2 h) or 24 h methanol treated (20.04% in 2 h) film has rapid drug release than fiber based system [87]. Mohammadi et al. investigated novel Gum tragacanth (GT) and PVA mixture was electrospun scaffold for

Table 5
Biological molecule loaded uni-axial polymer nanofibers.

Materials		Fiber Diameter	Application	Condition	Properties/Results	Ref. no.
Matrix	Biological molecule					
Silk fibroin (SF)	L-ascorbic acid 2-phosphate (VC-2-p)	362 ± 121 nm	Wound dressings	*In vitro*	VC-2-p release 60–70% in 20 min	[237]
Silk Fibroin	Fenugreek	309 ± 83 nm	Wound healing	*In vitro*	Fenugreek release 21.5 ± 0.9% in 24 h	[238]
PCL	Poly(citrate)-ε-poly-lysine (PCE)	212 ± 40 – 450 ± 100 nm	Wound healing	*In vivo and In vitro*	Water contact angle PCL nanofibers- 130 ± 1° PCL-30%PCE nanofibers- 41 ± 1°	[239]
PCL	Triiodothyronine hormone	300 ± 100 nm	Wound healing	*In vitro*	Initial burst release 70 ng in 1 h & cumulative release 340 ng in 4 days	[240]
PCL	Fibronectin	–	Wound healing	*In vivo*	Fibronectin activity Initiation time- 4 days	[241]
PCL	Type I collagen (Col I)	A- 583.3 ± 55 nm R- 556.3 ± 36 nm C- 573.3 ± 91 nm	Wound healing	*In vivo*	Tensile strength/wound recovery Aligned nanofibers (A)- 6.8 ± 0.2 Mpa/62% Random nanofibers (R)- 14.6 ± 1.2 Mpa/56% Crossed nanofibers (C)- 24.0 ± 0.9 Mpa/70%	[242]
PCL-poly(ethylenimine) [PEI]	Nucleic acids	–	Wound dressing	*In vivo*	Water contact angle Before methylation-102.11 ± 5.86° After methylation-13.00 ± 5.89°	[243]
Collagen/PCL	Bioactive glass nanoparticles	300–500 nm	Diabetic wound healing	*In vivo*	Wound recovery 90% in 14 days	[244]
PLGA-Collagen	Recombinant human platelet-derived growth factor (rhPDGF)	206.9 ± 120.1 nm	Diabetic wounds healing	*In vivo and In vitro*	Growth factor release rate 102 ± 3 ng ml^{-1} for 1 day 5 ng ml^{-1} for 21 days	[245]
PLGA	Collagen	250 nm	Wound dressing	–	Decreased wound area 5% in 21 days	[79]
Chitosan	Silk Fibroin	249.7 ± 157.1 nm	Wound dressing	*In vitro*	Tensile strength-4 MPa	[80]
Chitosan-EDTA/PVA	Lysozymeb	143–209 nm	Wound healing	*In vitro*	Lysozymeb release Initial 80% in 30 min & cumulative 90% in 4 h	[246]
Gelatin/Chitosan (G/C)	Bioactive glass (BG)	–	Wound dressing	*In vivo*	Water contact angle-94.6°	[247]
Gelatin	Curcumin	–	Acute wound healing	*In vivo*	Decreased wound area 2% in 15 days	[248]
Gelatin	Vitamin A Vitamin E	538 ± 176 nm 582 ± 131 nm	Wound dressing	*In vivo*	Vitamin A release Initial 20% in 8 h & cumulative 64% in 60 h Vitamin E release Initial 30% in 10 h & cumulative 72% in 60 h	[249]
Gelatin/poly-methyl vinyl ether-alt-maleic anhydride (PMVE/MA)	Nano zinc oxide	500–700 nm	Wound healing	*In vivo*	Wound closure 99.04 ± 0.46% in 10 days	[250]
CA	Gelatin/+Hydroxyapatite	316 ± 115 nm	Wound healing	*In vitro and in vivo*	Wound closure 66% in 7 days & 93% in 14 days	[251]
PU–CA	Zein + drug	400–700 nm	Wound dressing	*In vitro*	Zone of inhibition *E. coli*-12 mm B. subtilis-15 mm S. aureus- 8 mm	[252]
Polyhydroxybutyrate (PHB)/Gelatin (GEL)	Ostholamide + Collagen	80 ± 10 nm	Wound healing	*In vitro and in vivo*	Degradation rate 71.8% in 12 h	[253]
PU	Human umbilical vein endothelial cells (HUVECs)	200–500 nm	Wound healing	–	Cell attachment Anisotropic nanofibers − 5236 ± 2313 cells/cm^2 Random nanofibers- 2252 ± 683 cells/cm^2 Planar nanofibers- 1143 ± 521 cells/cm^2	[254]

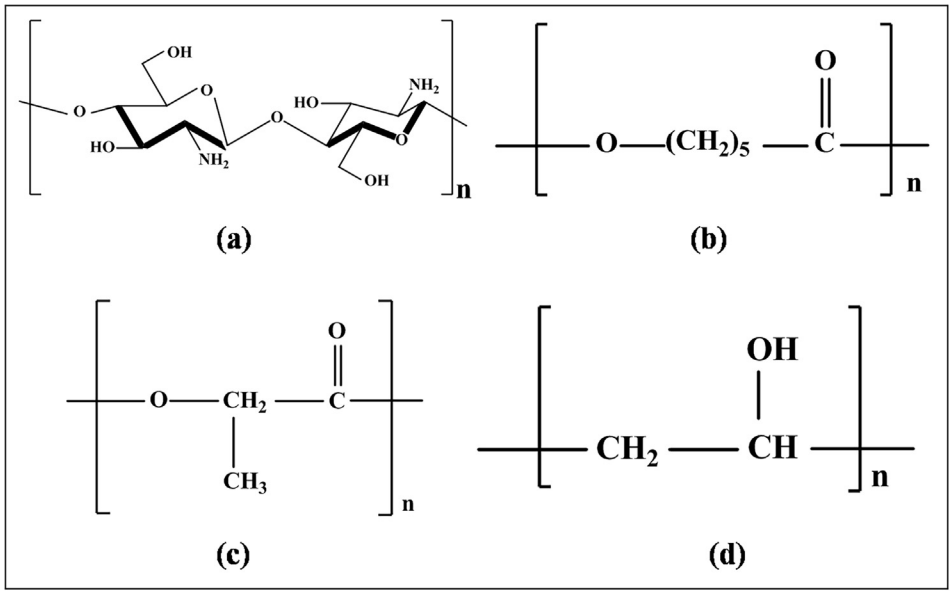

Fig. 9. Typical structure of (a) Chitosan (b) PCL (c) PLA (d) PLA.

wound dressing as the biodegradability, non-toxicity and biocompatibility of gum tragacanth facilitate the fibroblast cell adhesion and proliferation. Increase in viscosity prevented the electric field from stretching the fiber and hence diameter increases (140–210 nm). It was observed that as-prepared GT/PVA nanofibers have capability to resist *P. aeruginosa* and *S. aureus* bacteria [264]. Jiang et al. prepared Silica nanocapsules (SiNCs) containing octyl methoxycinnamate (OMC), peppermint oil (PO), amphiphilic octenidine (OCT) added PVA nanofibrous mat with additional UV protection for wound dressing. TGA analysis shows encapsulation content was 65% while theoretical content was 60%, this was results in enhanced UV absorbance of dispersion of SiNCs-OMC and Antibacterial study suggested that SiNC-PO/OCT has 99% resistance against *E. coli* K-12 and *B. Subtilis* [265]. Augustine et al. fabricated silver nanoparticles embedded PVA nanofibers via electrospinning technique for wound dressing application. Water uptake capacity study shows that swelling of pure PVA nanofibers (800% in 6 h) was higher than PVA/Ag nanoparticles nanofibers (525% in 6 h). Release study shows that 1.9 ppm of Ag was released in 48 h for 1 wt% Ag nanoparticles loaded PVA nanofibers. As the silver nanoparticles possess anti-bacterial effect, PVA/Ag nanofibers (10.47 ± 1.87 mm) showed higher zone of inhibition against *E. coli* compared to pure PVA nanofibers (6.00 ± 0 mm) [266]. Shoba et al. explored Papain (P)/Urea (U) loaded PVA nanofibers scaffold for wound debridement. Antibacterial activity shows that pristine PVA nanofibers have 50% bactericidal activity whereas the addition of Papain and urea stabilize the system for longer time against gram-negative bacteria (*E. coli*). The P-U/PVA and P/PVA nanofibers have initial burst release and then sustain release for 24 h, this behaviour was observed due to high surface area and surface porosity of the hydrophilic matrix [267]. Kataria et al. developed ciprofloxacin antibiotic amalgamated PVA-sodium alginate (NaAlg) nanofibers for transdermal patch. Degree of swelling was higher in case of PVA/NaAlg (190 ± 5.3% in 12 h) compared to ciprofloxacin loaded PVA/NaAlg (170 ± 4.3% in 12 h). In vitro drug release study shows that PVA nanofibers (initial 28.4% in 30 min & 98.6% in 5 h) has higher ciprofloxacin release rate than PVA/NaAlg composite nanofiber (initial 20% in 30 min & 80% in 5 h), both the formulation releases 99% drug in 24 h [268]. Zahedi et al. studied phenytoin sodium (PHT-Na)/PVA, PHT-Na/PCL as well as PHT-Na/PVA/PCL composite nanofibers for active wound dressing. The decreased wound area of 2% PHT-Na loaded PVA nanofibers (40%) have higher decreased wound closure rate compared to gauze dressing (65%) and commercial dressing such as Comfeel®Plus (60%). The drug release rate of PVA/PHT-Na nanofiber (90% in 48 h) was higher than PHT-Na/PVA/PCL composite nanofiber (45% in 48 h) than PCL/PHT-Na nanofiber (15% in 48 h) [269]. Jannesari et al. investigated the effect of novel PVA/poly(vinyl acetate) (PVAc) blend containing Ciprofloxacin HCl (CipHCl) composite nanofiber for controlled drug release. Fiber diameter of the entire formulations was declined by presence of 10 wt% CipHCl whereas degree of swelling decreases by addition of CipHCl. Drug releases study reveal that PVAc nanofibers have slower release profile (35% in 72 h), PVA/PVAc (50:50) composite nanofiber has moderate release profile (80% in 72 h) whereas the PVA nanofiber has rapid release profile (98% in 72 h), this was observed due to hydrophobic nature of PVAc polymer [270]. Lu et al. prepared graphene-based PVA/chitosan for wound healing. The antibacterial study shows that PVA/chitosan containing graphene resist the *E. coli* cells and Agrobacterium as they are prokaryotic but not yeast cell (eukaryotic), this unusual phenomena may be due to interaction between cell and graphene that easily transit electron from graphene to the cell but it was difficult to enter when cells has nuclear membrane such as eukaryotic cell, therefore, this transited electron breakdown the prokaryotic cell in which nuclear membrane was missing, as the most of the microbes has prokaryotic cell hence proliferation of microbes can be controlled with graphene [271]. Ahmed et al. reported electrospun zinc oxide embedded chitosan/PVA nanofibers for diabetic wound healing application. As-prepared nanofibers shows higher zone of inhibition against *E. coli*, *P. aeroginosa*, *B. subtilis* and *S. aureus* compared to pristine chitosan/PVA nanofibers. The wound contraction percentage with chitosan/PVA/ZnO nanofibers (90%) was greater than pristine chitosan/PVA nanofibers (80%) in 12 days [272]. Shalumon et al. explored Sodium alginate/poly(vinyl alcohol)/nano ZnO composite Nanofibrous mat for wound dressing, these nanofibers are stabilized by crosslinking with 2% glutyraldehyde vapor. The anti-bacterial study observed that higher ZnO (0.5–5%) content assist in enhanced inhibition zone diameter of S. aureus (15–16 mm) and *E. coli* bacteria (14–15 mm). Nanofibers containing maximum 1% ZnO successfully adhere and proliferate the L929 cells in 96 h [273]. PVA based drug dressing has slower drug release rate however it should not be less than minimum effective concentration of drug. Characteristics of Drug-loaded PVA based uni-axial nanofibers are consolidated in Table 7.

5.1.4.3. Drug-loaded PCL based nanofibers. Xue et al. developed the Metronidazole (MNA) antibiotic-loaded PCL nanofiber scaffold for

Table 6
Drug-loaded chitosan-based uni-axial nanofibers.

Materials		Fiber Diameter	Application	Condition	Properties/Results	Ref. no.
Matrix	Drug					
Chitosan (CS)	Garcinia mangostana extracts	205.56 nm	Wound healing	*In vivo*	Drug release Cumulative 80% in 60 min	[255]
CS/PEO	Chitin nanocrystals (ChNC)	223–966 nm	Wound dressing	*In vitro*	Water vapor transmission rate- 1434 g m^{-2} day^{-1}	[82]
CS/PEO	Metronidazole	124 ± 20 nm	Chronic wounds	*In vitro*	Drug release 60% in 10 min & cumulative 95% in 2 h Swelling rate-1000% in 1 h	[256]
CS/PEO	Cefazolin	60–100 nm	Wound healing	*In vitro and in vivo*	Drug release- Cumulative 65% in 24 h	[257]
CS/PVA	Silver nanoparticles (AgNPs)	150 nm	Wound dressing	–	Drug release rate 15.8% in 7 days	[258]
Chitosan(CS)-hydroxybenzotriazole (HOBt), CS-ethylenediaminetetraacetic acid, CS-thiamine pyrophosphate (TPP)	PVA	146 ± 33 nm 100 ± 19 nm 94 ± 20 nm	Wound healing	*In vivo*	Decreased wound area 2% in 10 days	[259]
Grafted chitosan	Curcumin loaded polypropylene carbonate (PPC)	390 nm	Wound healing	*In vivo*	Drug release Initial 15% in 12 h & cumulative 40% in 12 days Wound closure 100% in 21 days	[260]
CS/PEO	Green tea extract	100 nm	Wound dressing	–	Drug release 58% in 48 days	[261]
CS/PEO	Silver Nanoparticles	130 nm	Wound healing	–	Zone of inhibition 0.48 mm against *E. coli*	[262]
CS/PEO	Phenytoin (Ph)	115 ± 20 nm	Wound dressing	*In vivo*	Drug release 33% in 48 h	[263]

Table 7
Drug-loaded PVA based uni-axial nanofibers.

Materials		Fiber Diameter	Application	Condition	Properties/Results	Ref. no.
Matrix	Drug					
PVA	Ketoprofen	0.5–1.5 μm	Wound dressing	*In vitro*	Drug release Initial 10.42% in 2 h & cumulative 34.68% in 2 week	[87]
PVA	Gum tragacanth	140–210 nm	Wound dressing	*In vitro*	Anti-bacterial resistance Anti-bacterial activity against *P. aeruginosa*	[264]
PVA	Silica nanocapsules (SiNCs)	200–300 nm	Wound dressing	–	Antibacterial resistance 99% resistance against *E. coli*	[265]
PVA	Silver nanoparticles	403 nm	Wound dressing	*In vitro*	Zone of inhibition against *E. coli* Pure PVA nanofibers- 6.00 mm PVA/Ag nanofibers- 10.47 mm	[266]
Urea loaded PVA	Papain	200–400 nm	Wound debridement	*In vitro*	Drug release Initial 43% in 1 h & cumulative 57% in 12 h	[267]
PVA-sodium alginate (NaAlg)	Ciprofloxacin	300–400 nm	Acute wound healing	*In vivo*	Drug release Initial 20% in 30 min & cumulative 97% in 6.5 h	[268]
PVA/PCL	Phenytoin sodium (PHT-Na)	240 nm	Wound healing	*In vitro and in vivo*	Drug release PVA/PCL (80/20) nanofibers- 45% in 48 h PCL nanofibers- 15% in 48 h PVA nanofibers- 90% in 48 h	[269]
PVA/PVAc	Ciprofloxacin HCl	405 nm	Wound dressing	*In vitro*	Drug release PVA nanofiber-100% in 80 h PVA:PVAc (50:50) nanofiber-85% in 250 h PVAc nanofiber- 35% in 250 h	[270]
PVA/chitosan	Graphene	120 nm	Wound healing	–	Antibacterial resistance Breakdown activity-Prokaryotic cell (against *E. coli* and Agrobacterium)	[271]
Chitosan/PVA	ZnO nanoparticles	279.34 ± 7.23 nm	Diabetic wound healing	*In vivo*	Wound contraction % Chitosan/PVA/ZnO nanofibers- 90% in 12 days Pristine chitosan/PVA nanofibers- 80% in 12 days	[272]
Sodium alginate (SA)/PVA	ZnO nanoparticles	190–240 nm	Wound dressing	–	Zone of inhibition S. aureus-16 mm *E. coli*- 15 mm	[273]

guided tissue regeneration. Drug encapsulation efficiency (above 80%) confirms the good dispersion of MNA drug in the vicinity of the PCL matrix. The drug release study states that cumulatively 90% MNA was released in 1 week with initial burst release and zone of inhibition increases with augmented MNA content [274]. Hinojos-Márquez *et al.* studied the antimicrobial silver nanoparticles (AgNPs) embedded PCL nanofibers mat for strong resistance against gram-positive and gram-negative bacteria. Increased Ag concentration (1–100 mM) helps for achieving fine nanofibers (234 ± 66 nm to 159 ± 79 nm) and on the contrary, lower AgNPs concentration of PCL nanofibers exhibit sufficient resistance to bacteria such as *S. aureus*, *E. coli*, *P. aeruginosa*, *S. pyogenes* and *K. pneumonia* [275]. Pal et al. investigated the Carbon nanodots (CND) incorporated PCL fluorescent nanofiber for monitoring of in vivo testing to enhanced full thickness wound dressing. As-prepared nanofiber was stabilized via N-hydroxysuccinimide (NHS)/1-ethyl-3-(3-dimethylaminopropyl) carbodiimide (EDC) solution. The CND incorporated PCL (82.75 ± 1.5%) exerted wound recovery which was higher than pristine PCL (51.75 ± 3.2%) and an open wound (13.8 ± 5.1%) and controlled CNDs release was also observed [276]. Augustine et al. prepared europium hydroxide nanorods (EHNs) added PCL electrospun scaffold. The mechanical properties such as elongation at break of 0.25% EHN loaded PCL (235 ± 16 MPa) was higher than pristine PCL nanofibers (316 ± 14 MPa). Cell culture test clearly indicates that proliferation of human umbilical vein endothelial cells (HUVECs) in 0.5 wt% EHNs added PCL from 158 ± 16 cells/mm^2 (within 24 h) to 284 ± 17 cells/mm^2 (within 120 h) [277]. Augustine et al. reported Electrospun ZnO nanoparticles loaded PCL membrane for accelerated fibroblast proliferation and wound healing. Cell density study shows that cell density in pure PCL membrane was increased from 20 ± 6 cells per mm^2 (after 5 days of implantation) to 212 ± 12 cells per mm^2 (after 20 days of implantation) whereas, cell density with 1% ZnO loaded PCL membrane increased from 38 ± 8 cells per mm^2 (after 5 days of implantation) to 316 ± 6 cells per mm^2 (after 20 days of implantation). Percentage of wound healing with ZnO loaded PCL membrane (100%) was greater than pure PCL membrane (85%) after 25 days of implantation [278]. Preem et al. studied the interaction between antibiotic chloramphenicol (CAM), polymeric matrix and exogenous bacteria for dressing of the infectious wound. The average fiber diameter of PCL/PEO fibers was higher than PCL/PEO/CAM fibers, this was observed may be due to interaction between drug and polymer increases the viscosity followed by decrease in fiber elongation. Drug release study reveals that 60% drug releases in 78 h with initial 19% burst release in PCL/CAM fibers whereas 92% drug release in 15 min was observed in PCL/PEO/CAM fibers [279]. Yu et al. fabricated PCL/PLA nanofibers via electrospinning and $CaCuSi_4O_{10}$ nanoparticles spin-coated on as-spun nanofibers for skin tissue regeneration. Photothermal effect due to presence of $CaCuSi_4O_{10}$ nanoparticles releases the Cu^{2+} and SiO_4^{4-} ions enhance the angiogenesis and epidermis formation. This nanoparticles also has 33.8% photothermal conversion efficiency, therefore, it was utilized for photothermal therapy of cancer [280]. Xue et al. explored the Metronidazole (MNA) loaded PCL–gelatin nanofiber for guided tissue regeneration implants. Addition of MNA in higher concentration (5–40%) leads to decrease (53.6–31.4°) in water contact angle whereas the pristine PCL nanofibers have 129.6° water contact angle. The drug release profile indicates that burst release for 1 day and slower release for the remaining 6 days, but this initial release was lower in 10 wt% MNA than 40 wt% MNA [281]. Yang et al. investigated multidrug-resistance (MDR) bacteria wound infection with APA-coated Au nanoparticles embedded PCL/gelatin nanofibers fabricated via electrospinning technique. Release study shows that as-spun nanofiber has 80% APA-coated Au nanoparticles release within 14 days in saline solution. It also shows excellent biocompatibility and high bacterial resistance against *E. coli* and MDR *E. coli* [282]. Motealleh et al. developed the chamomile impregnated poly(ε-caprolactone)/polystyrene nanofibers for wound dressing. The chamomile impregnated PCL nanofiber has faster drug release rate (75% in 12 h) than chamomile impregnated PCL/PS (65:35) nanofibers (58% in 12 h) and chamomile impregnated PS nanofiber (26% in 12 h), this was observed due to PS nanofiber (40%) exert lower swelling than PCL/PS (65:35) nanofibers (275%) and PCL nanofiber (400%) [283]. Liu et al. evaluated the performance of hydrophobic (ketoprofen) or hydrophilic (captopril) dug embedded thermo-sensitive poly(N-vinylcaprolactam-*co*-methacrylic acid) (PNVCL-*co*-MAA) nanofibers for controlled drug release. All the nanofibers samples show adhesion and proliferation of fibroblast cells for both drugs. The increased MMA content in NVCL:MAA causes rapid release of captopril drug e.g. 20% captopril embedded PNVCL-*co*-MAA(1:0.08) nanofibers (75% in 48 h) slower release was observed than 20% captopril embedded PNVCL-*co*-MAA(1:0.20) nanofibers (90% in 48 h) at 40 °C, similar behaviour was observed in ketoprofen drug with lower drug release due to its hydrophobicity, it was also observed that at 40 °C (above the lower critical solution temperature LCST) drug release was slow and at 20 °C (below the LCST) drug release was fast [284]. Pristine PCL based wound dressing has slower degradation rate, thus this can delay the drug release in the wound area therefore for tuning the degradation rate, PCL can be blended with higher degradation rate polymers such as chitosan, PEO etc. Characteristics of Drug-loaded PCL based uni-axial nanofibers are consolidated in Table 8.

5.1.4.4. Drug-loaded PLA based nanofibers. Wold et al. fabricated thiol added poly(lactic-*co*-glycolic-*co*-hydroxymethyl propionic acid) (PLGH) nanofiber for nitric oxide (NO) release to enhance wound healing. Antibacterial study shows that 23.3 mg PLGH-cysteamine SNO film and 19.4 mg material required to achieve 96% bacterial count reduction. The NO release in S-nitrosated PLGH-cysteamine nanofibers (0.281 ± 0.016 mmol·g^{-1}) were similar to spin-coated films (0.241 ± 0.004 mmol·g^{-1}) [285]. Kenawy et al. investigated the Tetracycline hydrochloride (TCH) loaded PLA/PEVA (50:50) blend nanofibers scaffold for wound dressing. Drug release of 5% TCH loaded PEVA electrospun fibers (62% in 120 h) were rapid than 5% TCH loaded PLA/PEVA (50:50) blend nanofibers (38% in 120 h) and amount of tetracycline HCl released by 5% TCH loaded PLA/PEVA (50:50) blend nanofibers (0.24 mg) were slower than commercially available wound dressing Actisite (0.8 mg) [286]. Zhang et al. prepared Captopril (CPL) impregnated Poly(lacticco-caprolactone) (PLCL) for drug release. The swelling study reveals that for PLCL nanofiber (165% in 50 min under 7.4 pH) reduced swelling percentage than PLLA (480% in 50 min under 7.4 pH) and PLGA (290% in 50 min under 7.4 pH) nanofibers. Initial burst release of PLLA and PLGA nanofiber (90% in 2 h) was greater than PLCL nanofiber (66% in 2 h) and PLCL nanofiber under 7.4 pH (90% in 250 h) has greater drug release rate than 6.8 pH (50% in 250 h) [88]. Loiola et al. studied Acetaminophen (AC) and celecoxib (CL) embedded PLLA–PEO–PPO block copolymers electrospun nanofiber for wound healing. Drug release of 5 wt% CL embedded PEPELA nanofibers (20% in 12 h) has slower release than 5 wt% AC embedded PEPL nanofibers (40% in 12 h) [287]. Glycolic acid or Caprolactone copolymerized PLA dressing shows appropriate drug release rate. Characteristics of Drug-loaded PLA based uni-axial nanofibers are consolidated in Table 9.

5.1.4.5. Other polymeric material based nanofibers. Li et al. explored 5-FU-Hydrophilic/Paeonolum-hydrophobic added PEO with mixed surfactant cetyltrimethylammonium bromide (CTAB)/sodium dodecylbenzenesulfonate (SDBS) nanofiber for drug release behaviour. Cumulative 5-FU release of CTAB/SDBS molar ratio 2:8 nanofiber (25% in 400 min) was slower than surfactant free nanofiber (96% in 400 min) also cumulative paeonolum release of CTAB/SDBS molar ratio 8:2 nanofiber (40% in 400 h) was slower than CTAB/SDBS molar ratio 2:8 nanofiber (70% in 400 h) [288]. Xing et al. developed silver nanoparticles (AgNPs) loaded Poly-(3-hydroxybutyrate-*co*-3-hydroxyvalerate) (PHBV). Antibacterial study shows that 1% AgNPs

Table 8
Drug-loaded PCL based uni-axial nanofibers.

Materials		Fiber Diameter	Application	Condition	Properties/Results	Ref. no.
Matrix	Drug					
PCL	Metronidazole	250–500 nm	Wound healing	*In vivo*	Drug release 90% in 1 week	[274]
PCL	Silver nanoparticles	183 ± 59 nm	Wound healing	–	Zone of inhibition > 8 mm against S. aureus, *E. coli*, *P. aeruginosa*, *S. pyogenes* and *K. pneumonia*	[275]
PCL	Carbon nanodots (CND)	698 ± 420 nm	Full thickness wound healing	*In vivo*	Wound recovery 82.75 ± 1.5% in 7 days	[276]
PCL	Europium hydroxide nanorods (EHNs)	1250 nm	Wound healing	*In vitro and in vivo*	HUVECs proliferation 158 ± 16 cells/mm^2 in 24 h	[277]
PCL	ZnO	–	Wound healing	*In vivo*	Wound healing % Pure PCL membrane- 85% in 25 days ZnO loaded PCL membrane- 100% in 25 days	[278]
PCL/PEO	Chloramphenicol (CAM)	496 ± 339 nm	Wound dressing	*In vitro*	Drug release PCL/PEO nanofibers- 92% in 15 min PCL nanofibers- 60% in 78 h	[279]
PCL/PLA	$CaCuSi_4O_{10}$ nanoparticles	1–1.5 μm	Skin tissue regeneration	*In vitro and in vivo*	Photothermal conversion efficiency- 33.8%	[280]
PCL/Gelatin	Metronidazole (MNA)	280–470 nm	Wound healing	*In vitro*	Drug release Initial 58% in 2 h & cumulative 98% in 14 h	[281]
PCL/gelatin	6-aminopenicillanic acid, (APA)-coated gold nanoparticles	–	Wound healing	*In vivo*	Drug release Initial 30% in 2 days & cumulative 80% in 14 days	[282]
PCL/polystyrene	Chamomile	175 nm	Wound dressing	*In vitro and in vivo*	Drug release PCL nanofibers-65% in 5 h & 78% in 48 h PCL/PS (65:35) nanofibers-35% in 5 h & 75% in 48 h PS nanofibers-15% in 5 h & 35% in 48 h	[283]
Poly(N-vinylcaprolactam-*co*-methacrylic acid) (PNVCL-*co*-MMA)	Captopril Ketoprofen	–	Wound healing	*In vitro*	Drug release At 20 °C (PNVCL-*co*-MMA) + Captopril-80% within 240 h (PNVCL-*co*-MMA) + Ketoprofen-60% within 240 h At 40 °C (PNVCL-*co*-MMA) + Captopril-85% within 48 h (PNVCL-*co*-MMA) + Ketoprofen-40% within 48 h	[284]

Table 9
Drug-loaded PLA based uni-axial nanofibers.

Materials		Fiber Diameter	Application	Condition	Properties/Results	Ref. no.
Matrix	Drug					
Poly(lactic-*co*-glycolic-*co*-hydroxymethyl propionic acid) (PLGH)	Thiol	200–410 nm	Wound healing	*In vitro*	Reduction in bacterial count PLGH film- 23.3 mg required for 96% PLGH nanofibers- 19.4 mg required for 96%	[285]
PLLA Poly(ethylene-*co*-vinylacetate) PLA/PEVA(50:50)	Tetracycline hydrochloride	1–3 μm	Wound dressing	–	Drug release PLA/PEVA (50:50) nanofibers- 50% in 120 h	[286]
Poly(L-lactic acid) (PLLA) Poly(lactic-*co*-glycolic acid) (PLGA) Poly(lacticco-caprolactone) (PLCL)	Captopril (CPL)	738 ± 211 nm	Wound healing	*In vitro*	Drug release PLLA and PLGA nanofibers- 90% in 2 h PLCL nanofibers- 66% in 2 h	[88]
Poly(L-lactide)-*b*-PEO-*b*-poly(L-lactide) (PELA) Poly(L-lactide)-bPEO-*b*-poly (propylene oxide)-*b*-PEO-*b*-poly(L-lactide) (PEPELA)	Acetaminophen (AC) and Celecoxib (CL)	400–530 nm	Wound healing	*In vitro*	Drug release AC-PELA nanofibers- 40% in 12 h CL-PEPELA nanofibers- 20% in 12 h	[287]

loaded PHBV nanofibers (99% against Klebsiella pneumonia and S. aureus) exert higher growth inhibition percentage than pristine PHBV nanofibers (10% against Klebsiella pneumonia and S. aureus). The drug release study reveals that 0.55 ppm AgNPs release within 30 days [289]. GhavamiNejad et al. also evaluated silver nanoparticles impregnated poly(dopamine methacrylamide-*co*-methyl methacrylate) (MADO) nanofibers for wound dressing application. Anti-bacterial study indicates that MADO-AgNPs exhibits *E. coli* (165%), which has higher percentage increase in diameter S. aureus (120%) and *P. aeruginosa* (130%). Drug release studies disclose that MADO-AgNPs nanofiber shows initial burst release (16 μg in day 1) and then sustain drug release (25 μg in day 7) in 7 days [290]. Fayemi et al. investigated Moringa Extract embedded Polyacrylonitrile nanofibers for accelerated wound healing. The wound closure study indicates that 0.5 g moringa extracts embedded Polyacrylonitrile exhibit 95% wound closure on day 7, also the highest bactericidal effect was observed in 0.5 g of moringa with inhibition zone 12 mm for S. aureus and 15 mm for *E. coli* [291]. Wu et al. prepared Ag nanoparticles added Thermoplastic polyurethanes (TPUs) nanofibers for wound dressing. Swelling study indicates that water uptake of 1 wt% $AgNO_3$ electrospun mat (517 ± 36%) was greater compared to 1 wt% $AgNO_3$ cast film (474 ± 25%). SEM images evidenced that $AgNO_3$ exhibit microbial activity against *E. coli*. [292]. Wang et al. studied Keratin (K) and silver nanoparticles (AgNPs) loaded polyurethane (PU) nanofibers bactericidal for wound healing. SEM images confirmed that NIH 3 T3 cells growth on PU/K and PU/K/AgNP was superior to PU mat. Bactericidal study shows that zone inhibition diameter *E. coli* (3.1 mm) was higher than S. aureus (1.9 mm). Exudate absorption characteristic of nanofibers were evaluated via water absorption in PBS, as the water absorption of 195.2 ± 7.8% was higher than PU (44.4 ± 4.2%) and PU/K/AgNPs (101.5 ± 5.1%) [293]. Ahmed et al. investigated the feasibility of Amphotericin B (AMB) and Itraconazole (ITZ) loaded polyvinylidene fluoride, poly(methyl methacrylate), poly(N-isopropylacrylamide), and polyvinylpyridine (PVP) fibers for drug delivery function fabricated via electrospinning and pressure gyration technique. The morphological studies shows that electrospun drug loaded PVP fibers has finer diameter compared with pressurized gyration technique as well as drug dissolution profile also confirm that drug-loaded PVP fibers significantly enhance the dissolution of Amphotericin B and Itraconazole. The drug release profile shows that for the initial 15 min electrospun PVP fibers shows rapid release whereas after 15 min gyrospun fibers exhibit accelerated drug release [294]. Characteristics of Drug-loaded other polymer uniaxial nanofibers are consolidated in Table 10.

Researchers enormously explored the drug-loaded uniaxial electrospun nanofibers with varying concentration of drug, hydrophilic drug, hydrophobic drug and electrospinning parameters such as flow rate, tip to electrode distance, in case of polymer blend matrix individual polymer content for wound healing, wound dressing applications. But these nanofibers are most of the times useful only for bactericidal dressing.

5.1.5. Hybrid nanofibers

Hybrid nanofibers contain more than one drug or the combination of drug and biological molecule, these nanofibers had better chances of effective bacterial resistance as well as wound healing. Mohammadi et al. investigated curcumin-embedded PCL/gum tragacanth (GT) (PCL/GT/Cur) nanofibers mat for wound healing. Antibacterial study shows the antibacterial activity of 99.99% and 85.14% against gram-negative bacteria such as methicillin resisyant staphylococcus aureus (MRSA) and gram-positive bacteria such as extended spectrum b lactamase (ESBL). Decreased wound healing area of controlled growth sample was higher than that of (PCL/GT/Cur) nanofibers mat [90]. Zhao et al. reported multi-drug dual layer system with nitrofurazone (NFZ)-loaded poly(L-lactide) (PLLA)/sericin nanofibers in which first layer contains NFZ-loaded PLLA/sericin nanofibers whereas second layer contains NFZ-loaded PLLA nanofibers. PLLA was a hydrophilic but 2% NFZ shows hydrophobicity (125.7°) as the NFZ exert hydrophobic nature, thus the hydrophobicity can be controlled by addition of sericin (66°). Drug release study shows that single layer of 0.2% loaded PLLA/sericin exhibit burst release (98% in 10 min) whereas the single layer of 2% NFZ loaded PLLA exhibit sustain release (17.6% in 48 h), these release profile again modified with dual layer of PLLA/SS(2:1)-0.2NFZkPLLA-2NFZ nanofiber mat (11.2% in 48 h) [295]. Sarhan et al. attempted the Allium sativum extract (AE) and Cleome droserifolia extract (CE) incorporated honey/chitosan nanofiber for enhanced wound healing. SEM micrograph reveals that higher AE content decreases the fiber diameter and wound closure study (day 1-day 12) confirm that honey/polyvinyl alcohol/chitosan/AE nanofibers were better than commercially available Aquacel®Ag dressing. The antibacterial study disclosed that honey/polyvinyl alcohol/chitosan/AE and honey/polyvinyl alcohol/chitosan/AE/CE nanofibers scaffold have complete inhibition against S. aureus compared to commercial wound dressing [296]. Dubey et al. prepared the PEGylated graphene oxide (GO) - silver nanoparticle (Ag NP)-curcumin (CUR) loaded chitosan (CS)/PVA nanofibers hybrid system for wound dressing. The water contact angle study shows that pristine CS/PVA nanofiber (27°) has lower water contact angle than GO loaded CS/PVA nanofiber (58°) and GO-CUR loaded CS/PVA nanofiber (88°), this behaviour was observed mainly due to hydrophobic nature of GO as well as curcumin. The drug release study reveals that initial burst release of silver (10%) and curcumin (4%) followed by slow controlled release of silver (90% in 36 h) and curcumin (80% in 48 h) [297]. Ramanathan et al. explored collagen coated coccinia grandisplant extracts (CPE) impregnated Poly (3-hydroxybutyric acid)-gelatin (PG) nanofiber for ECM mimicking wound dressing. The swelling study states that collagen coated PG nanofibers (400%) has undergone greater swelling than PG-CPE nanofibers (300%) and PG-CPE-COL nanofibers (200%). The 0.3 mg/10 × 10 mm^2 CPE

Table 10
Drug-loaded other polymer uni-axial nanofibers.

Materials		Fiber diameter	Application	Condition	Properties/Results	Ref. no.
Matrix	Drug					
PEO	5-FU	140–380 nm	Wound healing	–	Drug release 25% in 400 min	[288]
Poly-(3-hydroxybutyrate-*co*-3-hydroxyvalerate) (PHBV)	Silver nanoparticles (AgNPs)	630 ± 20 nm	Wound dressing	*In vivo*	Drug release 0.55 ppm AgNPs release in 30 days	[289]
Poly(dopamine methacrylamide-*co*-methyl methacrylate) (MADO)	Silver Nanoparticles	800 nm	Wound dressing	*In vitro and in vivo*	Drug release Initial 16 μg in day 1 & cumulative 25 μg in 7 days	[290]
Polyacrylonitrile	Moringa Extract	–	Wound healing	–	Wound closure 95% in 7 days	[291]
Thermoplastic polyurethanes (TPUs)	Silver nanoparticles	150 nm	Wound dressing	–	Water uptake 517 ± 36%	[292]
Polyurethane	Keratin + silver nanoparticles (AgNPs)	593 ± 187 nm	Wound dressing	*In vivo*	Water absorption 101.5 ± 5.1%	[293]
Polyvinylpyridine	Amphotericin B Itraconazole	0.88 ± 0.35 μm 0.94 ± 0.34 μm	Wound healing	*In vitro*	Drug release PVP/AMB fibers- 90% in 60 min PVP/ITZ fibers- 95% in 60 min	[294]

embedded PG exhibits antimicrobial activity against S. aureus and *E. coli* as well as fibroblast adhesion and proliferation was also observed [298]. Cheng et al. developed Tetracycline hydrochloride (TH) embedded poly(3-hydroxybutyrate-*co*-3-hydroxyvalerate) (PHBV)/Cellulose nanocrystals (CNC) nanofibers to achieve durable drug release. Augmented CNC content in PHBV (1–10%) increases the viscosity (0.45–1.71 Pa s) as well as conductivity (0.18–1.05 μS cm^{-1}). Drug release study shows that initial drug release of PHBV nanofibers (36.1% in 50 h) were slower than PHBV/CNC nanofibers but the cumulative release of PHBV/CNC nanofibers (86% in 50 h) were higher than PHBV nanofibers (37.6% in 540 h) [299]. Peh et al. investigated vitamin C + hydrocortisone + Insulin + triiodothyronine + epidermal growth factor (EGF) + 1,25-dihydroxyvitamin D3 (VD3) [CHITED] added Poly (DL-lactide-*co*-glycolide) (PLGA)/bovine atelocollagen nanofiber for skin wound healing. The main intension of CHITED was to provide drug or biological stimulator for pathophysiological events like fibroblast proliferation can be stimulated by EGF, vitamin C assist the fibroblast to secrete type I collagen etc. drug release profile demonstrated that sustain release of bioactive molecules such as hydrocortisone and EGF (97% in 8 h), T3 and insulin (80% in 8 h), Vitamin C (55% in 4 h followed by 30% in the next 4 h), VD3 (30% in 12 h) were observed [300]. Mira et al. reported 5-aminolevulinic acid (5-ALA) incorporated in poly (methyl vinyl ether-alt-maleic acid) (PMVEMA-Ac) and poly(methyl vinyl ether-alt-maleic ethyl monoester) (PMVEMA-Es) electrospun nanofibers for wound healing application. According to high-performance chromatography results, the encapsulation efficiency of 5-ALA was 97 ± 1% and drug release profile reveal that PMVEMA-Es nanofibers (55% in 50 min) release rapid 5-ALA than PMVEMA-Ac nanofibers (15% in 50 min) [301]. Hybrid nanofibers have multi-drug carrying capacity but, the basic problem of burst drug release cannot be rectified with uni-axial nanofibers, as a result, researchers started exploring coaxial electrospun nanofibers for efficient drug release. Characteristics of uni-axial hybrid nanofibers are consolidated in Table 11.

5.2. Coaxial nanofibers

Coaxial nanofibers are fabricated via coaxial electrospinning technique; these nanofibers facilitate to carry sensitive drug or biological molecule without disturbing their structural integrity and also keeping safe from environmental fluctuations with the help of sheath barrier. This barrier also has crucial importance because they enhance the drug release efficiency and minimizes the severity of burst release. Coaxial nanofibers are divided into four types: (1) Polymer nanofibers having different polymer in core and sheath, (2) Biological molecule embedded nanofibers having biological molecule in core and polymer matrix in sheath, (3) Drug-loaded polymer nanofibers having drug in core and polymer in sheath and (4) Hybrid nanofibers having more than one drug in the core or in both core and sheath.

5.2.1. Polymer nanofibers

Zhao et al. reported the gelatin-coated poly(ε-caprolactone) nanofiber as the gelatin is well known for cells adhesion and proliferation whereas the PCL imparts the mechanical stability to the core/shell nanofibers. The gelatin layer was stabilized by glutaraldehyde solution. Cross-linked nanofibers scaffold had lesser porosity than as-prepares nanofibers scaffold [302]. Ojha et el. attempted the electrospinning of chitosan/PEO nanofibers for wound healing as well as wound dressing application. Tensile strength of pristine PEO nanofibers (10.0 ± 0.2 MPa) were greater than chitosan-PEO nanofibers (4.0 ± 0.3 MPa). The 3 wt% chitosan and 4 wt% PEO has core diameter 100 nm whereas shell diameter was 250 nm. The porosity of 84% was helpful for exudates absorption [303]. Nguyen et al. prepared poly (lactic acid) (PLA)-chitosan (CS) nanofiber for wound dressing. Increase in core feed rate (1.0–4.0 μL/min) augmented the water contact angle (24.1–52.9°) and on the contrary decline the bacterial inhibition rate (52–22%). Mechanical properties such as tensile strength of PLA

Table 11
Uni-axial hybrid nanofibers.

Materials		Fiber Diameter	Application	Condition	Properties/Results	Ref. no.
Matrix	Drug					
PCL	Curcumin-loaded/Gum tragacanth (GT)	50–500 nm	Diabetic wound healing	*In vivo*	Wound closure 100% in 15 days	[90]
Poly(L-lactide) (PLLA)	Nitrofurazone (NFZ) + Sericin (SS)	413 nm	Wound dressing	*In vivo*	Drug release PLLA/sericin nanofibers-98% in 10 min PLLA nanofibers-17.6% in 48 h of PLLA/SS(2:1)-0.2NFZkPLLA-2NFZ-11.2% in 48 h	[295]
Chitosan/PVA	Honey + Allium sativum extract (AE) Honey + Cleome droserifolia extract (CE)	145 nm	Wound healing	*In vivo*	Wound closure 100% in 12 days	[296]
Chitosan/PVA	Grafted PEG functionalized graphene oxide + Silver nanoparticle (Ag NP) + Curcumin	147 nm	Wound dressing	*In vitro*	Drug release Silver-90% in 36 h and curcumin- 80% in 48 h	[297]
Poly (3-hydroxybutyric acid)-Gelatin (PG)	Coccinia grandisplant extracts (CPE) + Collagen	240 ± 30 nm	Wound dressing	*In vitro*	Swelling rate- 400% in 48 h	[298]
Poly(3-hydroxybutyrate-*co*-3-hydroxyvalerate) (PHBV)/Cellulose Nanocrystals	Tetracycline hydrochloride (TH)	1052 ± 55 nm	Wound healing	*In vitro*	Drug release PHBV/CNC nanofibers- 86% in 50 h	[299]
Poly(DL-lactide-*co*-glycolide)/bovine atelocollagen	Vitamin C + hydrocortisone + Insulin + triiodothyronine + epidermal growth factor (EGF) + 1,25-dihydroxyvitamin D3 (VD3) [CHITED]	210 ± 62 nm	Wound healing	*In vitro*	Drug release Hydrocortisone & EGF- 97% in 8 h, T3 & insulin- 80% in 8 h, Vitamin C- 55% in 4 h,VD3- 30% in 12 h	[300]
Poly(methyl vinyl ether-alt-maleic acid) (PMVEMA-Ac) Poly(methyl vinyl ether-alt-maleic ethyl monoester) (PMVEMA-Es)	5-aminolevulinic acid (5-ALA) + conjugated with polyelectrolyte	150 nm	Wound healing	*In vitro*	Drug release PMVEMA-Ac nanofibers-15% in 50 min PMVEMA-Es nanofibers-55% in 50 min	[301]

Table 12
Co-axial polymer nanofibers.

Materials		Fiber Diameter	Application	Properties/Results	Ref. no.
Core	Shell				
PCL	Gelatin coating	1.13 μm	Wound dressing	Tensile strength Inner dope feed rate of 2 mL/h-1.16 MPa Inner dope feed rate of 5 mL/h-1.56 MPa	[302]
Chitosan	PEO	250 nm	Wound healing dressing	Porosity-84% Tensile strength- 4.0 ± 0.3 MPa	[303]
PLLA	Chitosan (CS)	236 ± 87 nm 303 ± 165 nm 396 ± 336 nm	Wound healing	Antibacterial efficiency (*E. coli* inhibition)- PLA/CS (core feed rate 1.0 μL/min)- 52% after 24 h PLA/CS (core feed rate 2.0 μL/min)- 44% after 24 h PLA/CS (core feed rate 4.0 μL/min)- 22% after 24 h	[304]
PEO	Chitosan	150–190 nm	Wound dressing	Specific surface area theoretical-16.7 m^2/g Experimental-15 ± 1.5 m^2/g	[305]
PEO	Chitosan	597.08 nm	Wound dressing	Maximum working temperature PEO/chitosan nanofiber-70 °C	[306]

nanofibers (3.3 MPa) were greater than CS nanofibers (0.5 MPa) [304]. Pakravan et al. explored PEO-chitosan nanofibers for wound dressing application as it possesses high specific surface area. The theoretical specific surface area of nanofibers 16.7 m^2/g were similar to experimental specific surface area (15 ± 1.5 m^2/g) [305]. Zhang et al. also investigated the PEO/Chitosan scaffold for wound care. The TEM images reveal that sharp interfaces between core and shell layer. Higher CS content expands the shell layer and as-prepared core/shell nanofiber was only sustain up to 70 °C [306]. Characteristics of Co-axial polymer nanofibers are consolidated in Table 12.

5.2.2. Biological molecule loaded nanofibers

Rubert et al. reported FGF2 and Bovine serum albumin (BSA)-Evans blue embedded in PEO/PCL core/shell electrospun nanofibers. Pristine PEO has 20° contact angle whereas pristine PCL has 118°. Drug release study evinces the initial burst release (10.6% in 1 h) and then sustain release (52.9% in day 1 to day 9) of FGF2 from core/shell nanofibers scaffold [307]. Zhang et al. attempted the fabrication of fluorescein isothiocyanate-conjugated bovine serum albumin (fitcBSA) loaded PEG/PCL core/shell nanofiber for sustain drug release. Variation in inner flow rate (0.2–0.6 mL/h) increases the fiber diameter (270–380 nm) and In vitro release study confirms that PCL/fitcBSA/PEG blend nanofiber (35.7% in 3 h) has initial burst release compared to PCL-r-fitcBSA/PEG core/shell nanofiber (31.2% in 4 h) [308]. Jiang et al. prepared lysozyme and Bovine serum albumin individual bioactive molecule added PEG/PCL core/shell nanofibers to achieve controlled release. Sustain release was observed in 1.96% BSA containing nanofiber (inner feed rate-0.6 mL/h) (50% within 24 day) than 5.56% BSA containing nanofiber (inner feed rate-2 mL/h) (95% within 24 day) [309]. Hyperglycemia was one of the main reason that causes a delay in the healing process, this was rectified by stabilizing with hypoxia-inducible factor 1 α (HIF-1α), thus Gao et al. studied Dimethyloxalylglycine (DMOG)/Col I embedded PCL core/shell nanofibers for diabetic wound healing. Drug release study demonstrates that DMOG/Col I blend nanofibers (53.3 ± 2.7% in 12 h) has rapid drug release than DMOG/Col I core/shell nanofibers (17 ± 2.1% in 12 h) [310]. Characteristics of Biological molecule loaded co-axial polymer nanofibers are consolidated in Table 13.

5.2.3. Drug loaded nanofibers

Ren et al. explored Dimethyloxalylglycine (DMOG)-loaded mesoporous silica nanoparticles (DS)/PLLA nanofibers for accelerated wound healing of diabetic patient. In vivo wound healing test shows that 10 wt% DS/PLLA nanofibers has higher wound healing ratio than pristine PLLA and controlled (open) wound, as well as on day 15, 10 wt % DS/PLLA nanofibers has higher wound healing ratio than pristine PLLA and controlled (open) wound. Cells (human umbilical vein endothelial cells) proliferation was increased via combined effect of DMOG drug and Si ion [75]. He et al. developed Tetracycline hydrochloride (TCH)/PLLA core/shell nanofibers for sustain drug delivery. As the higher PLLA content (5–10 wt%) augmented the fiber diameter (360–1312 nm) and Drug release profile indicate that 5 wt% PLLA nanofibers (55% within 30 days) has greater drug release than 10 wt% PLLA nanofibers (44% within 30 days) [89]. Qi et al. evaluated halloysite nanotubes (HNTs) incorporated tetracycline hydrochloride/PLGA core/shell nanofibers for sustain release. The mechanical properties of HNTs/PLGA were better than pristine PLGA nanofibers. In vitro drug release study indicate that 1 wt% TCH/PLGA nanofibers has a rapid drug release profile than 1 wt% TCH/HNT nanofibers TCH incorporated HNT/PLGA nanofibers. SEM images, as well as MTT cell proliferation assay, confirm the biocompatibility of the as-prepared nanofibers [311]. Sultanova et al. investigated Ampicillin/PCL core/shell nanofibers for controlled release of drug by varying the shell flow rate. Dilute core concentration assists to achieve fine fiber. Drug release study shows that core nanofiber has 85% drug release within 4 h (burst release) but in Ampicillin/PCL nanofiber (0.5 ml/h) and Ampicillin/PCL nanofiber (0.5 ml/h) has 16% and 7% drug release within 4 h respectively [76]. He et al. reported PCL containing metronidazole drug/zein core/shell nanofibers for tissue regeneration. Pristine Zein nanofibers (146° ± 0.8°) has higher water contact angle than MND-PCL/zein nanofibers (139° ± 1.4°) and pristine PCL nanofibers (126° ± 1.2°). the core to shell flow rate ratio variation affect on the release of the drug such as MND-PCL/zein nanofibers (1.4:3) (22.3% in 2 h) has rapid drug release than PCL/zein nanofibers (0.7:3) (16.5% in 2 h) and PCL/zein nanofibers (1:3) (12.2% in 2 h) [312]. Najafi-Taher et al. prepared ascorbic acid (ACA)/PVA-chitosan (CS) core/shell nanofibers and ACA embedded PVA/CS blend nanofibers for transdermal delivery. As-prepared nanofibers were stabilized by glutaraldehyde vapors. Crosslinked-blend nanofibers (33% within 4 h) have higher burst release compared to coaxial nanofibers (27% within 4 h) and also cumulative release of crosslinked coaxial nanofibers (74% in 30 h) were higher than blend nanofibers (63% in 30 h) [313]. Zupanč ic et al. explored monolithic PVA/poly(methyl methacrylate) (PMMA) and PVA and PMMA blend/ciprofloxacin hydrochloride (CIP) core/shell nanofibers for skin wound dressing. According to drug release study, it was observed that drug release can be tuned by varying core flow rate PVA in PVA/PMMA nanofibers and varying PMMA:PVA ratio in PVA-PMMA blend/CIP nanofibers [314]. Zhu et al. attempted to fabricate Asiaticoside/Alginate, PVA and chitosan (alginate/PVA/CS) core/shell nanofibers for burn wound dressing. As-prepared core/shell nanofiber has wound healing ratio above 99% whereas the centella triterpenes cream treated has 99.2% and cumulative drug release of centella triterpenes cream treated wound and coaxial nanofibers were 82% within 24 h [315]. Li et al. evaluated sodium alginate (SA)-calcium ions/Rana chensinensis skin peptides (RCSPs) nanofibers for effective wound dressing. Calcium ion provides thermal stability to the as-prepared coaxial nanofiber and In vivo drug release study indicated that SA@Ca2 + /RCSPs nanofibers has 46.6% wound healing within 5 days whereas SA@Ca2 + nanofibers has 35.03% wound recovery within 5 days [316]. Yu et al. investigated Ketoprofen/CA core/shell nanofibers for wound dressing. SEM images shown wrinkles on the fiber surface, this mainly due to contact of barometric pressure while solvent

Table 13
Biological molecule loaded co-axial polymer nanofibers.

Materials		Fiber Diameter	Application	Condition	Properties/Results	Ref. no.
Core	Shell					
Bovine serum albumin (BSA)-Evans blue/PEO	PCL	6.5 μm	Wound healing	*In vitro*	Drug release Core/Shell nanofiber −10.6% in 1 h and 52.9% in 9 days	[307]
fitcBSA/PEG	PCL	277 ± 140 nm	Wound healing	*In vitro*	Drug release Blend nanofiber – 35.7% in 3 h and 60–70% in 2 days Core/Shell nanofiber – 31.2% in 4 h and 45–65% in 2 days	[308]
PEG-Lysozyme PEG-Bovine Serum Albumin (BSA)	PCL	571 nm	Wound healing	–	Drug release Cumulative release- 50% in 24 day	[309]
Dimethyloxalylglycine (DMOG)	PCL/Col I	200–500 nm	Wound healing	*In vivo*	Drug release Blend nanofibers-53.3 ± 2.7% in 12 h and 72.6 ± 6.5% in 24 h Core/Shell nanofibers-17 ± 2.1% in 12 h and 36.1 ± 4.2% in 24 h	[310]

Table 14
Drug-loaded co-axial polymer nanofibers.

Materials		Fiber diameter	Application	Condition	Properties/Results	Ref. no.
Core (Drug)	Shell (matrix)					
Dimethyloxalylglycine (DMOG)/Mesoporous silica nanoparticles (DS)	PLLA	–	Diabetic wound, chronic wound	*In vivo*	Wound healing ratio-97% in 15 days Cumulative release- 0.04 mg/ml in 12 days	[75]
Tetracycline hydrochloride (TCH)	PLLA	360 nm	Wound dressing	*In vitro*	Drug release 44% in 30 days	[89]
Halloysite nanotubes (HNTs)/Tetracycline hydrochloride	PLGA	298 nm	Wound healing	*In vitro*	Drug release 30% in 28 days	[311]
Ampicillin	PCL	464 ± 214 nm	Wound healing	*In vitro*	Drug release 94.8% of the drug within 72 h	[76]
PCL/Metronidazole	Zein	0.6 ± 0.04 μm	Wound healing	*In vitro*	Drug release 12.2% in 2 h	[312]
Ascorbic acid	PVA-Chitosan	159 ± 34 nm	Wound healing	*In vitro*	Drug release Initial-27% in 4 h and cumulative 74% in 30 h	[313]
Monolithic PVA PVA and PMMA blend	Poly(methyl methacrylate) (PMMA) Ciprofloxacin hydrochloride (CIP)	1010 ± 165 nm	Wound healing	*In vitro*	Drug release Intial-7% in 6 h and cumulative 90% in 28 days	[314]
Asiaticoside	Alginate/PVA/chitosan	168.5 nm	Wound healing of burn injury	*In vitro*	Drug release Intial-55% in 5 h and cumulative 82% within 24 h Healing ratio High dose (5%) – 99.2% in 21 day	[315]
Sodium alginate (SA)/calcium ions	Rana chensinensisskin peptides (RCSPs)	87.58 nm	Wound healing	*In vivo*	Drug release Cumulative-99% in 10 sec Wound healing rate 46.6% wound healing within 5 days	[316]
Ketoprofen	CA	240 ± 30 nm	Wound healing	*In vitro*	Drug release Initial-9.1% in 1 h and cumulative 98.9% in 144 h	[83]
Polyurethanes without dendrimer	Polyurethanes with NO-releasing dendrimer	393 ± 157 nm	Wound dressing	*In vitro*	NO release study ~9 h with a half-life ($t_{1/2}$) of ~25 min	[317]

evaporation. Interestingly the drug release rate of ketoprofen loaded nanofibers were slightly slower than ketoprofen/CA core/shell nanofibers [83]. Worley et al. prepared Polyurethane without dendrimer (PU)/polyurethane with NO-releasing dendrimer (PU-NO) core/shell nanofibers for wound dressing. The PU nanofibers have higher porosity than PU-NO nanofibers but PU nanofibers have lower water absorption than PU-NO nanofibers. As-prepared nanofibers releases 0.027–0.072 μmol NO/mg and exhibit bactericidal activity against S. aureus [317]. Characteristics of drug loaded co-axial polymer nanofibers are consolidated in Table 14.

5.2.4. Hybrid nanofibers

Li et al. reported the regenerated silk fibroin (RSF) nanosphere + curcumin (core)/regenerated silk fibroin (RSF) based solution-doxorubicin hydrochloride (shell) nanofibers for wound healing. Wettability study observed that the water annealing treated at 60 °C of dual drug loaded RSF nanofibers has a higher water contact angle than treated nanofibers at 45 °C and untreated nanofibers. Rapid drug release was observed in CUR embedded RSF nanospheres (65% in 10 h) compared to RSF nanofibers loaded with CUR-RSF nanospheres (35% in 10 h) and RSF nanofibers-CUR embedded nanospheres/RSF nanofibers-DOX embedded nanospheres core/shell nanofibers (30% in 10 h) [318]. Ranjbar-Mohammadi et al. explored the Gum tragacanth (GT) and Tetracycline hydrochloride (TCH)/PLGA core/shell nanofibers were used for wound dressing. Wettability study demonstrates that GT-TCH/PLGA nanofibers (92°) have lower water contact angle than PLGA:GT 50:50 nanofibers (42°) and Pristine PLGA nanofibers (135°). Drug release study shows that PLGA/GT core/shell nanofibers (20% in 2 h) and PLGA nanofibers (25% in 2 h) undergone sustain drug release than PLGA/GT (50:50) blend nanofibers (48% in 2 h) [319]. Characteristics of drug loaded co-axial hybrid nanofibers are consolidated in Table 15. The co-axial electrospun fiber based dressing minimizes rapid drug release rate wherein the polymer acts as a shell that allow to permeate the drug (core) as degradation begins, therefore, polymer can be elected in such a way that the rate of drug release can be tuned by choosing polymer sheath with faster or slower polymer degradation rate, therefore tri-axial nanofibers are potential option to avoid burst drug release.

5.3. Tri-axial nanofibers

Tri-axial nanofibers are fabricated via tri-axial electrospinning technique which consists of a middle layer between the inner core and outer sheath. These nanofibers are not so much explored amongst all of the electrospun nanofibers but their properties render them as a potential candidate for drug delivery application.

Yang et al. evaluated the hollow nanofibers fabricated via tri-axial electrospinning technique, in which Lecithin-diclofenac sodium (PL-DS)/Methacrylic acid-Methylmethacrylate (MAA-MMA) blend/Ethanol was a core/middle/sheath layers. Ethanol protects the middle layer from environmental fluctuations, as well as post-drying, evaporates and MAA-MMA blend/PL-DS core/shell nanofibers were finally analyzed. Drug release study implies nanofibers have sustained release (15% in 3 h) and DS particles have burst release (75% in 3 h), this release profile was observed owing to nanofibers shell dissolve in 1 pH whereas the PL-DS dissolve in 7 pH [320]. Khalf et al. investigated Mineral oil/CA/PCL tri-axial nanofibers having a break strength of 5 N. It was also observed that Human Umbilical Vein Endothelial Cells (HUVEC-2) proliferate successfully, thus tissue regeneration was confirmed [219]. Liu et al. prepared the tri-axial nanofiber, which consists of gelatin core as well as sheath layer and PCL as a middle layer. The shell, core and middle layer contain 1.7 wt%, 10 wt% and 11 wt% respectively. All three layers had unique role to play in wound healing such as sheath has cell adhesion and proliferation, middle layer provides mechanical strength whereas core contains drug or growth factor for sustain release [321]. Han et al. reported nisin loaded polyvinylpyrrolidone (PVP)/PCL/Nylon 6 core/middle/shell tri-axial nanofiber for extended anti-microbial activity. The bacterial resistance of pristine nanofiber (8.6 wt% nisin loaded PCL), 19 wt% nisin loaded PVP/PCL coaxial nanofiber and triaxial nanofibers has 19 wt% PVP/PCL/CA tri-axial nanofiber exerts 1 day, 2 day and 6 days respectively, this extended microbial resistance was observed in tri-axial nanofibers due to sheath and middle layers slow down the drug release of the core [322]. Khalf et al. explored doxycycline embedded PCL-Gelatin(GT)/Hydrophilic Gelatin (GT)/PCL-Hydrophilic Gelatin (GT) tri-axial nanofibers for controlled drug release. Drug release profile depicted that PCL/GT blend nanofiber (95% in 24 h) have rapid drug release than GT/PCL core/shell nanofibers (50% in 24 h) and Triaxial nanofibers (85% in 24 h), this drug release behavior was due to poor homogeneity in thickness as well as in layers although the permeability of tri-axial fibers (3.5 μm/h) were lower than coaxial (6 μm/h) and blend fibers (12 μm/h) [323]. Yu et al. evaluated ethyl cellulose tri-axial fiber with varying ketoprofen (KET) drug concentration for zero order drug release. The surface area of middle layer was smaller than outer and inner layer. Drug release study confirms that as-prepared tri-axial fibers shows sustain release 10% in 2 h as well as they also have cumulative release of 90% drug in 24 h [324]. Han *at el.* investigated PCL-KAU dye/PCL/Polyvinylpyrrolidone (PVP) + KAB dye triaxial nanofibers for dual release. Middle solution flow rate variation has significant effect on drug release, such as 0.8 mL/h triaxial electrospun fibers (55% KAB in 4 h) shows rapid KAB release than 1.2 mL/h tri-axial electrospun fibers (26% KAB in 4 h), whereas 0.8 mL/h tri-axial electrospun fibers (98% KAU in 4 h) shows rapid KAU release than 1.2 mL/h tri-axial electrospun fibers (85% KAU in 4 h) [325]. Although drug release control in the tri-axial nanofibers is much better than uni-axial and coaxial nanofibers, the post-spinning solvent evaporation and selection of polymers are critical issues in the fabrication of tri-axial nanofibers. Characteristics of Tri-axial polymer nanofibers are consolidated in Table 16.

6. Smart wound dressing

Scientists have developed the long lasting and smart dressing which can detect drug release concentration and also has real-time monitoring facility [326,327]. Jin et al. developed photosensitive PCL/Poly(3-hexylthiophene) (P3HT) blend nanofibers for light stimulating dressing as different formulations were studied by varying the Poly(3-hexylthiophene) (P3HT) concentration. It was observed that PCL/P3HT (150:20) nanofibers have higher photon to electron transformation capability than PCL/P3HT (150:10) and PCL/P3HT (150:2) nanofibers. Biocompatibility of as-prepared nanofibers were confirm via culturing human dermal fibroblast and found that PCL/P3HT(150:10) nanofibers

Table 15
Co-axial hybrid nanofibers.

Materials		Fiber Diameter	Application	Condition	Properties/Results	Ref. no.
Core	Shell					
Regenerated silk fibroin (RSF) nanosphere/ Curcumin	Regenerated silk fibroin (RSF) based solution/Doxorubicin hydrochloride	1224 nm	Wound healing	*In vitro*	Drug release 30% in 10 h	[318]
Gum tragacanth (GT) + Tetracycline hydrochloride (TCH)	PLGA	180–460 nm	Periodontal regeneration	*In vitro*	Drug release 20% in 2 h	[319]

Table 16
Tri-axial polymer nanofibers.

Materials			Fiber Diameter	Application	Condition	Properties/Results	Composition	Ref. no.
Sheath layer	Middle layer	Core layer						
Ethanol/Hollow	Methacrylic acid/Methyl Methacrylate	Lecithin-Diclofenac sodium (PL-DS)	0.55 ± 0.06 μm	Oral colon-targeted drug delivery	*Ex vivo*	Drug release 15% in 3 h	P	[320]
PCL PCL CA	CA PVA PCL	Mineral oil/Hollow (H)	8.50 ± 1.57 μm 7.16 ± 1.59 μm 11.6 ± 3.92 μm	Wound healing	–	Break strength PCL/CA/H – 5 N PCL/PVA/H – 2 N CA/PCL/H – 1 N	P	[219]
Gelatin (GT)	PCL	Gelatin	1 μm	Wound healing	–	Composition GT:PCL:GT-17 wt%:11 wt%:10 wt%	P	[321]
CA	PCL	Polyvinylpyrrolidone (PVP) + Nisin	0.8 μm	Wound dressing	–	Antimicrobial resistance Triaxial fiber-6 days Coaxial fiber-2 days	DC	[322]
PCL-Hydrophilic Gelatin (GT)	Hydrophilic Gelatin (GT)	PCL-Hydrophilic Gelatin(GT) + Hydrophilic Doxycycline	30.0 ± 17.0 μm	Drug delivery	*In vitro*	Drug release PCL/GT blend fiber-95% in 24 h GT/PCL core/shell fibers-50% in 24 h Triaxial fibers-85% in 24 h	DC	[323]
Ethyl cellulose (EC) + Ketoprofen (KET)	Ethyl cellulose (EC) + Ketoprofen (KET)	Ethyl cellulose (EC) + Ketoprofen (KET)	0.74 ± 0.06 μm	Wound dressing	*In vitro*	Drug release 10% in 2 h	DC	[324]
Polyvinylpyrrolidone (PVP) + keyacid blue (KAB) dye	PCL	PCL + keyacid uranine (KAU) dye	0.702 μm	Wound dressing	–	Drug release 26% KAB in 4 h 85% KAU in 4 h	DC	[325]

P-Polymer nanofibers, DC-Drug loaded nanofibers.

has better cell adhesion and proliferation than other nanofibers formulations. Cell proliferation rate was higher in stimulated nanofibers scaffold than non-stimulated scaffold [328]. Patra et al. fabricated polyaniline-multiwall carbon nanotube/poly(N-isopropylacrylamide), (PANI-MWCNT/PNIPAm) multi-component nanofibers for advanced tissue restoration. It was found that tumor necrosis factor (presence of TNFα) assists in higher cell migration than absence of TNFα, thus these customized experimentation confirm the inflammation sensitive dressing competence. The polyaniline has lower critical solution temperature at 32 °C above which it shows hydrophobic interaction, as water molecule appear and makes the structure disintegrate, this event ease the cell migration and reduces the time required for tissue regeneration [329]. Tan et al. reported silver nitrate post-treated chitosan, gelatin and shape memory polyurethane (SMPU) blend nanofibers (CNM) for smart wound healing. Pristine SPMU nanofiber (135.7 ± 1.2°) has greater contact angle than CNM nanofibers (122.3 ± 2.5°) and pristine gelatin nanofibers (84.4 ± 2.8°), thus wettability data indicates that SPMU exerts hydrophobic behaviour which helps scaffold to become stable while water erosion. During wound healing most of the dressing tends to contract or expand according to scar formation, temperature fluctuations whereas the as-prepared nanofibers has capability to retain their shape even at low and high-temperature fluctuation owing to shape memory effect exerted by SPMU [330].

7. Drug delivery

The drug delivery is an important segment in wound healing owing to sudden increase in drug concentration in human body may lead to toxic effect [331] whereas slower sluggish release decreases the therapeutic efficiency. To design a controlled drug release system, drug release prediction was necessary thus mathematical models were utilized to determine exact mass transport and quantitative prediction of drug released. In general, hydrophilic drug release through simple diffusion whereas hydrophobic drug release through swelling or erosion of polymer matrix [332]. Drug release consists of zero order and first order release, thus zero order provides initial rapid release and first order release provides sustained release.

7.1. Mathematical models for drug release

A mathematical model based on distinct mathematical functions assists to evaluate the release profile. After selecting suitable function, mathematical models were applied. The important mathematical models are zero order, first order, Higuchi, Hixson–Crowell, Korsmeyer–Peppas, Baker–Lonsdale, Weibull, Gompertz, Ritger–Peppas, Korsmeyer–Peppas model and Hopfenberg, out of which zero order, first order, Hopfenberg model, Ritger–Peppas and Korsmeyer–Peppas models focuses on drug release profile of polymeric systems.

7.1.1. Zero order kinetics

The drug concentration in blood resides for short period of time mainly due to rapid absorption as well as rapid elimination. The time taken by bioactive agent to come out and exert the release effect is called therapeutic range. As the lower therapeutic range necessitates the repetitive dosing and hence controlling drug release become difficult. The velocity of dissolution demonstrates the amount of drug dissolved in specific time as considering the dissolution in kinetic process.

The equation of zero-order kinetics was mathematically represented as

$$f_i = K_0 t \tag{1}$$

where $f_i = 1 - (w_i/w_0)$ shows W_i is a remaining mass of drug, W_o is an initial mass of the drug during time t and K_0 is a dissolution velocity constant.

Table 17
Release exponent values of drug release mechanism.

Drug release mechanism	Geometry	Release exponent (n)	Ref.
Fickian diffusion	Cylindrical	0.43	[333]
Anomalous transport	Cylindrical	0.45 < n < 0.89	
Case II transport	Cylindrical	0.89	
Super Case II transport	Cylindrical	n > 0.89	

$$C_t = C_0 + K_0 t \quad (2)$$

where C_t shows amount of active release of drug during time t, C_0 is initial concentration of active release generally C_0 is zero and zero order concentration represented by K_0.

In zero-order kinetics, the release was only time-dependent and constant rate of process is independent on active drug concentration.

7.1.2. First-order kinetics

This mathematical expression utilized to depict the absorption or elimination of drug. First order kinetics states that change in concentration with respect to change in time is dependent only on concentration.

$$\log Q_1 = \log Q_0 + \frac{k_1 t}{2.303} \quad (3)$$

where Q_1 is amount of drug release in time t, Q_0 is initial amount of drug dissolved and K_1 is first-order constant.

The curvature of graph resulted due to $k_1/2.303$ (angular coefficient) and linear nature is due to log Q_0 (linear coefficient) [333].

7.1.3. Korsmeyer–Peppas model and Ritger–Peppas model

Korsmeyer et al. and Ritger et al. developed drug release model for the polymeric system; this model established the exponential relationship between drug release and time [334,335].

$$f_1 = \frac{M_i}{M_\infty} = Kt^n \quad (4)$$

where f_i is mass of drug release, M_∞ is mass of drug at equilibrium state, M_i is mass of drug released in time t, K is structural and geometrical constant and n is the exponent of release (related to mechanism of release) in time t.

Further Kim et al. proposed the mathematical model for rapid initial drug release (burst effect) [336] is given by

$$\frac{M_i}{M_\infty} = Kt^n + b \quad (5)$$

where b is burst effect

7.1.4. Hopfenberg model

Katzhendler et al. reported drug release model for erodible polymers and different geometrical systems such as film, sphere and cylinders [337], thus the proposed equation is given below,

$$\frac{M_t}{M_\infty} = 1 - \left[1 - \frac{k_0 t}{C_0 a_0}\right]^n \quad (6)$$

where M_t is mass of drug release at time t, M_∞ is mass of drug release at infinite time, fraction of drug dissolved is M_t/M_∞, k_0 is erosion grade constant, C_0 is initial concentration of drug in matrix, a_0 is initial radius of the cylinder and n = 2 for cylinder.

7.2. Drug release mechanism

There are two types of drug release mechanism, Fickian and Non-Fickian mechanism.

7.2.1. Fickian mechanism (Case I)

The drug release is administered by diffusion, solvent transit rate, thus diffusion was higher than polymer chain relaxation process. As the surface absorption takes place at higher rate than solvent underneath the surface due to higher exposure time and diffusion is time-dependent phenomenon [338].

7.2.2. Non-Fickian mechanism

Non-Fickian mechanism (case II) is correlated via zero-order kinetics and swelling as well as relaxation of polymer chains drives the drug release. Swelling produces the jelly region outside and vitreous region inside of polymeric geometry. Thus in initial stage, diffusion of jelly region is greater than vitereous region. At last accelerated absorption rate was observed due to forces exerted by swelling on viterous region. Non-Fickian (Anomalous transport) mechanism executed via combined effect of diffusion and swelling in which gradually rearrangement of polymer chains occurs and concurrently diffusion motivate the anomalous transport. Non-Fickian (Super Case II) mechanism is an intense form of transport accomplished by solvent crazing which is the breaking and tension of polymeric chain while absorption. Outer layer exerts the compression stress on the nucleus, thus extended stress break the nucleus. The main difference between Case II, Anomalous transport and super case II was velocity of diffusion [339]. Release exponent (n) values of drug release mechanisms are consolidated in Table 17.

8. Life Cycle Assessment (LCA)

The wound dressing should be designed considering its impact on environmental and at last, the cost of the dressing as the commercial viability of product depends on the cost. Life cycle assessment is an entire analysis of the product from its origin to its post end use management. Truong et al. reviewed the commercial wound dressing products such as noncellular dermal matrix, Integra, Dermagraft-TC, Dermalogen, or Alloderm and compared their performance with control group. Alloderm was a collagen-based matrix acquired from human skin, Dermagraft-TC is made up of nitted absorbant biopolymer porous film from polylactic and polyglycolic acids, Dermalogen consist of human dermal collagen matrix in powder form. Integra was a human skin biomimetic film contains bovin collagen which was crosslinked with the help of shark chondroitin-6-sulfate. Wound contraction results shows that Dermagraft-TC (50% ± 22%) has higher wound contraction than Integra (46% ± 12%), Dermalogen (39% ± 9%) and controlled wound (34% ± 7%) [340]. Comparison data of commercial dressing are consolidated in Table 18.

The cost of individual passive dressing was less compared to vapour-permeable nanofibers dressing but as shown in Fig. 10 passive dressing is need to change in every 3–4 times per day so the overall cost of the passive dressing ($ 110) was greater than air permeable nanofiber based dressing ($ 8) [341]. The commercial products are based on the biological molecules such as growth factor, proteins embedded polymer matrix where the biological molecule imparts excellent biocompatibility, cell adhesion, as well as proliferation and polymer matrix, assist in safe delivery of biological molecule by acting as a carrier which disintegrates after post delivery. Currently, Dermagraft-TC is one of the promising dressing to heal faster although research is necessary to enhance the efficiency of the carrier and further reduces the wound contraction time.

9. Conclusion and future perspectives

The wound care management is growing faster day by day due to increase in world population (8.223 billion in 2016), chronic wound incidents also increases although appropriate medication can successfully defeat the slow wound healing and inhibit wound infection, therefore, dermatologist, pharmacologist and engineers need to work

Table 18
Nanofiber-based commercial dressings.

Commercial product	Cost/100 cm^2	Materials	Structural form	Application	Manufacturer
Integra™	$ 49.5	Silicone/collagen	Bilayer matrix	Ulcer wound	Integra Life Sciences (http://www.ilstraining.com/default.html)
Dermafill™	$ 120.5	Cellulose	Foam	Accidental wound	DERMAFILL (http://www.dermafill.fr/)
Kerlix AMD™	$ 0.222	Polyhexamethylene biguanide	Gauze/Spong	Antibacterial dressing	Kendall (http://hrhealthcare.co.uk/)
Biobrane™	$ 1.7	Silicon/nylon/collagen	Fibers	Superficial and partial-thickness wounds	Smith & Nephew (http://www.smith-nephew.com/)
AlloDerm®	$ 2475	Collagen matrix	Fibers	Regenerative tissue	AlloDerm SELECT (http://hcp.alloderm.com/)
Apligraf®	$ 27.1	Bovine collagen	Membrane	Chronic venous leg ulcers and diabetic foot ulcers	Novartis (http://www.apligraf.com/)
DuoDERM®	$ 0.412	–	Hydrocolloids	Dry to lightly exuding wounds	Convatec (https://www.convatec.com/)
Permacol™	$ 14.6	Collagen	–	Surgical wound	Medtronic (http://www.medtronic.com/covidien/en-us/index.html)

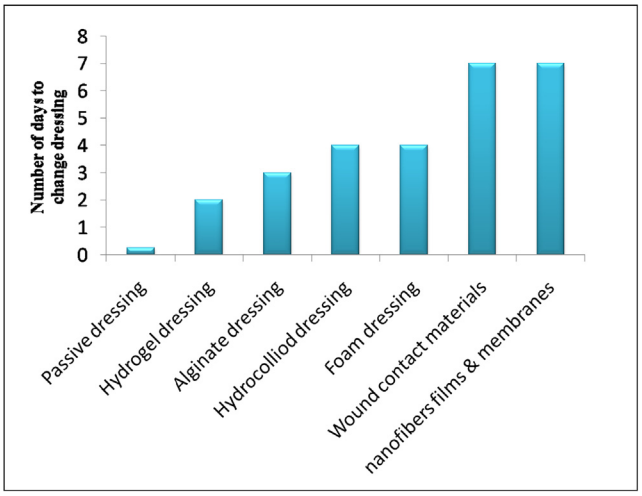

Fig. 10. Graphical demonstration of No. of days to change dressing versus topological forms of dressing.

together in this direction for better understanding of wound healing events, improved drug effectiveness and improved drug delivery system for sustain release profile respectively. This review paper describes the intricate wound healing process and events related to them as well as the comprehensive nano/micro-fibres based wound healing scaffold according to the improved efficiency of drug release. Mathematical models were also explained where the drug release profile and theoretical drug release profile can also be predicted and correlated with these models. The tri-axial electrospun fiber based scaffold shows better drug release due to its dual barrier layer which slowed down the diffusion of the drug from scaffold even multiple drug incorporation can also be possible, since it has a high specific surface area, high porosity and oxy-permeability and bacterial resistance. As limited research data is present in the world on tri-axial nanofibers dressing, this can be a potential area of research in future. The dressing can be made in such a way that they have the combination of drugs and biological molecule which should be release according to wound healing stages and help individual stage for accelerated wound healing. Thus this is only possible with the tri-axial nanofibers and careful selection of polymer matrix according to their degradation time. The advanced technology in emerging smart dressing can also assist in better care of the wound and for real-time monitoring. Life cycles assessment shows that nanofibers based dressing have better properties compared to conventional dressing in the context of cost, wound healing time and efficient drug delivery.

Acknowledgement

The authors would like to thank Dr. C. P. Ramanarayanan, Vice-Chancellor, DIAT (DU), Pune, for constant encouragement and support. The authors would also like to acknowledge Mr. Prakash Gore, Mr. Swaroop Gharde, Mr. Deepak Prajapati, and Mr. Jay Korde for technical discussions and support.

References

[1] G. Broughton, J.E. Janis, C.E. Attinger, A brief history of wound care, Plast. Reconstr. Surg. 117 (2006) 6–11, https://doi.org/10.1097/01.prs.0000225429.76355.dd.
[2] M. Gizaw, J. Thompson, A. Faglie, S.-Y. Lee, P. Neuenschwander, S.-F. Chou, Electrospun fibers as a dressing material for drug and biological agent delivery in wound healing applications, Bioengineering 5 (2018) 9, https://doi.org/10.3390/bioengineering5010009.
[3] P. Beldon, Basic science of wound healing, Surgery 28 (2010) 409–412, https://doi.org/10.1016/j.mpsur.2010.05.007.
[4] M.A. Fonder, G.S. Lazarus, D.A. Cowan, B. Aronson-Cook, A.R. Kohli, A.J. Mamelak, Treating the chronic wound: a practical approach to the care of

nonhealing wounds and wound care dressings, J. Am. Acad. Dermatol. 58 (2008) 185–206, https://doi.org/10.1016/j.jaad.2007.08.048.
[5] S. Bhattacharya, Wound healing through the ages, Indian J. Plast. Surg. 45 (2012) 177, https://doi.org/10.4103/0970-0358.101255.
[6] M. Loukas, A. Lanteri, J. Ferrauiola, R.S. Tubbs, G. Maharaja, M.M. Shoja, A. Yadav, V.C. Rao, Anatomy in ancient India: a focus on the Susruta Samhita, J. Anat. 217 (2010) 646–650, https://doi.org/10.1111/j.1469-7580.2010.01294.x.
[7] V. Sreedevi, R. Tripathy, A.N. Nj, N.S. John, P. Suresh, Conventional care of wounded in Susruta Samhita — a review, Int. J. Ayurvedic Med. 7 (2016) 21–23 Review Article.
[8] A.J.M. Boulton, The diabetic foot, 2019. https://doi.org/10.1016/j.mpmed.2018.11.001.
[9] F. Köckerling, D. Köckerling, C. Lomas, Cornelius Celsus – ancient encyclopedist, surgeon-scientist, or master of surgery? Langenbeck's Arch. Surg. 398 (2013) 609–616, https://doi.org/10.1007/s00423-013-1050-0.
[10] I. Gibas, Helena Janik, Review: synthetic polymer hydrogels for biomedical applications, Chem. Chem. Technol. 4 (2010), https://doi.org/10.1016/S1044-7431(03)00174-X.
[11] G.D. Winter, Formation of the scab and the rate of epithelization of superficial wounds in the skin of the young domestic pig, Nature 193 (1962) 293–294, https://doi.org/10.1038/193293a0.
[12] M.S. Khil, D. Il Cha, H.Y. Kim, I.S. Kim, N. Bhattarai, Electrospun nanofibrous polyurethane membrane as wound dressing, J. Biomed. Mater. Res. - Part B Appl. Biomater. 67 (2003) 675–679, https://doi.org/10.1002/jbm.b.10058.
[13] F.L. Mi, S.S. Shyu, Y.B. Wu, S.T. Lee, J.Y. Shyong, R.N. Huang, Fabrication and characterization of a sponge-like asymmetric chitosan membrane as a wound dressing, Biomaterials 22 (2001) 165–173, https://doi.org/10.1016/S0142-9612(00)00167-8.
[14] W.K. Czaja, D.J. Young, M. Kawecki, R.M. Brown, The future prospects of microbial cellulose in biomedical applications, Biomacromolecules 8 (2007) 1–12, https://doi.org/10.1021/bm060620d.
[15] A. Davis, K. Balasubramanian, Bioactive hybrid composite membrane with enhanced antimicrobial properties for biomedical applications, Def. Sci. J. 66 (2016) 434–438, https://doi.org/10.14429/dsj.66.10218.
[16] R. Yadav, B. Kandasubramanian, Egg albumin PVA hybrid membranes for antibacterial application, Mater. Lett. 110 (2013) 130–133, https://doi.org/10.1016/j.matlet.2013.07.109.
[17] K. Ramdayal, Balasubramanian, antibacterial application of polyvinylalcohol-nanogold composite membranes, Colloids Surf. A Physicochem. Eng. Asp. 455 (2014) 174–178, https://doi.org/10.1016/j.colsurfa.2014.04.050.
[18] V. Verma, K. Balasubramanian, Experimental and theoretical investigations of Lantana camara oil diffusion from polyacrylonitrile membrane for pulsatile drug delivery system, Mater. Sci. Eng. C 41 (2014) 292–300, https://doi.org/10.1016/j.msec.2014.04.061.
[19] G. Sun, X. Zhang, Y.-I. Shen, R. Sebastian, L.E. Dickinson, K. Fox-Talbot, M. Reinblatt, C. Steenbergen, J.W. Harmon, S. Gerecht, Dextran hydrogel scaffolds enhance angiogenic responses and promote complete skin regeneration during burn wound healing, Proc. Natl. Acad. Sci. 108 (2011) 20976–20981, https://doi.org/10.1073/pnas.1115973108.
[20] F. Yoshii, Y. Zhanshan, K. Isobe, K. Shinozaki, K. Makuuchi, Electron beam crosslinked PEO and PEO/PVA hydrogels for wound dressing, Radiat. Phys. Chem. 55 (1999) 133–138, https://doi.org/10.1016/S0969-806X(98)00318-1.
[21] P.T. Sudheesh Kumar, V.K. Lakshmanan, T.V. Anilkumar, C. Ramya, P. Reshmi, A.G. Unnikrishnan, S.V. Nair, R. Jayakumar, Flexible and microporous chitosan hydrogel/nano ZnO composite bandages for wound dressing: In vitro and in vivo evaluation, ACS Appl. Mater. Interfaces 4 (2012) 2618–2629 https://doi.org/10.1021/am300292v.
[22] M. Kokabi, M. Sirousazar, Z.M. Hassan, PVA-clay nanocomposite hydrogels for wound dressing, Eur. Polym. J. 43 (2007) 773–781, https://doi.org/10.1016/j.eurpolymj.2006.11.030.
[23] K.K.G. Premika, K. Balasubramanian, Advanced Polymeric Materials From Macro- to Nano-Length Scales, CRC Press, 2016.
[24] P. Rastogi, B. Kandasubramanian, Breakthrough in the printing tactics for stimuli-responsive materials: 4D printing, Chem. Eng. J. 366 (2019) 264–304, https://doi.org/10.1016/j.cej.2019.02.085.
[25] S. Gharde, A. Surendren, J.M. Korde, S. Saini, N. Deoray, R. Goud, S. Nimje, B. Kandasubramanian, Recent advances in additive manufacturing of bio-inspired materials, in: Biomanufacturing, Springer International Publishing, Cham, 2019, pp. 35–68. http://doi.org/10.1007/978-3-030-13951-3_2.
[26] A.D. Sezer, F. Hatipoglu, E. Cevher, Z. Oğurtan, A.L. Bas, J. Akbuğa, Chitosan film containing fucoidan as a wound dressing for dermal burn healing: preparation and in vitro/in vivo evaluation, AAPS PharmSciTech. 8 (2007) E94–E101, https://doi.org/10.1208/pt0802039.
[27] Y. Pranoto, S.K. Rakshit, V.M. Salokhe, Enhancing antimicrobial activity of chitosan films by incorporating garlic oil, potassium sorbate and nisin, LWT – Food Sci. Technol. 38 (2005) 859–865, https://doi.org/10.1016/j.lwt.2004.09.014.
[28] T. Kitagawa, K. Yabuki, Physical properties of silk fibroin/chitosan blend films, J. Appl. Polym. Sci. 80 (2001) 928–934, https://doi.org/10.1002/app.1172.
[29] D. Altiok, E. Altiok, F. Tihminlioglu, Physical, antibacterial and antioxidant properties of chitosan films incorporated with thyme oil for potential wound healing applications, J. Mater. Sci. Mater. Med. 21 (2010) 2227–2236, https://doi.org/10.1007/s10856-010-4065-x.
[30] S. Anjum, A. Sharma, M. Tummalapalli, J. Joy, S. Bhan, B. Gupta, A novel route for the preparation of silver loaded polyvinyl alcohol nanogels for wound care systems, Int. J. Polym. Mater. Polym. Biomater. 64 (2015) 894–905, https://doi.org/10.1080/00914037.2015.1030660.
[31] M. Zafar, T. Shah, A. Rawal, E. Siores, Preparation and characterisation of thermoresponsive nanogels for smart antibacterial fabrics, Mater. Sci. Eng. C 40 (2014) 135–141, https://doi.org/10.1016/j.msec.2014.03.033.
[32] V.J. Cornelius, N. Majcen, M.J. Snowden, J.C. Mitchell, B. Voncina, Preparation of SMART wound dressings based on colloidal microgels and textile fibres, Int. Soc. Opt. Photon. 6413 (2006) 64130X, https://doi.org/10.1117/12.712573.
[33] K. Madhumathi, P.T. Sudheesh Kumar, S. Abhilash, V. Sreeja, H. Tamura, K. Manzoor, S.V. Nair, R. Jayakumar, Development of novel chitin/nanosilver composite scaffolds for wound dressing applications, J. Mater. Sci. Mater. Med. 21 (2010) 807–813, https://doi.org/10.1007/s10856-009-3877-z.
[34] M. Burkatovskaya, A.P. Castano, T.N. Demidova-Rice, G.P. Tegos, M.R. Hamblin, Effect of chitosan acetate bandage on wound healing in infected and noninfected wounds in mice, Wound Repair Regen. 16 (2008) 425–431, https://doi.org/10.1111/j.1524-475X.2008.00382.x.
[35] E.J. Chong, T.T. Phan, I.J. Lim, Y.Z. Zhang, B.H. Bay, S. Ramakrishna, C.T. Lim, Evaluation of electrospun PCL/gelatin nanofibrous scaffold for wound healing and layered dermal reconstitution, Acta Biomater. 3 (2007) 321–330, https://doi.org/10.1016/j.actbio.2007.01.002.
[36] X. Fan, K. Chen, X. He, N. Li, J. Huang, K. Tang, Y. Li, F. Wang, Nano-TiO2/collagen-chitosan porous scaffold for wound repairing, Int. J. Biol. Macromol. 91 (2016) 15–22, https://doi.org/10.1016/j.ijbiomac.2016.05.094.
[37] R. Yadav, K. Balasubramanian, Polyacrylonitrile/Syzygium aromaticum hierarchical hydrophilic nanocomposite as a carrier for antibacterial drug delivery systems, RSC Adv. 5 (2015) 3291–3298, https://doi.org/10.1039/c4ra12755b.
[38] A.E. Purushothaman, K. Thakur, B. Kandasubramanian, Development of highly porous, Electrostatic force assisted nanofiber fabrication for biological applications, Int. J. Polym. Mater. Polym. Biomater. (2019) 1–28, https://doi.org/10.1080/00914037.2019.1581197.
[39] M. Abrigo, S.L. McArthur, P. Kingshott, Electrospun nanofibers as dressings for chronic wound care: advances, challenges, and future prospects, Macromol. Biosci. 14 (2014) 772–792, https://doi.org/10.1002/mabi.201300561.
[40] M.Á.R. Calderón, W. Zhao, Applications of Polymer Nanofibers in Bio-Materials, Biotechnology and Biomedicine: A Review, TMS 2014 143rd Annu. Meet. Exhib., vol. 125, 2014, pp. 401–414. https://doi.org/10.1007/978-3-319-48237-8_50.
[41] R. Yadav, K. Balasubramanian, Bioabsorbable engineered nanobiomaterials for antibacterial therapy, Eng. Nanobiomater. Appl. Nanobiomater. Elsevier (2016) 77–117, https://doi.org/10.1016/B978-0-323-41532-3.00003-8.
[42] D.G. Castner, B.D. Ratner, Biomedical surface science: Foundations to frontiers, 2002. https://doi.org/10.1016/S0039-6028(01)01587-4.
[43] P.M. Gore, A. Purushothaman, M. Naebe, X. Wang, B. Kandasubramanian, Nanotechnology for Oil-Water Separation, in: 2019, pp. 299–339. https://doi.org/10.1007/978-3-030-02381-2_14.
[44] P.M. Gore, B. Kandasubramanian, Heterogeneous wettable cotton based superhydrophobic Janus biofabric engineered with PLA/functionalized-organoclay microfibers for efficient oil–water separation, J. Mater. Chem. A 6 (2018) 7457–7479, https://doi.org/10.1039/C7TA11260B.
[45] P.M. Gore, M. Dhanshetty, K. Balasubramanian, Bionic creation of nano-engineered Janus fabric for selective oil/organic solvent absorption, RSC Adv. 6 (2016) 111250–111260, https://doi.org/10.1039/C6RA24106A.
[46] E.K.F. Yim, E.M. Darling, K. Kulangara, F. Guilak, K.W. Leong, Nanotopography-induced changes in focal adhesions, cytoskeletal organization, and mechanical properties of human mesenchymal stem cells, Biomaterials 31 (2010) 1299–1306, https://doi.org/10.1016/j.biomaterials.2009.10.037.
[47] D. Pamfil, E. Butnaru, C. Vasile, Poly (vinyl alcohol)/chitosan cryogels as PH responsive ciprofloxacin carriers, J. Polym. Res. 23 (2016), https://doi.org/10.1007/s10965-016-1042-1.
[48] R.S. Ambekar, B. Kandasubramanian, A polydopamine-based platform for anticancer drug delivery, Biomater. Sci. (2019), https://doi.org/10.1039/c8bm01642a.
[49] P. Neeraja, V. Mohanachari, K. Indira, K.S. Swami, Metabolic changes in kidney of mice on alloxan treatment, Indian J. Exp. Biol. 18 (1980) 1331–1333, https://doi.org/10.1016/j.addr.2012.05.006.
[50] Y. Su, Q. Su, W. Liu, M. Lim, J.R. Venugopal, X. Mo, S. Ramakrishna, S.S. Al-Deyab, M. El-Newehy, Controlled release of bone morphogenetic protein 2 and dexamethasone loaded in core-shell PLLACL-collagen fibers for use in bone tissue engineering, Acta Biomater. 8 (2012) 763–771, https://doi.org/10.1016/j.actbio.2011.11.002.
[51] Y.-C. Chiu, E.L. Fong, B.J. Grindel, F.K. Kasper, D.A. Harrington, M.C. Farach-Carson, Sustained delivery of recombinant human bone morphogenetic protein-2 from perlecan domain I - functionalized electrospun poly (ε-caprolactone) scaffolds for bone regeneration, J. Exp. Orthop. 3 (2016) 25, https://doi.org/10.1186/s40634-016-0057-1.
[52] N. Manhas, K. Balasubramanian, P. Prajith, P. Rule, S. Nimje, PCL/PVA nanoencapsulated reinforcing fillers of steam exploded/autoclaved cellulose nanofibrils for tissue engineering applications, RSC Adv. 5 (2015) 23999–24008, https://doi.org/10.1039/C4RA17191H.
[53] H. Liu, Y. Zhou, S. Chen, M. Bu, J. Xin, S. Li, Current sustained delivery strategies for the design of local neurotrophic factors in treatment of neurological disorders, Asian J. Pharm. Sci. 8 (2013) 269–277, https://doi.org/10.1016/j.ajps.2013.10.003.
[54] Q. Liu, J. Huang, H. Shao, L. Song, Y. Zhang, Dual-factor loaded functional silk fibroin scaffolds for peripheral nerve regeneration with the aid of neovascularization, RSC Adv. 6 (2016) 7683–7691, https://doi.org/10.1039/c5ra22054h.
[55] C. Huang, Y. Ouyang, H. Niu, N. He, Q. Ke, X. Jin, D. Li, J. Fang, W. Liu, C. Fan, T. Lin, Nerve guidance conduits from aligned nanofibers: improvement of nerve regeneration through longitudinal nanogrooves on a fiber surface, ACS Appl.

Mater. Interfaces 7 (2015) 7189–7196, https://doi.org/10.1021/am509227t.
[56] Y. Yang, T. Xia, W. Zhi, L. Wei, J. Weng, C. Zhang, X. Li, Promotion of skin regeneration in diabetic rats by electrospun core-sheath fibers loaded with basic fibroblast growth factor, Biomaterials 32 (2011) 4243–4254, https://doi.org/10.1016/j.biomaterials.2011.02.042.
[57] H.J. Lai, C.H. Kuan, H.C. Wu, J.C. Tsai, T.M. Chen, D.J. Hsieh, T.W. Wang, Tailored design of electrospun composite nanofibers with staged release of multiple angiogenic growth factors for chronic wound healing, Acta Biomater. 10 (2014) 4156–4166, https://doi.org/10.1016/j.actbio.2014.05.001.
[58] M.W. Laschke, M.D. Menger, Vascularization in tissue engineering: angiogenesis versus inosculation, Eur. Surg. Res. 48 (2012) 85–92, https://doi.org/10.1159/000336876.
[59] R.S. Ambekar, B. Kandasubramanian, Progress in the advancement of porous biopolymer scaffold: tissue engineering application, Ind. Eng. Chem. Res. (2019), https://doi.org/10.1021/acs.iecr.8b05334 acs.iecr.8b05334.
[60] J.M. Korde, B. Kandasubramanian, Biocompatible alkyl cyanoacrylates and their derivatives as bio-adhesives, Biomater. Sci. 6 (2018) 1691–1711, https://doi.org/10.1039/c8bm00312b.
[61] K. Balasubramanian, K.M. Kodam, Encapsulation of therapeutic lavender oil in an electrolyte assisted polyacrylonitrile nanofibres for antibacterial applications, RSC Adv. 4 (2014) 54892–54901, https://doi.org/10.1039/C4RA09425E.
[62] K. Balasubramanian, R. Yadav, P. Prajith, Antibacterial nanofibers of polyoxymethylene/gold for pro-hygiene applications, Int. J. Plast. Technol. 19 (2015) 363–367, https://doi.org/10.1007/s12588-015-9127-y.
[63] Q. Zhang, Y. Li, Z.Y. William Lin, K.K.Y. Wong, M. Lin, L. Yildirimer, X. Zhao, Electrospun polymeric micro/nanofibrous scaffolds for long-term drug release and their biomedical applications, Drug Discov. Today 22 (2017) 1351–1366, https://doi.org/10.1016/j.drudis.2017.05.007.
[64] J. Ahmed, E. Altun, M.O. Aydogdu, O. Gunduz, L. Kerai, G. Ren, M. Edirisinghe, Anti-fungal bandages containing cinnamon extract, Int. Wound J. (2019), https://doi.org/10.1111/iwj.13090.
[65] E. Altun, M.O. Aydogdu, F. Koc, M. Crabbe-Mann, F. Brako, R. Kaur-Matharu, G. Ozen, S.E. Kuruca, U. Edirisinghe, O. Gunduz, M. Edirisinghe, Novel making of bacterial cellulose blended polymeric fiber bandages, Macromol. Mater. Eng. 303 (2018) 1700607, https://doi.org/10.1002/mame.201700607.
[66] E. Altun, M.O. Aydogdu, M. Crabbe-Mann, J. Ahmed, F. Brako, B. Karademir, B. Aksu, M. Sennaroglu, M.S. Eroglu, G. Ren, O. Gunduz, M. Edirisinghe, Co-culture of keratinocyte-Staphylococcus aureus on Cu-Ag-Zn/CuO and Cu-Ag-W nanoparticle loaded bacterial cellulose:PMMA bandages, Macromol. Mater. Eng. 304 (2019) 1800537, https://doi.org/10.1002/mame.201800537.
[67] P.L. Heseltine, J. Ahmed, M. Edirisinghe, Developments in pressurized gyration for the mass production of polymeric fibers, Macromol. Mater. Eng. 303 (2018) 1800218, https://doi.org/10.1002/mame.201800218.
[68] A.I. Freeman, E. Mayhew, Targeted drug delivery, in: Cancer, Elsevier, 1986, pp. 573–583. https://doi.org/10.1002/1097-0142(19860715)58:2+<573::AID-CNCR2820581328>3.0.CO;2-C.
[69] Y. Fu, W.J. Kao, Drug release kinetics and transport mechanisms of non-degradable and degradable polymeric delivery systems, Expert Opin. Drug Deliv. 7 (2010) 429–444, https://doi.org/10.1517/17425241003602259.
[70] Z.M. Huang, C.L. He, A. Yang, Y. Zhang, X.J. Han, J. Yin, Q. Wu, Encapsulating drugs in biodegradable ultrafine fibers through co-axial electrospinning, J. Biomed. Mater. Res. – Part A 77 (2006) 169–179, https://doi.org/10.1002/jbm.a.30564.
[71] J.J. Rogalski, C.W.M. Bastiaansen, T. Peijs, Rotary jet spinning review – a potential high yield future for polymer nanofibers, Nanocomposites 3 (2017) 97–121, https://doi.org/10.1080/20550324.2017.1393919.
[72] H. Lee, K. Watanabe, M. Kim, M. Gopiraman, K.H. Song, J.S. Lee, I.S. Kim, Handspinning enabled highly concentrated carbon nanotubes with controlled orientation in nanofibers, Sci. Rep. 6 (2016) 37590, https://doi.org/10.1038/srep37590.
[73] P.L. Heseltine, J. Hosken, C. Agboh, D. Farrar, S. Homer-Vanniasinkam, M. Edirisinghe, Fiber formation from silk fibroin using pressurized gyration, Macromol. Mater. Eng. 304 (2019) 1800577, https://doi.org/10.1002/mame.201800577.
[74] J. Tahalyani, S. Datar, K. Balasubramanian, Investigation of dielectric properties of free standing electrospun nonwoven mat, J. Appl. Polym. Sci. 135 (2018) 46121, https://doi.org/10.1002/app.46121.
[75] X. Ren, Y. Han, J. Wang, Y. Jiang, Z. Yi, H. Xu, Q. Ke, An aligned porous electrospun fibrous membrane with controlled drug delivery – an efficient strategy to accelerate diabetic wound healing with improved angiogenesis, Acta Biomater. 70 (2018) 140–153, https://doi.org/10.1016/j.actbio.2018.02.010.
[76] G. Kabay, A.E. Meydan, G. Kaleli Can, C. Demirci, M. Mutlu, Controlled release of a hydrophilic drug from electrospun amyloid-like protein blend nanofibers, Mater. Sci. Eng. C 81 (2017) 271–279, https://doi.org/10.1016/j.msec.2017.08.003.
[77] A. Prasad, B. Kandasubramanian, Fused deposition processing polycaprolactone of composites for biomedical applications, Polym. Technol. Mater. (2019) 1–34, https://doi.org/10.1080/25740881.2018.1563117.
[78] A. Aytimur, S. Koçyiıit, I. Uslu, F. Gökmeşe, Preparation and characterization of polyvinyl alcohol based copolymers as wound dressing fibers, Int. J. Polym. Mater. Polym. Biomater. 64 (2015) 111–116, https://doi.org/10.1080/00914037.2014.891118.
[79] S.J. Liu, Y.C. Kau, C.Y. Chou, J.K. Chen, R.C. Wu, W.L. Yeh, Electrospun PLGA/collagen nanofibrous membrane as early-stage wound dressing, J. Memb. Sci. 355 (2010) 53–59, https://doi.org/10.1016/j.memsci.2010.03.012.
[80] Z.X. Cai, X.M. Mo, K.H. Zhang, L.P. Fan, A.L. Yin, C.L. He, H.S. Wang, Fabrication of chitosan/silk fibroin composite nanofibers for wound-dressing applications, Int. J. Mol. Sci. 11 (2010) 3529–3539, https://doi.org/10.3390/ijms11093529.
[81] N. Abdolhi, A. Soltani, H.K. Fadafan, V. Erfani-Moghadam, A.D. Khalaji, H. Balakheyli, Preparation, characterization and toxicity evaluation of Co_3O_4 and NiO-filled multi-walled carbon nanotubes loaded to chitosan, Nano-Struct. Nano-Objects 12 (2017) 182–187, https://doi.org/10.1016/j.nanoso.2017.09.008.
[82] N. Naseri, C. Algan, V. Jacobs, M. John, K. Oksman, A.P. Mathew, Electrospun chitosan-based nanocomposite mats reinforced with chitin nanocrystals for wound dressing, Carbohydr. Polym. 109 (2014) 7–15, https://doi.org/10.1016/j.carbpol.2014.03.031.
[83] D.G. Yu, J.H. Yu, L. Chen, G.R. Williams, X. Wang, Modified coaxial electrospinning for the preparation of high-quality ketoprofen-loaded cellulose acetate nanofibers, Carbohydr. Polym. 90 (2012) 1016–1023, https://doi.org/10.1016/j.carbpol.2012.06.036.
[84] L. Bacakova, J. Pajorova, M. Bacakova, A. Skogberg, P. Kallio, K. Kolarova, V. Svorcik, Versatile application of nanocellulose: from industry to skin tissue engineering and wound healing, Nanomaterials 9 (2019) 164, https://doi.org/10.3390/nano9020164.
[85] M. Bacakova, J. Pajorova, T. Sopuch, L. Bacakova, Fibrin-modified cellulose as a promising dressing for accelerated wound healing, Materials (Basel). 11 (2018) 2314, https://doi.org/10.3390/ma11112314.
[86] N. Ninan, M. Muthiah, I.K. Park, N. Kalarikkal, A. Elain, T. Wui Wong, S. Thomas, Y. Grohens, Wound healing analysis of pectin/carboxymethyl cellulose/microfibrillated cellulose based composite scaffolds, Mater. Lett. 132 (2014) 34–37, https://doi.org/10.1016/j.matlet.2014.06.056.
[87] E.R. Kenawy, F.I. Abdel-Hay, M.H. El-Newehy, G.E. Wnek, Controlled release of ketoprofen from electrospun poly(vinyl alcohol) nanofibers, Mater. Sci. Eng. A 459 (2007) 390–396, https://doi.org/10.1016/j.msea.2007.01.039.
[88] H. Zhang, S. Lou, G.R. Williams, C. Branford-White, H. Nie, J. Quan, L.M. Zhu, A systematic study of captopril-loaded polyester fiber mats prepared by electrospinning, Int. J. Pharm. 439 (2012) 100–108, https://doi.org/10.1016/j.ijpharm.2012.09.055.
[89] C.L. He, Z.M. Huang, X.J. Han, L. Liu, H.S. Zhang, L.S. Chen, Coaxial electrospun poly(L-lactic acid) ultrafine fibers for sustained drug delivery, J. Macromol. Sci. Part B Phys. 45 B (2006) 515–524, https://doi.org/10.1080/00222340600769832.
[90] M.R. Mohammadi, S. Rabbani, S.H. Bahrami, M.T. Joghataei, F. Moayer, Antibacterial performance and in vivo diabetic wound healing of curcumin loaded gum tragacanth/poly(ε-caprolactone) electrospun nanofibers, Mater. Sci. Eng. C. 69 (2016) 1183–1191, https://doi.org/10.1016/j.msec.2016.08.032.
[91] P. Govindaraj, B. Kandasubramanian, K.M. Kodam, Molecular interactions and antimicrobial activity of curcumin (Curcuma longa) loaded polyacrylonitrile films, Mater. Chem. Phys. 147 (2014) 934–941, https://doi.org/10.1016/j.matchemphys.2014.06.040.
[92] K. Ghosal, C. Agatemor, Z. Špitálsky, S. Thomas, E. Kny, Electrospinning tissue engineering and wound dressing scaffolds from polymer-titanium dioxide nanocomposites, Chem. Eng. J. 358 (2019) 1262–1278, https://doi.org/10.1016/j.cej.2018.10.117.
[93] S.D. Lakshmi, P.K. Avti, G. Hegde, Activated carbon nanoparticles from biowaste as new generation antimicrobial agents: a review, Nano-Struct. Nano-Objects 16 (2018) 306–321, https://doi.org/10.1016/j.nanoso.2018.08.001.
[94] M. Hudlikar, K. Balasubramanian, K. Kodam, Towards the enhancement of antimicrobial efficacy and hydrophobization of chitosan, J. Chitin Chitosan Sci. 2 (2014) 273–279, https://doi.org/10.1166/jcc.2014.1080.
[95] I.B.J.G. Debats, T.G.A.M. Wolfs, T. Gotoh, J.P.M. Cleutjens, C.J. Peutz-Kootstra, R.R.W.J. van der Hulst, Role of arginine in superficial wound healing in man, Nitric Oxide – Biol. Chem. 21 (2009) 175–183, https://doi.org/10.1016/j.niox.2009.07.006.
[96] S.R. Young, M. Dyson, Effect of therapeutic ultrasound on the healing of full-thickness excised skin lesions, Ultrasonics 28 (1990) 175–180, https://doi.org/10.1016/0041-624X(90)90082-Y.
[97] M. Tsutsumi, M. Denda, Paradoxical effects of ??-estradiol on epidermal permeability barrier homeostasis, Br. J. Dermatol. 157 (2007) 776–779, https://doi.org/10.1111/j.1365-2133.2007.08115.x.
[98] F.M. Hendriks, D. Brokken, C.W.J. Oomens, D.L. Bader, F.P.T. Baaijens, The relative contributions of different skin layers to the mechanical behavior of human skin in vivo using suction experiments, Med. Eng. Phys. 28 (2006) 259–266, https://doi.org/10.1016/j.medengphy.2005.07.001.
[99] G.E. Pierard, N. Nikkels-Tassoudji, C. Pierard-Franchimont, Influence of the test area on the mechanical properties of skin, Dermatology 191 (1995) 9–15, https://doi.org/10.1159/000246472.
[100] K. Chiller, B.A. Selkin, G.J. Murakawa, Skin microflora and bacterial infections of the skin, J. Investig. Dermatology Symp. Proc. 6 (2001) 170–174, https://doi.org/10.1046/j.0022-202x.2001.00043.x.
[101] D.N. Fredricks, Microbial ecology of human skin in health and disease, J. Investig. Dermatol Symp. Proc. 6 (2001) 167–169, https://doi.org/10.1046/j.0022-202x.2001.00039.x.
[102] E.A. Grice, H.H. Kong, S. Conlan, C.B. Deming, J. Davis, A.C. Young, G.G. Bouffard, R.W. Blakesley, P.R. Murray, E.D. Green, M.L. Turner, J.A. Segre, Topographical and temporal diversity of the human skin microbiome, Science (80-) 324 (2009) 1190–1192, https://doi.org/10.1126/science.1171700.
[103] H. Silvola, P. Tala, R. Orko, Skin bacteriology and surgical wound infection, Scand. Cardiovasc. J. 1 (1967) 61–63, https://doi.org/10.3109/14017436709131843.
[104] R.W. Middleton, Wound infections, Med. J. Aust. 46 (1959) 426–428, https://doi.org/10.1001/jama.294.16.2122.
[105] G.S. Lazarus, D.M. Cooper, D.R. Knighton, D.J. Margolis, R.E. Percoraro, G. Rodeheaver, M.C. Robson, Definitions and guidelines for assessment of wounds

and evaluation of healing, Wound Repair Regen. 2 (1994) 165–170, https://doi.org/10.1046/j.1524-475X.1994.20305.x.
[106] S.V. Bharambe, A.B. Darekar, R.B. Saudagar, Wound healing dressings and drug delivery systems: a review, Int. J. Pharm. Technol. 5 (2013) 2764–2786, https://doi.org/10.1002/jps.21210.
[107] J.E. Alonso, J. Lee, A.R. Burgess, B.D. Browner, The management of complex orthopedic injuries, Surg. Clin. North Am. 76 (1996) 879–903, https://doi.org/10.1016/S0039-6109(05)70486-2.
[108] D.A. Dubay, M.G. Franz, Acute wound healing: the biology of acute wound failure, Surg. Clin. North Am. 83 (2003) 463–481, https://doi.org/10.1016/S0039-6109(02)00196-2.
[109] M.H. Katz, A.F. Alvarez, R.S. Kirsner, W.H. Eaglstein, V. Falanga, Human wound fluid from acute wounds stimulates fibroblast and endothelial cell growth, J. Am. Acad. Dermatol. 25 (1991) 1054–1058, https://doi.org/10.1016/0190-9622(91)70306-M.
[110] J. Li, J. Chen, R. Kirsner, Pathophysiology of acute wound healing, Clin. Dermatol. 25 (2007) 9–18, https://doi.org/10.1016/j.clindermatol.2006.09.007.
[111] O. Stojadinovic, H. Brem, C. Vouthounis, B. Lee, J. Fallon, M. Stallcup, A. Merchant, R.D. Galiano, M. Tomic-Canic, Molecular pathogenesis of chronic wounds: the role of β-catenin and c-myc in the inhibition of epithelialization and wound healing, Am. J. Pathol. 167 (2005) 59–69, https://doi.org/10.1016/S0002-9440(10)62953-7.
[112] B.C. Kim, H.T. Kim, S.H. Park, J.S. Cha, T. Yufit, S.J. Kim, V. Falanga, Fibroblasts from chronic wounds show altered TGF-β-signaling and decreased TGF-β type II receptor expression, J. Cell. Physiol. 195 (2003) 331–336, https://doi.org/10.1002/jcp.10301.
[113] B.G. Visavadia, J. Honeysett, M.H. Danford, Manuka honey dressing: an effective treatment for chronic wound infections, Br. J. Oral Maxillofac. Surg. 46 (2008) 55–56, https://doi.org/10.1016/j.bjoms.2006.09.013.
[114] M. Subrahmanyam, A prospective randomised clinical and histological study of superficial burn wound healing with honey and silver sulfadiazine, Burns 24 (1998) 157–161, https://doi.org/10.1016/S0305-4179(97)00113-7.
[115] J.J. Marler, J. Upton, R. Langer, J.P. Vacanti, Transplantation of cells in matrices for tissue regeneration, Adv. Drug Deliv. Rev. 33 (1998) 165–182, https://doi.org/10.1016/S0169-409X(98)00025-8.
[116] D.H. Roh, S.Y. Kang, J.Y. Kim, Y.B. Kwon, Y.K. Hae, K.G. Lee, Y.H. Park, R.M. Baek, C.Y. Heo, J. Choe, J.H. Lee, Wound healing effect of silk fibroin/alginate-blended sponge in full thickness skin defect of rat, J. Mater. Sci. Mater. Med. 17 (2006) 547–552, https://doi.org/10.1007/s10856-006-8938-y.
[117] W.A. Berk, R.D. Welch, B.F. Bock, Controversial issues in clinical management of the simple wound, Ann. Emerg. Med. 21 (1992) 72–78, https://doi.org/10.1016/S0196-0644(05)82245-0.
[118] J.W. Denham, M. Hauer-Jensen, The radiotherapeutic injury - a complex “wound”, Radiother. Oncol. 63 (2002) 129–145, https://doi.org/10.1016/S0167-8140(02)00060-9.
[119] S.G. Moran, S.T. Windham, J.M. Cross, S.M. Melton, L.W. Rue III, Vacuum-assisted complex wound closure with elastic vessel loop augmentation: a novel technique, J. Wound Care 12 (2003) 212–213, https://doi.org/10.12968/jowc.2003.12.6.26508.
[120] S.N.P. Guimarães, V.M. Hamza, Avanços na caracterização das estruturas geológicas em subsuperfície da provincia uranífera Lagoa Real (BA) a partir de dados aerogeofísicos, Geociencias 28 (2009) 273–286, https://doi.org/10.1053/ejso.2002.1308.
[121] J.H. Kendrick, R.E. Casali, N.P. Lang, R.C. Read, The complicated septic abdominal wound, Arch. Surg. 117 (1982) 464–468, https://doi.org/10.1001/archsurg.1982.01380280048010.
[122] T.R. Stevenson, J.G. Thacker, G.T. Rodeheaver, C. Bacchetta, M.T. Edgerton, R.F. Edlich, Cleansing the traumatic wound by high pressure syringe irrigation, J. Am. Coll. Emerg. Physicians 5 (1976) 17–21, https://doi.org/10.1016/S0361-1124(76)80160-8.
[123] G. Rodríguez, M. Ortegón, D. Camargo, L.C. Orozco, Iatrogenic mycobacterium abscessus infection: histopathology of 71 patients, Br. J. Dermatol. 137 (1997) 214–218, https://doi.org/10.1046/j.1365-2133.1997.18081891.x.
[124] D.H. Culver, T.C. Horan, R.P. Gaynes, W.J. Martone, W.R. Jarvis, T.G. Emori, S.N. Banerjee, J.R. Edwards, J.S. Tolson, T.S. Henderson, J.M. Hughes, National Nosocomial Infections Surveillance System, Surgical wound infection rates by wound class, operative procedure, and patient risk index, Am. J. Med. 91 (1991) S152–S157, https://doi.org/10.1016/0002-9343(91)90361-Z.
[125] D. Church, S. Elsayed, O. Reid, B. Winston, R. Lindsay, Burn wound infections, Clin. Microbiol. Rev. 19 (2006) 403–434, https://doi.org/10.1128/CMR.19.2.403-434.2006.
[126] B.A. Pruitt, A.T. McManus, S.H. Kim, C.W. Goodwin, Burn wound infections: current status, World J. Surg. 22 (1998) 135–145, https://doi.org/10.1007/s002689900361.
[127] B.S. Atiyeh, M. Costagliola, S.N. Hayek, S.A. Dibo, Effect of silver on burn wound infection control and healing: review of the literature, Burns. 33 (2007) 139–148, https://doi.org/10.1016/j.burns.2006.06.010.
[128] B.A. Pruitt, The diagnosis and treatment of infection in the burn patient, Burns 11 (1984) 79–91, https://doi.org/10.1016/0305-4179(84)90129-3.
[129] R. Maenthaisong, N. Chaiyakunapruk, S. Niruntraporn, C. Kongkaew, The efficacy of aloe vera used for burn wound healing: a systematic review, Burns 33 (2007) 713–718, https://doi.org/10.1016/j.burns.2006.10.384.
[130] D.O. Weber, J.J. Gooch, W.R. Wood, E.M. Britt, R.O. Kraft, Influence of operating room surface contamination on surgical wounds: a prospective study, Arch. Surg. 111 (1976) 484–488, https://doi.org/10.1001/archsurg.1976.01360220180031.
[131] M.C. Fernandez, M. Gottlieb, Blood transfusion and postoperative infection in orthopedic patients, Transfusion 32 (1992) 318–322, https://doi.org/10.1046/j.1537-2995.1992.32492263444.x.
[132] R.A. Garibaldi, D. Cushing, T. Lerer, Risk factors for postoperative infection, Am. J. Med. 91 (1991) 158S–163S, https://doi.org/10.1016/0002-9343(91)90362-2.
[133] N. Bhagavathula, R.L. Warner, M. Dasilva, S.D. McClintock, A. Barron, M.N. Aslam, K.J. Johnson, J. Varani, A combination of curcumin and ginger extract improves abrasion wound healing in corticosteroid-impaired hairless rat skin, Wound Repair Regen. 17 (2009) 360–366, https://doi.org/10.1111/j.1524-475X.2009.00483.x.
[134] T. Dai, G.P. Tegos, T. Zhiyentayev, E. Mylonakis, M.R. Hamblin, Photodynamic therapy for methicillin-resistant Staphylococcus aureus infection in a mouse skin abrasion model, Lasers Surg. Med. 42 (2010) 38–44, https://doi.org/10.1002/lsm.20887.
[135] C. Ker-Woon, N.A. Ghafar, C. Kien Hui, Y.A.M. Yusof, W.Z.W. Ngah, The effects of acacia honey on in vitro corneal abrasion wound healing model, BMC Cell Biol. 16 (2015) 2, https://doi.org/10.1186/s12860-015-0053-9.
[136] J.E. Fulton, The stimulation of postdermabrasion wound healing with stabilized aloe vera gel???polyethylene oxide dressing, J. Dermatol. Surg. Oncol. 16 (1990) 460–467, https://doi.org/10.1111/j.1524-4725.1990.tb00065.x.
[137] H. Brem, J. Balledux, T. Bloom, M.D. Kerstein, L. Hollier, Healing of diabetic foot ulcers and pressure ulcers with human skin equivalent: a new paradigm in wound healing, Arch. Surg. 135 (2000) 627–634, https://doi.org/10.1001/archsurg.135.6.627.
[138] A. Markova, E.N. Mostow, US skin disease assessment: ulcer and wound care, Dermatol. Clin. 30 (2012) 107–111, https://doi.org/10.1016/j.det.2011.08.005.
[139] M.G. Franz, P.D. Smith, T.L. Wachtel, T.E. Wright, M.A. Kuhn, F. Ko, M.C. Robson, Fascial incisions heal faster than skin: a new model of abdominal wall repair, Surgery 129 (2001) 203–208, https://doi.org/10.1067/msy.2001.110220.
[140] M. Gingrass, L. Perry, D. Hill, T. Wright, M. Robson, J. Fisher, Nondisruptive, in vivo method for biomechanical characterization of linear incision wound healing: preliminary report, Plast. Reconstr. Surg. 102 (1998) 801–806, https://doi.org/10.1097/00006534-199809010-00026.
[141] W.A. Dorsett-Martin, Rat models of skin wound healing: a review, Wound Repair Regen. 12 (2004) 591–599, https://doi.org/10.1111/j.1067-1927.2004.12601.x.
[142] B. Kaplan, B. Gönül, S. Dinçer, F.N.D. Kaya, A. Babül, Relationships between tensile strength, ascorbic acid, hydroxyproline, and zinc levels of rabbit full-thickness incision wound healing, Surg. Today 34 (2004) 747–751, https://doi.org/10.1007/s00595-004-2827-0.
[143] R. Hambley, P.A. Hebda, E. Abell, B.A. Cohen, B.V. Jegasothy, Wound healing of skin incisions produced by ultrasonically vibrating knife, scalpel, electrosurgery, and carbon dioxide laser, J. Dermatol. Surg. Oncol. 14 (1988) 1213–1217, https://doi.org/10.1111/j.1524-4725.1988.tb03478.x.
[144] S.A. Kramer, Effect of povidone-iodine on wound healing: a review, J. Vasc. Nurs. 17 (1999) 17–23, https://doi.org/10.1016/S1062-0303(99)90004-3.
[145] P.G. Hanson, J. Standridge, F. Jarrett, D.G. Maki, Freshwater wound infection due to aeromonas hydrophila, JAMA J. Am. Med. Assoc. 238 (1977) 1053–1054, https://doi.org/10.1001/jama.1977.03280110057026.
[146] J.E. Hollander, A.J. Singer, S.M. Valentine, F.S. Shofer, Risk factors for infection in patients with traumatic lacerations, Acad. Emerg. Med. 8 (2001) 716–720, https://doi.org/10.1111/j.1553-2712.2001.tb00190.x.
[147] B.S. Atiyeh, S.A. Dibo, S.N. Hayek, Wound cleansing, topical antiseptics and wound healing, Int. Wound J. 6 (2009) 420–430, https://doi.org/10.1111/j.1742-481X.2009.00639.x.
[148] D.A. Hudson, J.D. Knottenbelt, J.E.J. Krige, Closed degloving injuries: results following conservative surgery, Plast. Reconstr. Surg. 89 (1992) 853–855, https://doi.org/10.1097/00006534-199205000-00013.
[149] W.B. Kleinman, J.A. Dustman, Preservation of function following complete degloving injuries to the hand: use of simultaneous groin flap, random abdominal flap, and partial-thickness skin graft, J. Hand Surg. Am. 6 (1981) 82–89, https://doi.org/10.1016/S0363-5023(81)80017-2.
[150] H. Wannous, Y. Lucas, S. Treuillet, Enhanced assessment of the wound-healing process by accurate multiview tissue classification, IEEE Trans. Med. Imaging 30 (2011) 315–326, https://doi.org/10.1109/TMI.2010.2077739.
[151] H. Wannous, S. Treuillet, Y. Lucas, Supervised tissue classification from color images for a complete wound assessment tool, in: Annu. Int. Conf. IEEE Eng. Med. Biol. - Proc., IEEE, 2007: pp. 6031–6034. https://doi.org/10.1109/IEMBS.2007.4353723.
[152] P. Martin, Wound healing – aiming for perfect skin regeneration, Science(80-.) 276 (1997) 75–81, https://doi.org/10.1126/science.276.5309.75.
[153] K.A. Bielefeld, S. Amini-Nik, B.A. Alman, Cutaneous wound healing: recruiting developmental pathways for regeneration, Cell. Mol. Life Sci. 70 (2013) 2059–2081, https://doi.org/10.1007/s00018-012-1152-9.
[154] S.A. Eming, T. Krieg, J.M. Davidson, Inflammation in wound repair: molecular and cellular mechanisms, J. Invest. Dermatol. 127 (2007) 514–525, https://doi.org/10.1038/sj.jid.5700701.
[155] J.G. Merrell, S.W. McLaughlin, L. Tie, C.T. Laurencin, A.F. Chen, L.S. Nair, Curcumin-loaded poly(ε-caprolactone) nanofibres: diabetic wound dressing with anti-oxidant and anti-inflammatory properties, Clin. Exp. Pharmacol. Physiol. 36 (2009) 1149–1156, https://doi.org/10.1111/j.1440-1681.2009.05216.x.
[156] S.S. Ramasastry, Acute wounds, Clin. Plast. Surg. 32 (2005) 195–208, https://doi.org/10.1016/j.cps.2004.12.001.
[157] E. Kiwanuka, J. Junker, E. Eriksson, Harnessing growth factors to influence wound healing, Clin. Plast. Surg. 39 (2012) 239–248, https://doi.org/10.1016/j.cps.2012.04.003.
[158] H. Sorg, C. Krueger, B. Vollmar, Intravital insights in skin wound healing using the mouse dorsal skin fold chamber, J. Anat. 211 (2007) 810–818, https://doi.org/10.

1111/j.1469-7580.2007.00822.x.
[159] G.F. Pierce, T.A. Mustoe, B.W. Altrock, T.F. Deuel, A. Thomason, Role of platelet-derived growth factor in wound healing, J. Cell. Biochem. 45 (1991) 319–326, https://doi.org/10.1002/jcb.240450403.
[160] N.S. Gibran, S. Boyce, D.G. Greenhalgh, Cutaneous wound healing, J. Burn Care Res. 28 (2007) 577–579, https://doi.org/10.1097/BCR.0B013E318093E44C.
[161] Z. Xie, C.B. Paras, H. Weng, P. Punnakitikashem, L.C. Su, K. Vu, L. Tang, J. Yang, K.T. Nguyen, Dual growth factor releasing multi-functional nanofibers for wound healing, Acta Biomater. 9 (2013) 9351–9359, https://doi.org/10.1016/j.actbio.2013.07.030.
[162] S. Singh, A. Young, C.E. McNaught, The physiology of wound healing, Surg. (United Kingdom) 35 (2017) 473–477, https://doi.org/10.1016/j.mpsur.2017.06.004.
[163] M.C. Robson, D.L. Steed, M.G. Franz, Wound healing: biologic features and approaches to maximize healing trajectories, Curr. Probl. Surg. 38 (2001) A1, https://doi.org/10.1067/msg.2001.111167.
[164] V.L. Martins, M. Caley, E.A. O'Toole, Matrix metalloproteinases and epidermal wound repair, Cell Tissue Res. 351 (2013) 255–268, https://doi.org/10.1007/s00441-012-1410-z.
[165] M.P. Caley, V.L.C. Martins, E.A. O'Toole, Metalloproteinases and wound healing, Adv. Wound Care. 4 (2015) 225–234, https://doi.org/10.1089/wound.2014.0581.
[166] M.E. Swift, A.L. Burns, K.L. Gray, L.A. DiPietro, Age-related alterations in the inflammatory response to dermal injury, J. Invest. Dermatol. 117 (2001) 1027–1035, https://doi.org/10.1046/j.0022-202x.2001.01539.x.
[167] A. Gosain, L.A. DiPietro, Aging and wound healing, World J. Surg. 28 (2004) 321–326, https://doi.org/10.1007/s00268-003-7397-6.
[168] K.T. Keylock, V.J. Vieira, M.A. Wallig, L.A. DiPietro, M. Schrementi, J.A. Woods, Exercise accelerates cutaneous wound healing and decreases wound inflammation in aged mice, Am. J. Physiol. Integr. Comp. Physiol. 294 (2008) R179–R184, https://doi.org/10.1152/ajpregu.00177.2007.
[169] J.P. Godbout, R. Glaser, Stress-induced immune dysregulation: implications for wound healing, infectious disease and cancer, J. Neuroimmune Pharmacol. 1 (2006) 421–427, https://doi.org/10.1007/s11481-006-9036-0.
[170] L. Boyapati, H.L. Wang, The role of stress in periodontal disease and wound healing, Periodontology 2000 (44) (2007) 195–210, https://doi.org/10.1111/j.1600-0757.2007.00211.x.
[171] L. Vileikyte, Stress and wound healing, Clin. Dermatol. 25 (2007) 49–55, https://doi.org/10.1016/j.clindermatol.2006.09.005.
[172] R. Glaser, J.K. Kiecolt-Glaser, Stress-induced immune dysfunction: implications for health, Nat. Rev. Immunol. 5 (2005) 243–251, https://doi.org/10.1038/nri1571.
[173] D.A. Anaya, E.P. Dellinger, The obese surgical patient: a susceptible host for infection, Surg. Infect. (Larchmt) 7 (2006) 473–480, https://doi.org/10.1089/sur.2006.7.473.
[174] J.A. Greco, E.T. Castaldo, L.B. Nanney, J.J. Wendel, J.B. Summitt, K.J. Kelly, S.A. Braun, K.F. Hagan, R.B. Shack, The effect of weight loss surgery and body mass index on wound complications after abdominal contouring operations, Ann. Plast. Surg. 61 (2008) 235–242, https://doi.org/10.1097/SAP.0b013e318166d351.
[175] J.F. Guest, N. Ayoub, T. McIlwraith, I. Uchegbu, A. Gerrish, D. Weidlich, K. Vowden, P. Vowden, Health economic burden that wounds impose on the National Health Service in the UK, BMJ Open 5 (2015) e009283, https://doi.org/10.1136/bmjopen-2015-009283.
[176] J.A. Wilson, J.J. Clark, Obesity: impediment to wound healing, Crit. Care Nurs. Q. 26 (2003) 119–132, https://doi.org/10.1097/00002727-200304000-00006.
[177] P. Silverstein, Smoking and wound healing, Am. J. Med. 93 (1992) S22–S24, https://doi.org/10.1016/0002-9343(92)90623-J.
[178] L.T. Sørensen, L.N. Jorgensen, R. Zillmer, J. Vange, U. Hemmingsen, F. Gottrup, Transdermal nicotine patch enhances type I collagen synthesis in abstinent smokers, Wound Repair Regen. 14 (2006) 247–251, https://doi.org/10.1111/j.1743-6109.2006.00118.x.
[179] L.K.W. Chan, S. Withey, P.E.M. Butler, Smoking and wound healing problems in reduction mammaplasty: is the introduction of urine nicotine testing justified? Ann. Plast. Surg. 56 (2006) 111–115, https://doi.org/10.1097/01.sap.0000197635.26473.a2.
[180] C. Ahn, P. Mulligan, R. "Sal" Salcido, Smoking-the bane of wound healing, Adv. Skin Wound Care 21 (2008) 227–236, https://doi.org/10.1097/01.ASW.0000305440.62402.43.
[181] J.A. Jensen, W.H. Goodson, H.W. Hopf, T.K. Hunt, Cigarette smoking decreases tissue oxygen, Arch. Surg. 126 (1991) 1131–1134, https://doi.org/10.1001/archsurg.1991.01410330093013.
[182] T.R. Hayes, B. Su, Wound dressings, in: Electrospinning Tissue Regen, Elsevier, 2011, pp. 317–339. https://doi.org/10.1016/B978-1-84569-741-9.50015-X.
[183] D. Queen, H. Orsted, H. Sanada, G. Sussman, A dressing history, Int. Wound J. 1 (2004) 59–77, https://doi.org/10.1111/j.1742-4801.2004.0009.x.
[184] V. Jones, Wound dressings, Bmj 332 (2006) 777–780, https://doi.org/10.1136/bmj.332.7544.777.
[185] R. Uppal, G.N. Ramaswamy, C. Arnold, R. Goodband, Y. Wang, Hyaluronic acid nanofiber wound dressing-production, characterization, and in vivo behavior, J. Biomed. Mater. Res. - Part B Appl. Biomater. 97 B (2011) 20–29, https://doi.org/10.1002/jbm.b.31776.
[186] L. Van Der Schueren, T. De Meyer, I. Steyaert, Ö. Ceylan, K. Hemelsoet, V. Van Speybroeck, K. De Clerck, Polycaprolactone and polycaprolactone/chitosan nanofibres functionalised with the pH-sensitive dye Nitrazine Yellow, Carbohydr. Polym. 91 (2013) 284–293, https://doi.org/10.1016/j.carbpol.2012.08.003.
[187] A. Tamayol, A. Hassani Najafabadi, P. Mostafalu, A.K. Yetisen, M. Commotto, M. Aldhahri, M.S. Abdel-Wahab, Z.I. Najafabadi, S. Latifi, M. Akbari, N. Annabi, S.H. Yun, A. Memic, M.R. Dokmeci, A. Khademhosseini, Biodegradable elastic nanofibrous platforms with integrated flexible heaters for on-demand drug delivery, Sci. Rep. 7 (2017) 9220, https://doi.org/10.1038/s41598-017-04749-8.
[188] T.D. Stocco, N.J. Bassous, S. Zhao, A.E.C. Granato, T.J. Webster, A.O. Lobo, Nanofibrous scaffolds for biomedical applications, Nanoscale 10 (2018) 12228–12255, https://doi.org/10.1039/c8nr02002g.
[189] B. Kandasubramanian, P. Govindaraj, Peeling model for cell adhesion on electrospun polymer nanofibres, J. Adhes. Sci. Technol. 28 (2014) 171–185, https://doi.org/10.1080/01694243.2013.833402.
[190] J. Tahalyani, K.K. Rahangdale, R. Aepuru, B. Kandasubramanian, S. Datar, Dielectric investigation of a conducting fibrous nonwoven porous mat fabricated by a one-step facile electrospinning process, RSC Adv. 6 (2016) 36588–36598, https://doi.org/10.1039/c5ra23012h.
[191] K. Aruchamy, A. Mahto, S.K. Nataraj, Electrospun nanofibers, nanocomposites and characterization of art: insight on establishing fibers as product, Nano-Struct Nano-Objects 16 (2018) 45–58, https://doi.org/10.1016/j.nanoso.2018.03.013.
[192] J. Wang, M. Windbergs, Functional electrospun fibers for the treatment of human skin wounds, Eur. J. Pharm. Biopharm. 119 (2017) 283–299, https://doi.org/10.1016/j.ejpb.2017.07.001.
[193] S. Agarwal, J.H. Wendorff, A. Greiner, Progress in the field of electrospinning for tissue engineering applications, Adv. Mater. 21 (2009) 3343–3351, https://doi.org/10.1002/adma.200803092.
[194] S. Simon, K. Balasubramanian, Facile immobilization of camphor soot on electrospun hydrophobic membrane for oil-water separation, Mater. Focus. 7 (2018) 295–303, https://doi.org/10.1166/mat.2018.1511.
[195] S. Simon, A. Malik, B. Kandasubramanian, Hierarchical electrospun super-hydrophobic nanocomposites of fluoroelastomer, Mater. Focus. 7 (2018) 194–206, https://doi.org/10.1166/mat.2018.1499.
[196] R. Yadav, K. Balasubramanian, Metallization of electrospun PAN nanofibers via electroless gold plating, RSC Adv. 5 (2015) 24990–24996, https://doi.org/10.1039/c5ra03531g.
[197] R. Magisetty, P. Kumar, P.M. Gore, M. Ganivada, A. Shukla, B. Kandasubramanian, R. Shunmugam, Electronic properties of Poly(1,6-heptadiynes) electrospun fibrous non-woven mat, Mater. Chem. Phys. 223 (2019) 343–352, https://doi.org/10.1016/j.matchemphys.2018.11.020.
[198] D.I. Braghirolli, D. Steffens, P. Pranke, Electrospinning for regenerative medicine: a review of the main topics, Drug Discov. Today 19 (2014) 743–753, https://doi.org/10.1016/j.drudis.2014.03.024.
[199] Y. Badhe, K. Balasubramanian, Nanoencapsulated core and shell electrospun fibers of resorcinol formaldehyde, Ind. Eng. Chem. Res. 54 (2015) 7614–7622, https://doi.org/10.1021/acs.iecr.5b00929.
[200] P.D. Bhalara, K. Balasubramanian, B.S. Banerjee, Spider-web textured electrospun composite of graphene for sorption of Hg(II) ions, Mater. Focus 4 (2015) 154–163, https://doi.org/10.1166/mat.2015.1232.
[201] P.M. Gore, L. Khurana, S. Siddique, A. Panicker, B. Kandasubramanian, Ion-imprinted electrospun nanofibers of chitosan/1-butyl-3-methylimidazolium tetrafluoroborate for the dynamic expulsion of thorium (IV) ions from mimicked effluents, Environ. Sci. Pollut. Res. 25 (2018) 3320–3334, https://doi.org/10.1007/s11356-017-0618-6.
[202] J.H. Kim, J. Jang, Y.H. Jeong, T.J. Ko, D.W. Cho, Fabrication of a nanofibrous mat with a human skin pattern, Langmuir 31 (2015) 424–431, https://doi.org/10.1021/la503064r.
[203] X. Geng, O. Kwon, J. Jang, Electrospinning of chitosan dissolved in concentrated acetic acid solution, Biomaterials 26 (2005) 5427–5432, https://doi.org/10.1016/j.biomaterials.2005.01.066.
[204] Y.O. Kang, I.-S. Yoon, S.Y. Lee, D.-D. Kim, S.J. Lee, W.H. Park, S.M. Hudson, Chitosan-coated poly(vinyl alcohol) nanofibers for wound dressings, J. Biomed. Mater. Res. Part B Appl. Biomater 9999B (2009), https://doi.org/10.1002/jbm.b.31554 NA-NA.
[205] K.A. Rieger, R. Thyagarajan, M.E. Hoen, H.F. Yeung, D.M. Ford, J.D. Schiffman, Transport of microorganisms into cellulose nanofiber mats, RSC Adv. 6 (2016) 24438–24445, https://doi.org/10.1039/c6ra01394e.
[206] Y. Zhang, T.L. Chwee, S. Ramakrishna, Z.M. Huang, Recent development of polymer nanofibers for biomedical and biotechnological applications, J. Mater. Sci. Mater. Med. 16 (2005) 933–946, https://doi.org/10.1007/s10856-005-4428-x.
[207] K. Balasubramanian, S. Sharma, S. Badwe, B. Banerjee, Tailored non-woven electrospun mesh of poly-ethyleneoxide-keratin for radioactive metal ion sorption, J. Green Sci. Technol. 2 (2015) 10–19, https://doi.org/10.1166/jgst.2015.1032.
[208] P. Gore, M. Khraisheh, B. Kandasubramanian, Nanofibers of resorcinol–formaldehyde for effective adsorption of As (III) ions from mimicked effluents, Environ. Sci. Pollut. Res. 25 (2018) 11729–11745, https://doi.org/10.1007/s11356-018-1304-z.
[209] J. Zhang, K. Qiu, B. Sun, J. Fang, K. Zhang, H. Ei-Hamshary, S.S. Al-Deyab, X. Mo, The aligned core-sheath nanofibers with electrical conductivity for neural tissue engineering, J. Mater. Chem. B 2 (2014) 7945–7954, https://doi.org/10.1039/c4tb01185f.
[210] S.Y. Chew, R. Mi, A. Hoke, K.W. Leong, The effect of the alignment of electrospun fibrous scaffolds on Schwann cell maturation, Biomaterials 29 (2008) 653–661, https://doi.org/10.1016/j.biomaterials.2007.10.025.
[211] B. Wang, Q. Cai, S. Zhang, X. Yang, X. Deng, The effect of poly (L-lactic acid) nanofiber orientation on osteogenic responses of human osteoblast-like MG63 cells, J. Mech. Behav. Biomed. Mater. 4 (2011) 600–609, https://doi.org/10.1016/j.jmbbm.2011.01.008.
[212] A.K. Moghe, B.S. Gupta, Co-axial electrospinning for nanofiber structures:

preparation and applications, Polym. Rev. 48 (2008) 353–377, https://doi.org/10.1080/15583720802022257.
[213] S.J. Lee, J.J. Yoo, G.J. Lim, A. Atala, J. Stitzel, In vitro evaluation of electrospun nanofiber scaffolds for vascular graft application, J. Biomed. Mater. Res. - Part A 83 (2007) 999–1008, https://doi.org/10.1002/jbm.a.31287.
[214] L. Moroni, R. Schotel, J. Sohier, J.R. de Wijn, C.A. van Blitterswijk, Polymer hollow fiber three-dimensional matrices with controllable cavity and shell thickness, Biomaterials 27 (2006) 5918–5926, https://doi.org/10.1016/j.biomaterials.2006.08.015.
[215] K.L. Ou, C.S. Chen, L.H. Lin, J.C. Lu, Y.C. Shu, W.C. Tseng, J.C. Yang, S.Y. Lee, C.C. Chen, Membranes of epitaxial-like packed, super aligned electrospun micron hollow poly(l-lactic acid) (PLLA) fibers, Eur. Polym. J. 47 (2011) 882–892, https://doi.org/10.1016/j.eurpolymj.2011.02.001.
[216] Y. Dror, W. Salalha, R. Avrahami, E. Zussman, A.L. Yarin, R. Dersch, A. Greiner, J.H. Wendorff, One-step production of polymeric microtubes by co-electrospinning, Small 3 (2007) 1064–1073, https://doi.org/10.1002/smll.200600536.
[217] Y. Srivastava, C. Rhodes, M. Marquez, T. Thorsen, Electrospinning hollow and core/sheath nanofibers using hydrodynamic fluid focusing, Microfluid. Nanofluid. 5 (2008) 455–458, https://doi.org/10.1007/s10404-008-0285-5.
[218] A. Khalf, S.V. Madihally, Recent advances in multiaxial electrospinning for drug delivery, Eur. J. Pharm. Biopharm. 112 (2017) 1–17, https://doi.org/10.1016/j.ejpb.2016.11.010.
[219] A. Khalf, K. Singarapu, S.V. Madihally, Influence of solvent characteristics in triaxial electrospun fiber formation, React. Funct. Polym. 90 (2015) 36–46, https://doi.org/10.1016/j.reactfunctpolym.2015.03.004.
[220] D. Wu, X. Huang, X. Lai, D. Sun, L. Lin, High throughput tip-less electrospinning via a circular cylindrical electrode, J. Nanosci. Nanotechnol. 10 (2010) 4221–4226, https://doi.org/10.1166/jnn.2010.2194.
[221] T. Yoshioka, Y. Kawahara, A.K. Schaper, Cyclic or permanent? Structure control of the contraction behavior of regenerated bombyx mori silk nanofibers, Macromolecules 44 (2011) 7713–7718, https://doi.org/10.1021/ma2014172.
[222] R. Augustine, E.A. Dominic, I. Reju, B. Kaimal, N. Kalarikkal, S. Thomas, Electrospun poly(ε-caprolactone)-based skin substitutes: in vivo evaluation of wound healing and the mechanism of cell proliferation, J. Biomed. Mater. Res. - Part B Appl. Biomater. 103 (2015) 1445–1454, https://doi.org/10.1002/jbm.b.33325.
[223] D. Ishii, T.H. Ying, A. Mahara, S. Murakami, T. Yamaoka, W.K. Lee, T. Iwata, In vivo tissue response and degradation behavior of PLLA and stereocomplexed PLA nanofibers, Biomacromolecules 10 (2009) 237–242, https://doi.org/10.1021/bm8009363.
[224] I.S. Yeo, J.E. Oh, L. Jeong, T.S. Lee, S.J. Lee, W.H. Park, B.M. Min, Collagen-based biomimetic nanofibrous scaffolds: Preparation and characterization of collagen/silk fibroin bicomponent nanofibrous structures, Biomacromolecules 9 (2008) 1106–1116, https://doi.org/10.1021/bm700875a.
[225] S. Datta, A.P. Rameshbabu, K. Bankoti, P.P. Maity, D. Das, S. Pal, S. Roy, R. Sen, S. Dhara, Oleoyl-chitosan-based nanofiber mats impregnated with amniotic membrane derived stem cells for accelerated full-thickness excisional wound healing, ACS Biomater. Sci. Eng. 3 (2017) 1738–1749, https://doi.org/10.1021/acsbiomaterials.7b00189.
[226] A.A. Dongargaonkar, G.L. Bowlin, H. Yang, Electrospun blends of gelatin and gelatin-dendrimer conjugates as a wound-dressing and drug-delivery platform, Biomacromolecules 14 (2013) 4038–4045, https://doi.org/10.1021/bm401143p.
[227] F. Anjum, N.A. Agabalyan, H.D. Sparks, N.L. Rosin, M.S. Kallos, J. Biernaskie, Biocomposite nanofiber matrices to support ECM remodeling by human dermal progenitors and enhanced wound closure, Sci. Rep. 7 (2017) 10291, https://doi.org/10.1038/s41598-017-10735-x.
[228] M.O. Aydogdu, E. Altun, M. Crabbe-Mann, F. Brako, F. Koc, G. Ozen, S.E. Kuruca, U. Edirisinghe, C.J. Luo, O. Gunduz, M. Edirisinghe, Cellular interactions with bacterial cellulose: Polycaprolactone nanofibrous scaffolds produced by a portable electrohydrodynamic gun for point-of-need wound dressing, Int. Wound J. 15 (2018) 789–797, https://doi.org/10.1111/iwj.12929.
[229] S.L. Levengood, A.E. Erickson, F. chien Chang, M. Zhang, Chitosan-poly(caprolactone) nanofibers for skin repair, J. Mater. Chem. B 5 (2017) 1822–1833, https://doi.org/10.1039/C6TB03223K.
[230] V.T. Tchemtchoua, G. Atanasova, A. Aqil, P. Filée, N. Garbacki, O. Vanhooteghem, C. Deroanne, A. Noël, C. Jérome, B. Nusgens, Y. Poumay, A. Colige, Development of a chitosan nanofibrillar scaffold for skin repair and regeneration, Biomacromolecules 12 (2011) 3194–3204, https://doi.org/10.1021/bm200680q.
[231] M. Pakravan, M.C. Heuzey, A. Ajji, A fundamental study of chitosan/PEO electrospinning, Polymer (Guildf) 52 (2011) 4813–4824, https://doi.org/10.1016/j.polymer.2011.08.034.
[232] K. Zhang, X. Bai, Z. Yuan, X. Cao, X. Jiao, Y. Li, Y. Qin, Y. Wen, X. Zhang, Layered nanofiber sponge with an improved capacity for promoting blood coagulation and wound healing, Biomaterials 204 (2019) 70–79, https://doi.org/10.1016/j.biomaterials.2019.03.008.
[233] Y. Zhou, D. Yang, X. Chen, Q. Xu, F. Lu, J. Nie, Electrospun water-soluble carboxyethyl chitosan/poly(vinyl alcohol) nanofibrous membrane as potential wound dressing for skin regeneration, Biomacromolecules 9 (2008) 349–354, https://doi.org/10.1021/bm7009015.
[234] M. Ignatova, N. Manolova, N. Markova, I. Rashkov, Electrospun non-woven nanofibrous hybrid mats based on chitosan and PLA for wound-dressing applications, Macromol. Biosci. 9 (2009) 102–111, https://doi.org/10.1002/mabi.200800189.
[235] A.S. Asran, K. Razghandi, N. Aggarwal, G.H. Michler, T. Groth, Nanofibers from blends of polyvinyl alcohol and polyhydroxy butyrate as potential scaffold material for tissue engineering of skin, Biomacromolecules 11 (2010) 3413–3421, https://doi.org/10.1021/bm100912v.
[236] K.E. Park, H.K. Kang, S.J. Lee, B.-M. Min, W.H. Park, Biomimetic nanofibrous scaffolds: preparation and characterization of PGA/Chitin blend nanofibers, Biomacromolecules 7 (2006) 635–643, https://doi.org/10.1021/bm0509265.
[237] L. Fan, H. Wang, K. Zhang, Z. Cai, C. He, X. Sheng, X. Mo, Vitamin C-reinforcing silk fibroin nanofibrous matrices for skin care application, RSC Adv. 2 (2012) 4110–4119, https://doi.org/10.1039/c2ra20302b.
[238] S. Selvaraj, N.N. Fathima, Fenugreek incorporated silk fibroin nanofibers – a potential antioxidant scaffold for enhanced wound healing, ACS Appl. Mater. Interfaces 9 (2017) 5916–5926, https://doi.org/10.1021/acsami.6b16306.
[239] Y. Xi, J. Ge, Y. Guo, B. Lei, P.X. Ma, Biomimetic elastomeric polypeptide-based nanofibrous matrix for overcoming multidrug-resistant bacteria and enhancing full-thickness wound healing/skin regeneration, ACS Nano 12 (2018) 10772–10784, https://doi.org/10.1021/acsnano.8b01152.
[240] A. Satish, P.S. Korrapati, Fabrication of a triiodothyronine incorporated nanofibrous biomaterial: its implications on wound healing, RSC Adv. 5 (2015) 83773–83780, https://doi.org/10.1039/c5ra14142g.
[241] J. Xie, M.R. MacEwan, W.Z. Ray, W. Liu, D.Y. Siewe, Y. Xia, Radially aligned, electrospun nanofibers as dural substitutes for wound closure and tissue regeneration applications, ACS Nano 4 (2010) 5027–5036, https://doi.org/10.1021/nn101554u.
[242] L. Sun, W. Gao, X. Fu, M. Shi, W. Xie, W. Zhang, F. Zhao, X. Chen, Enhanced wound healing in diabetic rats by nanofibrous scaffolds mimicking the basket-weave pattern of collagen fibrils in native skin, Biomater. Sci. 6 (2018) 340–349, https://doi.org/10.1039/c7bm00545h.
[243] J. Kang, H.S. Yoo, Nucleic acid-scavenging electrospun nanofibrous meshes for suppressing inflammatory responses, Biomacromolecules 15 (2014) 2600–2606, https://doi.org/10.1021/bm500437e.
[244] W. Gao, W. Jin, Y. Li, L. Wan, C. Wang, C. Lin, X. Chen, B. Lei, C. Mao, A highly bioactive bone extracellular matrix-biomimetic nanofibrous system with rapid angiogenesis promotes diabetic wound healing, J. Mater. Chem. B 5 (2017) 7285–7296, https://doi.org/10.1039/c7tb01484h.
[245] C.H. Lee, Y.K. Chao, S.H. Chang, W.J. Chen, K.C. Hung, S.J. Liu, J.H. Juang, Y.T. Chen, F.S. Wang, Nanofibrous rhPDGF-eluting PLGA-collagen hybrid scaffolds enhance healing of diabetic wounds, RSC Adv. 6 (2016) 6276–6284, https://doi.org/10.1039/c5ra21693a.
[246] N. Charernsriwilaiwat, P. Opanasopit, T. Rojanarata, T. Ngawhirunpat, Lysozyme-loaded, electrospun chitosan-based nanofiber mats for wound healing, Int. J. Pharm. 427 (2012) 379–384, https://doi.org/10.1016/j.ijpharm.2012.02.010.
[247] W. Ma, X. Yang, L. Ma, X. Wang, L. Zhang, G. Yang, C. Han, Z. Gou, Fabrication of bioactive glass-introduced nanofibrous membranes with multifunctions for potential wound dressing, RSC Adv. 4 (2014) 60114–60122, https://doi.org/10.1039/c4ra10232k.
[248] X. Dai, J. Liu, H. Zheng, J. Wichmann, U. Hopfner, S. Sudhop, C. Prein, Y. Shen, H.G. Machens, A.F. Schilling, Nano-formulated curcumin accelerates acute wound healing through Dkk-1-mediated fibroblast mobilization and MCP-1-mediated anti-inflammation, e368-e368, NPG Asia Mater. 9 (2017), https://doi.org/10.1038/am.2017.31.
[249] H. Li, M. Wang, G.R. Williams, J. Wu, X. Sun, Y. Lv, L.M. Zhu, Electrospun gelatin nanofibers loaded with vitamins A and e as antibacterial wound dressing materials, RSC Adv. 6 (2016) 50267–50277, https://doi.org/10.1039/c6ra05092a.
[250] H. Chhabra, R. Deshpande, M. Kanitkar, A. Jaiswal, V.P. Kale, J.R. Bellare, A nano zinc oxide doped electrospun scaffold improves wound healing in a rodent model, RSC Adv. 6 (2016) 1428–1439, https://doi.org/10.1039/c5ra21821g.
[251] H. Samadian, M. Salehi, S. Farzamfar, A. Vaez, A. Ehterami, H. Sahrapeyma, A. Goodarzi, S. Ghorbani, In vitro and in vivo evaluation of electrospun cellulose acetate/gelatin/hydroxyapatite nanocomposite mats for wound dressing applications, Artif. Cells, Nanomed. Biotechnol. (2018) 1–11, https://doi.org/10.1080/21691401.2018.1439842.
[252] A.R. Unnithan, G. Gnanasekaran, Y. Sathishkumar, Y.S. Lee, C.S. Kim, Electrospun antibacterial polyurethane-cellulose acetate-zein composite mats for wound dressing, Carbohydr. Polym. 102 (2014) 884–892, https://doi.org/10.1016/j.carbpol.2013.10.070.
[253] S. Kandhasamy, S. Perumal, B. Madhan, N. Umamaheswari, J.A. Banday, P.T. Perumal, V.P. Santhanakrishnan, Synthesis and fabrication of collagen-coated ostholamide electrospun nanofiber scaffold for wound healing, ACS Appl. Mater. Interfaces 9 (2017) 8556–8568, https://doi.org/10.1021/acsami.6b16488.
[254] Y. Xi, H. Dong, K. Sun, H. Liu, R. Liu, Y. Qin, Z. Hu, Y. Zhao, F. Nie, S. Wang, Scab-inspired cytophilic membrane of anisotropic nanofibers for rapid wound healing, ACS Appl. Mater. Interfaces 5 (2013) 4821–4826, https://doi.org/10.1021/am4004683.
[255] N. Charernsriwilaiwat, T. Rojanarata, T. Ngawhirunpat, M. Sukma, P. Opanasopit, Electrospun chitosan-based nanofiber mats loaded with Garcinia mangostana extracts, Int. J. Pharm. 452 (2013) 333–343, https://doi.org/10.1016/j.ijpharm.2013.05.012.
[256] Š. Zupančič, T. Potrč, S. Baumgartner, P. Kocbek, J. Kristl, Formulation and evaluation of chitosan/polyethylene oxide nanofibers loaded with metronidazole for local infections, Eur. J. Pharm. Sci. 95 (2016) 152–160, https://doi.org/10.1016/j.ejps.2016.10.030.
[257] M. Sadri, Saede, A. Sorkhi, Preparation and characterization of CS/PEO/cefazolin nanofibers with in vitro and in vivo testing, Nanomed. Res. J. 2 (2017) 100–110, https://doi.org/10.22034/nmrj.2017.59850.1061.
[258] A.M. Abdelgawad, S.M. Hudson, O.J. Rojas, Antimicrobial wound dressing nanofiber mats from multicomponent (chitosan/silver-NPs/polyvinyl alcohol) systems, Carbohydr. Polym. 100 (2014) 166–178, https://doi.org/10.1016/j.carbpol.2012.12.043.
[259] N. Charernsriwilaiwat, T. Rojanarata, T. Ngawhirunpat, P. Opanasopit,

Electrospun chitosan/polyvinyl alcohol nanofibre mats for wound healing, Int. Wound J. 11 (2014) 215–222, https://doi.org/10.1111/j.1742-481X.2012.01077.x.
[260] L. Mei, R. Fan, X. Li, Y. Wang, B. Han, Y. Gu, L. Zhou, Y. Zheng, A. Tong, G. Guo, Nanofibers for improving the wound repair process: the combination of a grafted chitosan and an antioxidant agent, Polym. Chem. 8 (2017) 1664–1671, https://doi.org/10.1039/c7py00038c.
[261] M. Sadri, S. Arab-Sorkhi, H. Vatani, A. Bagheri-Pebdeni, New wound dressing polymeric nanofiber containing green tea extract prepared by electrospinning method, Fibers Polym. 16 (2015) 1742–1750, https://doi.org/10.1007/s12221-015-5297-7.
[262] D. Annur, Z.K. Wang, J. Der Liao, C. Kuo, Plasma-synthesized silver nanoparticles on electrospun chitosan nanofiber surfaces for antibacterial applications, Biomacromolecules 16 (2015) 3248–3255, https://doi.org/10.1021/acs.biomac.5b00920.
[263] I.H. Ali, I.A. Khalil, I.M. El-Sherbiny, Single-dose electrospun nanoparticles-in-nanofibers wound dressings with enhanced epithelialization, collagen deposition, and granulation properties, ACS Appl. Mater. Interfaces 8 (2016) 14453–14469, https://doi.org/10.1021/acsami.6b04369.
[264] M. Ranjbar-Mohammadi, S.H. Bahrami, M.T. Joghataei, Fabrication of novel nanofiber scaffolds from gum tragacanth/poly(vinyl alcohol) for wound dressing application: in vitro evaluation and antibacterial properties, Mater. Sci. Eng. C 33 (2013) 4935–4943, https://doi.org/10.1016/j.msec.2013.08.016.
[265] S. Jiang, B.C. Ma, J. Reinholz, Q. Li, J. Wang, K.A.I. Zhang, K. Landfester, D. Crespy, Efficient nanofibrous membranes for antibacterial wound dressing and UV protection, ACS Appl. Mater. Interfaces 8 (2016) 29915–29922, https://doi.org/10.1021/acsami.6b09165.
[266] R. Augustine, A. Hasan, V.K. Yadu Nath, J. Thomas, A. Augustine, N. Kalarikkal, A.E. Al Moustafa, S. Thomas, Electrospun polyvinyl alcohol membranes incorporated with green synthesized silver nanoparticles for wound dressing applications, J. Mater. Sci. Mater. Med. 29 (2018) 163, https://doi.org/10.1007/s10856-018-6169-7.
[267] E. Shoba, R. Lakra, M.S. Kiran, P.S. Korrapati, Design and development of papain-urea loaded PVA nanofibers for wound debridement, RSC Adv. 4 (2014) 60209–60215, https://doi.org/10.1039/c4ra10239h.
[268] K. Kataria, A. Gupta, G. Rath, R.B. Mathur, S.R. Dhakate, In vivo wound healing performance of drug loaded electrospun composite nanofibers transdermal patch, Int. J. Pharm. 469 (2014) 102–110, https://doi.org/10.1016/j.ijpharm.2014.04.047.
[269] P. Zahedi, I. Rezaeian, S.H. Jafari, In vitro and in vivo evaluations of phenytoin sodium-loaded electrospun PVA, PCL, and their hybrid nanofibrous mats for use as active wound dressings, J. Mater. Sci. 48 (2013) 3147–3159, https://doi.org/10.1007/s10853-012-7092-9.
[270] M. Jannesari, J. Varshosaz, M. Morshed, M. Zamani, Composite poly(vinyl alcohol)/poly(vinyl acetate) electrospun nanofibrous mats as a novel wound dressing matrix for controlled release of drugs, Int. J. Nanomed. 6 (2011) 993–1003, https://doi.org/10.2147/IJN.S17595.
[271] B. Lu, T. Li, H. Zhao, X. Li, C. Gao, S. Zhang, E. Xie, Graphene-based composite materials beneficial to wound healing, Nanoscale 4 (2012) 2978–2982, https://doi.org/10.1039/c2nr11958g.
[272] R. Ahmed, M. Tariq, I. Ali, R. Asghar, P. Noorunnisa Khanam, R. Augustine, A. Hasan, Novel electrospun chitosan/polyvinyl alcohol/zinc oxide nanofibrous mats with antibacterial and antioxidant properties for diabetic wound healing, Int. J. Biol. Macromol. 120 (2018) 385–393, https://doi.org/10.1016/j.ijbiomac.2018.08.057.
[273] K.T. Shalumon, K.H. Anulekha, S.V. Nair, S.V. Nair, K.P. Chennazhi, R. Jayakumar, Sodium alginate/poly(vinyl alcohol)/nano ZnO composite nanofibers for antibacterial wound dressings, Int. J. Biol. Macromol. 49 (2011) 247–254, https://doi.org/10.1016/j.ijbiomac.2011.04.005.
[274] J. Xue, M. He, Y. Niu, H. Liu, A. Crawford, P. Coates, D. Chen, R. Shi, L. Zhang, Preparation and in vivo efficient anti-infection property of GTR/GBR implant made by metronidazole loaded electrospun polycaprolactone nanofiber membrane, Int. J. Pharm. 475 (2014) 566–577, https://doi.org/10.1016/j.ijpharm.2014.09.026.
[275] J. Lopez-Esparza, L. Francisco Espinosa-Cristobal, A. Donohue-Cornejo, S.Y. Reyes-Lopez, Antimicrobial activity of silver nanoparticles in polycaprolactone nanofibers against gram-positive and gram-negative bacteria, Ind. Eng. Chem. Res. 55 (2016) 12532–12538, https://doi.org/10.1021/acs.iecr.6b02300.
[276] P. Pal, B. Das, P. Dadhich, A. Achar, S. Dhara, Carbon nanodot impregnated fluorescent nanofibers for: in vivo monitoring and accelerating full-thickness wound healing, J. Mater. Chem. B 5 (2017) 6645–6656, https://doi.org/10.1039/c7tb00684e.
[277] R. Augustine, S.K. Nethi, N. Kalarikkal, S. Thomas, C.R. Patra, Electrospun polycaprolactone (PCL) scaffolds embedded with europium hydroxide nanorods (EHNs) with enhanced vascularization and cell proliferation for tissue engineering applications, J. Mater. Chem. B 5 (2017) 4660–4672, https://doi.org/10.1039/c7tb00518k.
[278] R. Augustine, E.A. Dominic, I. Reju, B. Kaimal, N. Kalarikkal, S. Thomas, Electrospun polycaprolactone membranes incorporated with ZnO nanoparticles as skin substitutes with enhanced fibroblast proliferation and wound healing, RSC Adv. 4 (2014) 24777–24785, https://doi.org/10.1039/c4ra02450h.
[279] L. Preem, M. Mahmoudzadeh, M. Putriņš, A. Meos, I. Laidmäe, T. Romann, J. Aruväli, R. Härmas, A. Koivuniemi, A. Bunker, T. Tenson, K. Kogermann, Interactions between chloramphenicol, carrier polymers, and bacteria-implications for designing electrospun drug delivery systems countering wound infection, Mol. Pharm. 14 (2017) 4417–4430, https://doi.org/10.1021/acs.molpharmaceut.7b00524.
[280] Q. Yu, Y. Han, T. Tian, Q. Zhou, Z. Yi, J. Chang, C. Wu, Chinese sesame stick-inspired nano-fibrous scaffolds for tumor therapy and skin tissue reconstruction, Biomaterials 194 (2019) 25–35, https://doi.org/10.1016/j.biomaterials.2018.12.012.
[281] J. Xue, M. He, Y. Liang, A. Crawford, P. Coates, D. Chen, R. Shi, L. Zhang, Fabrication and evaluation of electrospun PCL-gelatin micro-/nanofiber membranes for anti-infective GTR implants, J. Mater. Chem. B 2 (2014) 6867–6877, https://doi.org/10.1039/c4tb00737a.
[282] X. Yang, J. Yang, L. Wang, B. Ran, Y. Jia, L. Zhang, G. Yang, H. Shao, X. Jiang, Pharmaceutical intermediate-modified gold nanoparticles: against multidrug-resistant bacteria and wound-healing application via an electrospun scaffold, ACS Nano 11 (2017) 5737–5745, https://doi.org/10.1021/acsnano.7b01240.
[283] B. Motealleh, P. Zahedi, I. Rezaeian, M. Moghimi, A.H. Abdolghaffari, M.A. Zarandi, Morphology, drug release, antibacterial, cell proliferation, and histology studies of chamomile-loaded wound dressing mats based on electrospun nanofibrous poly(ε-caprolactone)/polystyrene blends, J. Biomed. Mater. Res. - Part B Appl. Biomater. 102 (2014) 977–987, https://doi.org/10.1002/jbm.b.33078.
[284] L. Liu, S. Bai, H. Yang, S. Li, J. Quan, L. Zhu, H. Nie, Controlled release from thermo-sensitive PNVCL-co-MAA electrospun nanofibers: the effects of hydrophilicity/hydrophobicity of a drug, Mater. Sci. Eng. C 67 (2016) 581–589, https://doi.org/10.1016/j.msec.2016.05.083.
[285] K.A. Wold, V.B. Damodaran, L.A. Suazo, R.A. Bowen, M.M. Reynolds, Fabrication of biodegradable polymeric nanofibers with covalently attached no donors, ACS Appl. Mater. Interfaces 4 (2012) 3022–3030, https://doi.org/10.1021/am300383w.
[286] E.R. Kenawy, G.L. Bowlin, K. Mansfield, J. Layman, D.G. Simpson, E.H. Sanders, G.E. Wnek, Release of tetracycline hydrochloride from electrospun poly(ethylene-co-vinylacetate), poly(lactic acid), and a blend, J. Control. Release 81 (2002) 57–64, https://doi.org/10.1016/S0168-3659(02)00041-X.
[287] L.M.D. Loiola, P.R. Cortez Tornello, G.A. Abraham, M.I. Felisberti, Amphiphilic electrospun scaffolds of PLLA-PEO-PPO block copolymers: preparation, characterization and drug-release behaviour, RSC Adv. 7 (2017) 161–172, https://doi.org/10.1039/c6ra25023h.
[288] W. Li, T. Luo, Y. Yang, X. Tan, L. Liu, Formation of controllable hydrophilic/hydrophobic drug delivery systems by electrospinning of vesicles, Langmuir 31 (2015) 5141–5146, https://doi.org/10.1021/la504796v.
[289] Z.C. Xing, W.P. Chae, J.Y. Baek, M.J. Choi, Y. Jung, I.K. Kang, In vitro assessment of antibacterial activity and cytocompatibility of silver-containing phbv nanofibrous scaffolds for tissue engineering, Biomacromolecules 11 (2010) 1248–1253, https://doi.org/10.1021/bm1000372.
[290] A. GhavamiNejad, A. Rajan Unnithan, A. Ramachandra Kurup Sasikala, M. Samarikhalaj, R.G. Thomas, Y.Y. Jeong, S. Nasseri, P. Murugesan, D. Wu, C. Hee Park, C.S. Kim, Mussel-inspired electrospun nanofibers functionalized with size-controlled silver nanoparticles for wound dressing application, ACS Appl. Mater. Interfaces 7 (2015) 12176–12183, https://doi.org/10.1021/acsami.5b02542.
[291] O.E. Fayemi, A.C. Ekennia, L. Katata-Seru, A.P. Ebokaiwe, O.M. Ijomone, D.C. Onwudiwe, E.E. Ebenso, Antimicrobial and wound healing properties of polyacrylonitrile-moringa extract nanofibers, ACS Omega 3 (2018) 4791–4797, https://doi.org/10.1021/acsomega.7b01981.
[292] J. Wu, S. Hou, D. Ren, P.T. Mather, Antimicrobial properties of nanostructured hydrogel webs containing silver, Biomacromolecules 10 (2009) 2686–2693, https://doi.org/10.1021/bm900620w.
[293] Y. Wang, P. Li, P. Xiang, J. Lu, J. Yuan, J. Shen, Electrospun polyurethane/keratin/AgNP biocomposite mats for biocompatible and antibacterial wound dressings, J. Mater. Chem. B 4 (2016) 635–648, https://doi.org/10.1039/c5tb02358k.
[294] J. Ahmed, R.K. Matharu, T. Shams, U.E. Illangakoon, M. Edirisinghe, A comparison of electric-field-driven and pressure-driven fiber generation methods for drug delivery, Macromol. Mater. Eng. 303 (2018) 1700577, https://doi.org/10.1002/mame.201700577.
[295] R. Zhao, X. Li, B. Sun, Y. Tong, Z. Jiang, C. Wang, Nitrofurazone-loaded electrospun PLLA/sericin-based dual-layer fiber mats for wound dressing applications, RSC Adv. 5 (2015) 16940–16949, https://doi.org/10.1039/c4ra16208k.
[296] W.A. Sarhan, H.M.E. Azzazy, I.M. El-Sherbiny, Honey/chitosan nanofiber wound dressing enriched with allium sativum and cleome droserifolia: enhanced antimicrobial and wound healing activity, ACS Appl. Mater. Interfaces 8 (2016) 6379–6390, https://doi.org/10.1021/acsami.6b00739.
[297] P. Dubey, P. Gopinath, PEGylated graphene oxide-based nanocomposite-grafted chitosan/polyvinyl alcohol nanofiber as an advanced antibacterial wound dressing, RSC Adv. 6 (2016) 69103–69116, https://doi.org/10.1039/c6ra12192f.
[298] G. Ramanathan, S. Singaravelu, M.D. Raja, N. Nagiah, P. Padmapriya, K. Ruban, K. Kaveri, T.S. Natarajan, U.T. Sivagnanam, P.T. Perumal, Fabrication and characterization of a collagen coated electrospun poly(3-hydroxybutyric acid)-gelatin nanofibrous scaffold as a soft bio-mimetic material for skin tissue engineering applications, RSC Adv. 6 (2016) 7914–7922, https://doi.org/10.1039/c5ra19529b.
[299] M. Cheng, Z. Qin, S. Hu, S. Dong, Z. Ren, H. Yu, Achieving long-term sustained drug delivery for electrospun biopolyester nanofibrous membranes by introducing cellulose nanocrystals, ACS Biomater. Sci. Eng. 3 (2017) 1666–1676, https://doi.org/10.1021/acsbiomaterials.7b00169.
[300] P. Peh, N.S.J. Lim, A. Blocki, S.M.L. Chee, H.C. Park, S. Liao, C. Chan, M. Raghunath, Simultaneous delivery of highly diverse bioactive compounds from blend electrospun fibers for skin wound healing, Bioconjug. Chem. 26 (2015)

1348–1358, https://doi.org/10.1021/acs.bioconjchem.5b00123.
[301] A. Mira, C.R. Mateo, R. Mallavia, A. Falco, Poly(methyl vinyl ether-alt-maleic acid) and ethyl monoester as building polymers for drug-loadable electrospun nanofibers, Sci. Rep. 7 (2017) 17205, https://doi.org/10.1038/s41598-017-17542-4.
[302] P. Zhao, H. Jiang, H. Pan, K. Zhu, W. Chen, Biodegradable fibrous scaffolds composed of gelatin coated poly(??-caprolactone) prepared by coaxial electrospinning, J. Biomed. Mater. Res. - Part A 83 (2007) 372–382, https://doi.org/10.1002/jbm.a.31242.
[303] V. Padmavathy, P. Vasudevan, S.C. Dhingra, Thermal and spectroscopic studies on sorption of nickel(II) ion on protonated baker's yeast, Chemosphere 52 (2003) 1807–1817, https://doi.org/10.1021/bm800551q.
[304] T.T.T. Nguyen, O.H. Chung, J.S. Park, Coaxial electrospun poly(lactic acid)/chitosan (core/shell) composite nanofibers and their antibacterial activity, Carbohydr. Polym. 86 (2011) 1799–1806, https://doi.org/10.1016/j.carbpol.2011.07.014.
[305] M. Pakravan, M.C. Heuzey, A. Ajji, Core-shell structured PEO-chitosan nanofibers by coaxial electrospinning, Biomacromolecules 13 (2012) 412–421, https://doi.org/10.1021/bm201444v.
[306] J.F. Zhang, D.Z. Yang, F. Xu, Z.P. Zhang, R.X. Yin, J. Nie, Electrospun core-shell structure nanofibers from homogeneous solution of poly(ethylene oxide)/chitosan, Macromolecules 42 (2009) 5278–5284, https://doi.org/10.1021/ma900657y.
[307] M. Rubert, J. Dehli, Y.F. Li, M.B. Taskin, R. Xu, F. Besenbacher, M. Chen, Electrospun PCL/PEO coaxial fibers for basic fibroblast growth factor delivery, J. Mater. Chem. B 2 (2014) 8538–8546, https://doi.org/10.1039/c4tb01258e.
[308] Y.Z. Zhang, X. Wang, Y. Feng, J. Li, C.T. Lim, S. Ramakrishna, Coaxial electrospinning of (fluorescein isothiocyanate-conjugated bovine serum albumin)-encapsulated poly(ε-caprolactone) nanofibers for sustained release, Biomacromolecules 7 (2006) 1049–1057, https://doi.org/10.1021/bm050743i.
[309] H. Jiang, Y. Hu, Y. Li, P. Zhao, K. Zhu, W. Chen, A facile technique to prepare biodegradable coaxial electrospun nanofibers for controlled release of bioactive agents, J. Control. Release 108 (2005) 237–243, https://doi.org/10.1016/j.jconrel.2005.08.006.
[310] W. Gao, L. Sun, X. Fu, Z. Lin, W. Xie, W. Zhang, F. Zhao, X. Chen, Enhanced diabetic wound healing by electrospun core-sheath fibers loaded with dimethyloxalylglycine, J. Mater. Chem. B 6 (2018) 277–288, https://doi.org/10.1039/c7tb02342a.
[311] R. Qi, R. Guo, M. Shen, X. Cao, L. Zhang, J. Xu, J. Yu, X. Shi, Electrospun poly (lactic-co-glycolic acid)/halloysite nanotube composite nanofibers for drug encapsulation and sustained release, J. Mater. Chem. 20 (2010) 10622–10629, https://doi.org/10.1039/c0jm01328e.
[312] M. He, H. Jiang, R. Wang, Y. Xie, C. Zhao, Fabrication of metronidazole loaded poly (ε-caprolactone)/zein core/shell nanofiber membranes via coaxial electrospinning for guided tissue regeneration, J. Colloid Interface Sci. 490 (2017) 270–278, https://doi.org/10.1016/j.jcis.2016.11.062.
[313] R. Najafi-Taher, M.A. Derakhshan, R. Faridi-Majidi, A. Amani, Preparation of an ascorbic acid/PVA-chitosan electrospun mat: a core/shell transdermal delivery system, RSC Adv. 5 (2015) 50462–50469, https://doi.org/10.1039/c5ra03813h.
[314] Š. Zupančič, S. Sinha-Ray, S. Sinha-Ray, J. Kristl, A.L. Yarin, Controlled release of ciprofloxacin from core-shell nanofibers with monolithic or blended core, Mol. Pharm. 13 (2016) 1393–1404, https://doi.org/10.1021/acs.molpharmaceut.6b00039.
[315] L. Zhu, X. Liu, L. Du, Y. Jin, Preparation of asiaticoside-loaded coaxially electrospinning nanofibers and their effect on deep partial-thickness burn injury, Biomed. Pharmacother. 83 (2016) 33–40, https://doi.org/10.1016/j.biopha.2016.06.016.
[316] R. Li, Z. Cheng, R. Wen, X. Zhao, X. Yu, L. Sun, Y. Zhang, Z. Han, Y. Yuan, L. Kang, Novel SA@Ca2+/RCSPs core-shell structure nanofibers by electrospinning for wound dressings, RSC Adv. 8 (2018) 15558–15566, https://doi.org/10.1039/c8ra00784e.
[317] B.V. Worley, R.J. Soto, P.C. Kinsley, M.H. Schoenfisch, Active release of nitric oxide-releasing dendrimers from electrospun polyurethane fibers, ACS Biomater. Sci. Eng. 2 (2016) 426–437, https://doi.org/10.1021/acsbiomaterials.6b00032.
[318] H. Li, J. Zhu, S. Chen, L. Jia, Y. Ma, Fabrication of aqueous-based dual drug loaded silk fibroin electrospun nanofibers embedded with curcumin-loaded RSF nanospheres for drugs controlled release, RSC Adv. 7 (2017) 56550–56558, https://doi.org/10.1039/c7ra12394a.
[319] M. Ranjbar-Mohammadi, M. Zamani, M.P. Prabhakaran, S.H. Bahrami, S. Ramakrishna, Electrospinning of PLGA/gum tragacanth nanofibers containing tetracycline hydrochloride for periodontal regeneration, Mater. Sci. Eng. C 58 (2016) 521–531, https://doi.org/10.1016/j.msec.2015.08.066.
[320] C. Yang, D.G. Yu, D. Pan, X.K. Liu, X. Wang, S.W.A. Bligh, G.R. Williams, Electrospun pH-sensitive core-shell polymer nanocomposites fabricated using a triaxial process, Acta Biomater. 35 (2016) 77–86, https://doi.org/10.1016/j.actbio.2016.02.029.
[321] W. Liu, C. Ni, D.B. Chase, J.F. Rabolt, Preparation of multilayer biodegradable nanofibers by triaxial electrospinning, ACS Macro Lett. 2 (2013) 466–468, https://doi.org/10.1021/mz4000688.
[322] D. Han, S. Sherman, S. Filocamo, A.J. Steckl, Long-term antimicrobial effect of nisin released from electrospun triaxial fiber membranes, Acta Biomater. 53 (2017) 242–249, https://doi.org/10.1016/j.actbio.2017.02.029.
[323] A. Khalf, S.V. Madihally, Modeling the permeability of multiaxial electrospun poly (ε-caprolactone)-gelatin hybrid fibers for controlled doxycycline release, Mater. Sci. Eng. C 76 (2017) 161–170, https://doi.org/10.1016/j.msec.2017.03.093.
[324] D.G. Yu, X.Y. Li, X. Wang, J.H. Yang, S.W.A. Bligh, G.R. Williams, Nanofibers fabricated using triaxial electrospinning as zero order drug delivery systems, ACS Appl. Mater. Interfaces 7 (2015) 18891–18897, https://doi.org/10.1021/acsami.5b06007.
[325] D. Han, A.J. Steckl, Triaxial electrospun nanofiber membranes for controlled dual release of functional molecules, ACS Appl. Mater. Interfaces 5 (2013) 8241–8245, https://doi.org/10.1021/am402376c.
[326] F. Qu, J.L. Holloway, J.L. Esterhai, J.A. Burdick, R.L. Mauck, Programmed biomolecule delivery to enable and direct cell migration for connective tissue repair, Nat. Commun. 8 (2017) 1780, https://doi.org/10.1038/s41467-017-01955-w.
[327] T.R. Dargaville, B.L. Farrugia, J.A. Broadbent, S. Pace, Z. Upton, N.H. Voelcker, Sensors and imaging for wound healing: a review, Biosens. Bioelectron. 41 (2013) 30–42, https://doi.org/10.1016/j.bios.2012.09.029.
[328] G. Jin, M.P. Prabhakaran, D. Kai, M. Kotaki, S. Ramakrishna, Electrospun photosensitive nanofibers: potential for photocurrent therapy in skin regeneration, Photochem. Photobiol. Sci. 12 (2013) 124–134, https://doi.org/10.1039/c2pp25070e.
[329] H.K. Patra, Y. Sharma, M.M. Islam, M.J. Jafari, N.A. Murugan, H. Kobayashi, A.P.F. Turner, A. Tiwari, Inflammation-sensitive in situ smart scaffolding for regenerative medicine, Nanoscale 8 (2016) 17213–17222, https://doi.org/10.1039/c6nr06157e.
[330] L. Tan, J. Hu, H. Huang, J. Han, H. Hu, Study of multi-functional electrospun composite nanofibrous mats for smart wound healing, Int. J. Biol. Macromol. 79 (2015) 469–476, https://doi.org/10.1016/j.ijbiomac.2015.05.014.
[331] O.S. Fenton, K.N. Olafson, P.S. Pillai, M.J. Mitchell, R. Langer, Advances in biomaterials for drug delivery, Adv. Mater. 30 (2018) 1705328, https://doi.org/10.1002/adma.201705328.
[332] G. Agnes, E. J., Gonzales Ortega, Mathematical models and physicochemical of diffusion, 2003.
[333] Marcos Luciano Bruschi, Mathematical models of drug release, in: Strateg. to Modify Drug Release from Pharm. Syst., Elsevier, 2015, pp. 63–86. https://doi.org/10.1016/B978-0-08-100092-2.00005-9.
[334] R.W. Korsmeyer, R. Gurny, E. Doelker, P. Buri, N.A. Peppas, Mechanisms of solute release from porous hydrophilic polymers, Int. J. Pharm. 15 (1983) 25–35, https://doi.org/10.1016/0378-5173(83)90064-9.
[335] B.M. Cheknev, O rabote Alta??skogo meditsinskogo instituta, Zdravookhr. Ross. Fed. 12 (1968) 44–46, https://doi.org/10.1016/0168-3659(87)90034-4.
[336] H. Kim, R. Fassihi, Application of binary polymer system in drug release rate modulation. 2. Influence of formulation variables and hydrodynamic conditions on release kinetics, J. Pharm. Sci. 86 (1997) 323–328, https://doi.org/10.1021/js960307p.
[337] I. Katzhendler, A. Hoffman, A. Goldberger, M. Friedman, Modeling of drug release from erodible tablets, J. Pharm. Sci. 86 (1997) 110–115, https://doi.org/10.1021/js9600538.
[338] N.A. Peppas, Analysis of Fickian and non-Fickian drug release from polymers, Pharm. Acta Helv. 60 (1985) 110–111.
[339] C.M. Klech, A.P. Simonelli, Examination of the moving boundaries associated with non-fickian water swelling of glassy gelatin beads: effect of solution pH, J. Memb. Sci. 43 (1989) 87–101, https://doi.org/10.1016/S0376-7388(00)82355-8.
[340] M. Carlson, D.C. Wheelock, Interbank markets and banking crises: new evidence on the establishment and impact of the federal reserve, Am. Econ. Rev. 106 (2016) 533–537, https://doi.org/10.1257/aer.p20161044.
[341] B. Marasli, P. Nguyen, J.M. Wallace, A calibration technique for multiple-sensor hot-wire probes and its application to vorticity measurements in the wake of a circular cylinder, 1993. https://doi.org/10.1007/BF00189888.